Technische Universität München
TUM School of Life Sciences

Chemical evolution of acetylene under hydrothermal volcanic conditions

Philippe Christophe Maxime Diederich

Vollständiger Abdruck der von der TUM School of Life Sciences der Technischen Universität München zur Erlangung eines

Doktors der Naturwissenschaften (Dr. rer. nat.)

genehmigten Dissertation.

Vorsitz: Prof. Dr. Wilfried Schwab

Prüfende der Dissertation:

1. apl. Prof. Dr. Philippe Schmitt-Kopplin
2. Prof. Dr. Job Boekhoven

Die Dissertation wurde am 13.09.2024 bei der Technischen Universität München eingereicht und durch die TUM School of Life Sciences am 23.12.2024 angenommen.

Danksagung

The findings and experiences resulting from this thesis are all linked to a multitude of different people I met during my time at the BGC. I am however especially thankful to Prof. Philippe Schmitt-Kopplin, who supervised me during my whole journey. My passion for analytical chemistry was only able to develop due to the environment he created over many years at BGC. An environment of scientific freedom, where scientists can perform their research with nearly no restrictions, enhanced by the presence of the most state-of-the-art analytical instruments. The access to those instruments was a blessing that cannot be overstated.

I also want to thank Dr. Claudia Huber, who was always available for calls or to discuss any findings. Her yearlong experience in the field was invaluable for me and it was always a pleasure to learn about all the exciting experiments she performed in the past. I also want to thank Thomas and Christian who were never tried to produce a new reaction bottle for me, no matter what special wishes I had.

A final big thanks goes to all my collogues at BGC who made the good times better and the bad times less bad (if not caused by them). I want to thank Kristina for all the discussions and time we spend together. I also want to thank Leo, Stefan, Liesa, Michelle and Lance for either helping me with my research or letting me help them with their projects. In general everyone at BGC made my time there special and I cannot thank you enough.

Abstract

The aim of this study is to explore whether acetylene gas could have been a key component in the emergence of life. Acetylene is a reactive gas formed from the photolysis of methane in planetary atmospheres, including that of the primordial Earth. The study demonstrates that acetylene, in combination with other prebiotically relevant reactants such as carbon monoxide, water, and nickel sulfide, has the potential to transform into a variety of small molecules with properties that prebiotic chemists are looking for.

The study is divided into three major parts, each representing a publication analyzing different reaction products emerging from acetylene. The investigation revealed a promising similarity to the C2-metabolism of extant organisms, particularly *Pelobacter acetylenicus*. This microorganism thrives in anaerobic aqueous environments and can use acetylene as its sole carbon source.

Through ^{13}C-labelling, we discovered that acetylene is converted into a C2-building block in the system and is used to increase the mass of all detected compound classes. This discovery, along with the detection of thioacetic acid and higher thio acids, made this pathway even more reminiscent of the metabolism of *Pelobacter acetylenicus*, which converts acetylene into acetaldehyde and then into acetyl-CoA, a thio acid ester.

The experimental conditions changed over time due to the formation of a complex mixture. This led to an autoregulation of the compounds produced from newly formed acetaldehyde. Basic conditions led to the formation of amino acids if ammonium and cyanate were present in the system. Older systems changed to a more acidic pH due to the formation of carboxylic and sulfonic acids. This pH switch altered the reaction route taken by acetaldehyde and resulted in lactic acid, an α-hydroxy acid. Both amino and α-hydroxy acids possess useful characteristics for the origin of life.

The formation pathway of acetaldehyde could be further elucidated by detecting an organo-nickel complex in the form of nickel-bis(dithiolene). This complex formed quickly in the early stages of the reaction setup and was then transformed

into acetaldehyde and formic acid. This transformation is highly interesting, as the enzymatic transformation of acetylene into acetaldehyde in *Pelobacter acetylenicus* is catalyzed by a pterin co-factor containing a metal-bis(dithiolene) core.

Altogether, the research presented in this thesis clearly documents the promising role of acetylene as an essential Origin-of-Life building block.

Zusammenfassung

Diese Studie untersucht das Potenzial von Acetylen Gas als Baustein für den Ursprung des Lebens. Acetylen ist ein reaktives Gas, das durch Fotolyse von Methan in der Atmosphäre von Planeten, einschließlich der der urzeitlichen Erde, entstehen konnte. Unsere Studie zeigt, dass Acetylen in Kombination mit anderen präbiotisch-relevanten Reaktanten wie Kohlenmonoxid, Wasser und Nickelsulfid zu einer Vielzahl von kleinen Molekülen mit Eigenschaften, die von präbiotischen Chemikern gesucht werden, führt.

Die Studie ist in drei Hauptteile gegliedert, von denen jeder eine Veröffentlichung darstellt, die verschiedene Reaktionsprodukte analysiert, die aus Acetylen entstehen. Die Untersuchung ergab eine vielversprechende Ähnlichkeit zum C2-Stoffwechsel von existierenden Organismen, insbesondere *Pelobacter acetylenicu*s. Dieser Mikroorganismus überlebt in anaeroben wässrigen Umgebungen und kann Acetylen als einzige Kohlenstoffquelle nutzen.

Durch ^{13}C-Markierung wurde entdeckt, dass Acetylen in unserem System als C2-Baustein genutzt wird und zur Erhöhung der Masse aller nachgewiesenen Verbindungsklassen verwendet wird. Diese Entdeckung, zusammen mit dem Nachweis von Thioessigsäure und höheren Thiosäuren, machte dieses Reaktionssystem dem Stoffwechsel von *Pelobacter acetylenicus* noch ähnlicher: Dieser Mikroorganismus wandelt Acetylen in Acetaldehyd und dann in Acetyl-CoA, einem Thiosäureester, um.

Die experimentellen Bedingungen änderten sich im Laufe der Zeit aufgrund der Bildung eines komplexen Gemisches. Dies führte zu einer Autoregulation der produzierten Verbindungen aus neu gebildetem Acetaldehyd. Basische Bedingungen führten zur Bildung von Aminosäuren, wenn Ammonium und Cyanat im System vorhanden waren. Ältere Systeme wurden saurer aufgrund der Bildung von Carbonsäuren und Sulfonsäuren. Dieser pH-Wechsel änderte den Reaktionsweg von Acetaldehyd und führte zu Milchsäure, einer α-Hydroxysäure. Sowohl Aminosäuren als auch α-Hydroxysäuren besitzen nützliche Eigenschaften für den Ursprung des Lebens.

Der Bildungsweg von Acetaldehyd konnte weiter durch den Nachweis eines Organo-Nickel-Komplexes in Form von Nickel-bis(Dithiolene) aufgeklärt werden. Dieser Komplex bildete sich schnell in den frühen Stadien des Reaktionsaufbaus und wurde dann in Acetaldehyd und Ameisensäure umgewandelt. Diese Umwandlung ist hochinteressant, da die enzymatische Umwandlung von Acetylen zu Acetaldehyd in *Pelobacter acetylenicus* durch einen Pterin-Co-Faktor katalysiert wird, der einen Metall-bis(Dithiolene)-Kern enthält.

Insgesamt dokumentieren die in dieser Dissertation vorgestellten Forschungsergebnisse die vielversprechende Rolle von Acetylen als wesentlichen Baustein für den Ursprung des Lebens.

List of contributed articles

Publications in the context of this doctoral thesis

All results have been published in peer-reviewed journals:

- **Diederich, P., Geisberger, T., Yan, Y. *et al.* Formation, stabilization and fate of acetaldehyde and higher aldehydes in an autonomously changing prebiotic system emerging from acetylene.** *Commun Chem* **6**, 38 (2023). https://doi.org/10.1038/s42004-023-00833-5

- **Diederich, P., Ruf, A., Geisberger, T. *et al.* C2-addition patterns emerging from acetylene and nickel sulfide in simulated prebiotic hydrothermal conditions.** *Commun Chem* **6**, 220 (2023). https://doi.org/10.1038/s42004-023-01021-1

- **Diederich, P., Seitz, C., Buckett, L. *et al.* Nickel-organo compounds as potential enzyme precursors under simulated early Earth conditions.** *Commun Chem* **7**, 33 (2024). https://doi.org/10.1038/s42004-024-01119-0

- **Geisberger, T., Diederich, P., Kaiser, C.J.O. *et al.* Formation of vesicular structures from fatty acids formed under simulated volcanic hydrothermal conditions.** *Sci Rep* **13**, 15227 (2023). https://doi.org/10.1038/s41598-023-42552-w

- **Geisberger, T.; Diederich, P.; Steiner, T.; Eisenreich, W.; Schmitt-Kopplin, P.; Huber, C. Evolutionary Steps in the Analytics of Primordial Metabolic Evolution.** *Life* **9**, 50 (2019). https://doi.org/10.3390/life9020050

Other publications

The candidate was also involved in other projects, resulting in additional publications:

- **Pieczonka, S.A., Zarnkow, M., Diederich, P. *et al.* Archeochemistry reveals the first steps into modern industrial brewing.** *Sci Rep* **12**, 9251 (2022). https://doi.org/10.1038/s41598-022-12943-6

- **Michelle T. Berger, Daniel Hemmler, Philippe Diederich, Michael Rychlik, James W. Marshall, and Philippe Schmitt-Kopplin*. Open Search of Peptide Glycation Products from Tandem Mass Spectra**. *Analytical Chemistry* **94** *(15), 5953-5961(2022). https://doi.org/10.1021/acs.analchem.2c00388*

- **Harlacher E, Schulte C, Vondenhoff S, Schmitt-Kopplin P, Diederich P, Hemmers C, Moellmann J, Wollenhaupt J, Veltrop R, Biessen E, Lehrke M, Peters B, Schlieper G, Kuppe C, Floege J, Jankowski V, Marx N, Jankowski J and Noels H. Increased levels of a mycophenolic acid metabolite in patients with kidney failure negatively affect cardiomyocyte health.** *Front. Cardiovasc. Med.* 11:1346475. doi: 10.3389/fcvm.2024.1346475

Abbreviations

A	Adenine
APCI	Atmospheric pressure chemical ionization
APPI	Atmospheric pressure photoionization
C	Cytosine
CaO	Calcium oxide
CO	Carbon monoxide
COT	Cyclooctatetraene
DI-MS	Direct-infusion mass spectrometry
DNA	Deoxyribonucleic acid
ESI	Electrospray ionization
Fe	Iron
FID	Free induction decay
FT-ICR-MS	Fourier-transform ion cyclotron resonance mass spectrometry
G	Guanine
HCN	Hydrogen cyanide
kJ	Kilo Joule
LC	Liquid chromatography
MS	Mass spectrometry
Ni	Nickel
NMR	Nuclear magnetic resonance
OA	Oxalic acid
r(TCA)	Reversed tricarboxylic acid cycle
RNA	Ribonucleic acid
T	Thymine
TCA	Tricarboxylic acid cycle
ToF	Time of flight
U	Uracil
UHR-MS	Ultrahigh-resolution mass spectrometry
UV	Ultra-violet

Table of content

1. Introduction

1.1 The Origin of Life

The origin of life is an unanswered question humankind has been trying to solve since the earliest stages of its existence. The quest for an answer led to many hypotheses resulting in diverse philosophical and religious worldviews. With the emergence of the scientific method also came the wish to investigate routes leading to life in agreement with the laws of natural science(1, 2). To investigate the origin of life scientifically, however, it is necessary to define what the "origin of life" means. This question can be approached differently, and researchers followed different routes.

Even though the most direct interpretation of the question suggests that the goal is to find out how life emerged on Earth, this is commonly seen as the most unlikely question to be answered(3). Therefore, the question is often understood as how life could have emerged on Earth(4). Scientists try to discover one way that leads to a living organism without proving that this is the real way. An even broader view on the topic tries to answer how life can appear anywhere without any constraints on location or resources(5).

Synthetic biology is an approach that aims at engineering an organism without any restrictions on materials or complexity. Specifically, synthetic biologists do not refrain from interfering with the process at any given time(6). This human interference strongly contrasts the prebiotic approach, as the word prebiotic already suggests. If we stay on the other extreme of the spectrum, any interference from outside is forbidden. An optimal experiment for this line of thinking would be a closed system with all the necessary ingredients resulting in a living cell simply by waiting long enough - an experiment mimicking the emergence of life on a prebiotic planet.

A second question that must be considered is the general definition of life and, therefore, at what stage a reaction product of small molecules is considered alive. What conditions must this product fulfill to be the goal of chemical evolution?

NASA defines life as follows:

> "A self-sustaining chemical system capable of Darwinian evolution."

This definition contains two key requirements. The system must be self-sustaining. This condition emphasizes that external interference is not permitted. The system must "live" independently without external energy input or other resources from a higher entity. A second aspect is adaptability, represented by the term Darwinian evolution(7). The chemical system has to be able to alter itself and adapt to changing environments. This change is performed through imperfect replication of the system. This evolution also contains the characteristic of inheritance. The system inherits a specific amount of information to its replicate. The quality of this inherited information relative to its environment results in its overall fitness in the actual environment(8).

1.2 The Chemical Origin of Life

Prebiotic chemistry aims to synthesize molecules that are directly relevant to extant living organisms or compounds that could have been metabolic intermediates leading to those relevant molecules(9). Prebiotic chemists start at the boundary between inorganic and organic chemistry(10). Transforming inorganic molecules like water, nitrogen, and inorganic carbon species into organic molecules is the most fundamental step to establishing a chemical system that can be considered life(11). This concept often adheres to a more rigid interpretation of "how life could emerge on earth". Therefore, organic biological building blocks are synthesized in conditions and with reactants that are plausible for early Earth(12). The plausibility of reactants and conditions is an ever-evolving topic, and new knowledge from geology, astronomy, and computer modeling continuously alters the most popular opinions on acceptable experimental parameters(13). These parameters are defined not only by the expected conditions on early Earth at a specific time but also by the specific environment on early Earth at a specific time. Prebiotic chemists simulate many environments in the lab, ranging from extreme to extreme. While some scientists investigate the response of reactants to drastic temperature changes in freeze-thaw experiments(14), other scientists utilize the energy provided by volcanic lightning(15) or hot sulfur ponds(16).

- The **top-down approach** looks at life today and tries to break it into its basic molecular units following a retro-synthetic concept(17).
- The second approach, encompassing the chemical origin of life, starts with supposedly prebiotically plausible elemental units and describes the result of their interaction to converge to the most promising pathway leading to a product considered life(18). This approach is commonly called the **bottom-up approach** and is followed in this work.

1.3 The Building Blocks of Life

The bottom-up approach requires products that can be converted; therefore, defining which building blocks are required or relevant for the origin of life is important. Here, scientists look at the most basic units known to modern biology(19). Sugars, fatty acids, nucleobases, and amino acids are considered the essential building blocks of modern organisms and were chosen as targets for prebiotic synthesis. Synthetic chemists quickly synthesized those relevant compounds with varying degrees of prebiotic probability(20).

1.3.1 Sugars

The origin of sugars is largely seen in formaldehyde, the most primitive aldehyde. This aldehyde is frequently observed in the interstellar medium and was also produced in early Earth experimental simulations(21). Experimental proof for the synthesis of sugars from formaldehyde emerged as early as 1861 when Butlerov(22) discovered the formation of a complex mixture of sugars from an alkaline aqueous formaldehyde solution. However, this synthesis pathway proved insufficient. The mixture quickly turned into a tar-like water-insoluble mass(23). It only yielded low amounts of ribose, the sugar necessary for nucleoside synthesis and an essential component of the genetic material we know today. Another problem is the instability of relevant sugars, specifically ribose, in aqueous solution. Ribose was found to have a half-life of 73 minutes in neutral (pH 7) water at 100°C(24). The addition of borate ions, however, an element found in the upper continental crust, interacts with glyceraldehyde (the first condensation product of formaldehyde) and leads to a more selective synthesis of

ribose. In addition to this increased selectivity, borate stabilizes ribose and prevents the mixture from turning into its tar-like state(25). Alternatively, scientists also proposed ribose-independent precursors of nucleosides like peptide nucleic acids, which would partially circumvent the need for a prebiotically plausible way of sugar synthesis(26).

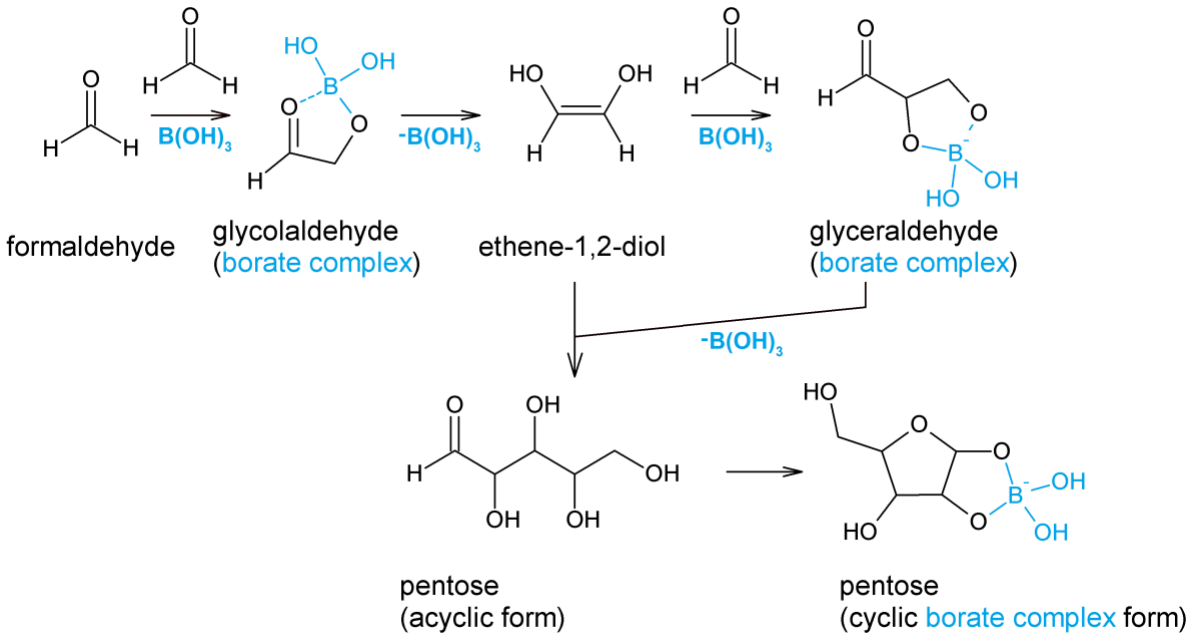

Figure 1: Formose reaction starting from formaldehyde. Modified with borate (in blue) to selectively yield pentose, as Benner et al. (2012) described.

1.3.2 DNA building blocks

The molecules that make up our DNA are another category of necessary building blocks for life as we know it today. These nucleotide building blocks are synthesized by combining nucleobases and ribose(27), the sugar resulting from the selective borate-catalyzed synthesis from formaldehyde. Nucleobases are next to sugars, the second critical part of the genetic material of extant organisms. The educts, catalysts, and conditions for their abiotic formation are more diverse, and multiple plausible routes have been proposed over the years(27, 28). Nucleobases exist in five different forms in our DNA and RNA: Adenine (A), guanine (G), cytosine (C), thymine (T), and uracil (U) are found in both DNA and RNA, whereas T is exclusive for DNA and is replaced by U in RNA. The nucleobases can be further divided into two different

chemical classes. Adenine and guanine belong to the class of purines; cytosine, thymine, and uracil are pyrimidines. Adenine was the first nucleotide to be synthesized under prebiotic conditions. Oro observed the formation of adenine in 1960 after heating ammonium cyanide for multiple days at temperatures around 100°C(29). This synthesis showed, however, the problem of over-polymerization and tar formation(30). Adenine was only discovered after removing the tar and adding hydrochloric acid to the residual solution(31). Different research groups analyzed this polymerization more thoroughly, and the exact mechanism was elucidated(32). The research invested into this reaction yielded more than just adenine. Guanine was discovered later in the same experimental setup at low concentrations(32). The synthesis of nucleobases of the pyrimidine class wasn't achieved by mere polymerization of cyanide. Pyrimidines require more ingredients. One successful attempt at synthesizing cytosine resulted in reacting cyanoacetylene with cyanide(33). Condensation of those two molecules leads to the desired nucleobase. However, a major drawback of cyanoacetylene is its reduced water stability(34, 35). In alkaline water, cyanoacetylene hydrolyses quickly into cyanoacetaldehyde. Luckily, this hydrolysis is not a problem, as cyanoacetaldehyde reacts with urea or guanidine to form cytosine and uracil(36). Here, the reaction with guanidine is much more efficient and succeeds even at very low concentrations (5mM).

Nucleobases can also be formed via a completely different route. Formamide, in conjunction with mineral catalysts, reacts to purines and pyrimidines if heated to temperatures over the boiling point of water(37, 38). An advantage of formamide over the otherwise used hydrogen cyanide is its boiling point. With a boiling point above 200°C, formamide can be concentrated in ponds or lagoons if water evaporates, an effect that is impossible for hydrogen cyanide with its low boiling point if the pH of the water is below the pKa of 9.2 of HCN(9). However, the concentration of HCN isn't unthinkable, as freezing of aqueous HCN solutions leads to an extreme concentration of HCN at -21°C(39).

Nucleobases all share a common problem. Nucleobases have limited stability in neutral water at elevated temperatures. Cytosine is the most unstable, with a half-life of only 19 days. All other nucleobases show half-lives of 1 to 56 years(40). Therefore, the accumulation of nucleobases in the ocean at a pace higher than their degradation

is seen with much doubt(33, 41). Only specialized reducing environments with high concentrations of HCN can be seen as potential candidates for nucleobase synthesis.

Meteorites are a completely different source of nucleobases. A variety of purines and pyrimidines was discovered, especially in carbonaceous chondrites. The concentrations rarely reach more than 500 ppb. Therefore, meteorites are only proof of the feasibility of abiotic purine and pyrimidine formation and are unlikely to be the main source of nucleobases for the origin of life on Earth(42, 43).

After synthesizing nucleobases, their reaction with ribose must be considered to form nucleotides. The final biological macromolecule formed by nucleotides is DNA. DNA is first transcribed to RNA,

1.3.3 Amino acids

RNA encodes proteins made of amino acids. This fact requires the prebiotic chemist to find ways to provide those amino acids in an origin-of-life context. Amino acids were discovered during the famous experiment by Miller and Urey in 1953(44). These pioneers built a setup that mimicked the composition of an early Earth atmosphere or what was accepted as prebiotically plausible at that time. The setup contained water, hydrogen, ammonia, and methane. Those reactants were then reacted with each other via electrical discharge. Later, however, the scientific community heavily criticized those conditions as unlikely. Nonetheless, Miller and Urey produced four of the twenty proteinogenic amino acids with this simple setup. They hypothesized the Strecker reaction to be the chemical pathway leading to those amino acids. The Strecker reaction requires aldehydes, hydrogen cyanide, and ammonia(45). This pathway became one of the most popular pathways for chemists in this field to produce amino acids(46).

α,β-unsaturated aldehydes belong to another important subgroup of aldehydes. Acrolein, combined with methanethiol or hydrogen cyanide, yields methionine or glutamine(47). Erythrose, an aldose, reacts to histidine if formamidine is added and water can be removed(48). Aldehydes are, however, not the only path to amino acids. Cyanoacetylene was also used as a reagent with ammonia and hydrogen cyanide to form asparagine(49). A further compound containing an ethinyl group, namely

phenylacetylene, was reacted into phenylalanine and tyrosine(50). Aminoacetonitrile yields valine and isoleucine if combined with the ketones acetone (for valine) and methyl ethyl ketone (for isoleucine)(51).

α-hydroxy acids are interesting side products of amino acid synthesis(52). Those molecules can be produced via the Strecker reaction under the same conditions as amino acids, with the pH determining the ratio between the two compound classes(45). Alkaline pH favors amino acid production, whereas acidic pH favors α-hydroxy acid production. Moving from an alkaline amino acid-producing system to an acidic α-hydroxy acid-producing system would be an interesting event, as α-hydroxy acids were shown to enhance peptide bond formation between amino acids during dry-down experiments(53).

Abiotic synthesis of amino acids was heavily investigated in hydrothermal vent systems. This environment presents perfect starting conditions for the Strecker reaction in the presence of elevated concentrations of formaldehyde, hydrogen cyanide, and ammonia(54).

1.3.4 Fatty acids

The strongest argument against Oparin's prebiotic soup theory, proposed as early as 1924, is the problem of diffusion and concentration(55). If the primitive ocean on early Earth is seen as a reaction vessel, then the production of biomolecules is very unlikely to have been sufficient to reach critical concentrations. Living beings and individual cellular entities are also physically constrained and have a barrier to the outside. This barrier provides the ability to concentrate biomolecules inside an organism or cell. The smallest organisms comprise a single cell, which possesses a barrier in the form of a lipidic membrane. Membranes of modern cells are made of a lipid bilayer of glycerol phosphate phospholipids(56). However, these membranes are very rigid and lack the ability of growth, division, and ion permeability(57). Modern cells solve this problem with elaborate biochemical tools like ion channels inserted into the membrane. Primitive cells most certainly lacked these tools and needed to resort to membrane components that allowed for the division and uptake of nutrients. Fatty acids showed promising results in experiments that tried to achieve compartmentalization(58). Fatty acids found in carbonaceous chondrites formed vesicles in an alkaline aqueous

mixture(59). A terrestrial pathway to fatty acids is the Fischer-Tropsch synthesis(60). This reaction turns CO and H_2 gas into a mixture of saturated unbranched alkanes. Fatty acids and alcohols are side products of this reaction. A main drawback of this synthesis is the requirement of a gas phase. Experiments in the liquid phase mainly produce methane(61). This reaction is even enhanced in the presence of Ni/Fe minerals(62). Another route to fatty acids is the action of UV irradiation(63), shock heating(64), or electric discharge(65). Those experiments yielded fatty acids up to C_{12}-chains.

A more recent approach included acetylene as a reactant for fatty acid synthesis(66). Reppe pioneered this synthesis in 1953 when he reacted carbon monoxide with acetylene in the presence of water and a nickel catalyst to form highly unsaturated fatty acids in varying chain lengths(67). This reaction was reinterpreted in a prebiotic setting by Wächtershäuser in a setting more akin to hydrothermal vents. A carbon monoxide and acetylene atmosphere over water containing a nickel sulfide catalyst could form unsaturated fatty acids with a carbon number of up to 9 carbons. This reaction does not require a gas phase, and the presence of acetylene becomes a more and more discussed topic in the origin of life(68-70).

1.4 Acetylene chemistry

1.4.1 Acetylene as a feedstock molecule in the chemical industry

In the first half of the 20th century, acetylene became a crucial component of the chemical industry after introducing its hydration into acetaldehyde in 1916(71). Kutscheroff first discovered this process in 1881(72). He discovered that hydration occurs in an aqueous solution when a mercury catalyst is present(73).

Acetylene was replaced by ethylene and other olefins due to their numerous advantages, such as safer handling and lower price(74). In the early 20th century, with the shift from a coal to petroleum-based chemistry, ethylene became an affordable reagent for the chemical industry. The advent of crude oil opened a new route to small hydrocarbons and moved the focus of industrial chemists from acetylene to ethylene. Acetylene production was not financially viable due to high energy costs, leading to declined interest(75). Also, safety was a big factor. Ethylene and other slow-mass

olefins are much easier to handle than acetylene. Acetylene is highly explosive when in contact with oxygen. Ironically, this aspect of acetylene also maintains one dominant use of acetylene. Acetylene is the gas with the highest welding performance due to its maximum flame temperature of 3170°C(76). As the oil market becomes increasingly unpredictable, there are talks of bringing back acetylene as a feedstock molecule. Combining energy-intensive processes with renewable energy sources like wind and solar power is a smart solution. By utilizing the excess energy produced during peak times, we can avoid losing it due to inadequate storage methods. Indeed, the plant will be shut down during low energy availability(74).

- The calcium carbide process is a long-established route of producing acetylene from coal. In this process, calcium oxide (CaO, quicklime) is heated with coke (a product of coal pyrolysis) at around 2100°C in an electric arc furnace(77). This step also releases carbon monoxide, another relevant gas for the origin of life(78). The resulting calcium carbide can then be reacted with water to release the gaseous acetylene. This method produces pure acetylene.
- A second class of processes to produce acetylene is cracking. Cracking was introduced along with crude oil. Crude oil or fuel is injected into a reaction chamber and partially burned. The resulting heat of 1200°C then leads to thermal cracking. Cracked hydrocarbons release hydrogen and methyl radicals, which are then recombined and undergo chain reactions to produce a mixture of hydrocarbons, including acetylene(79).

Nevertheless, it should be remembered that acetylene is more reactive and often requires fewer process steps. The resulting higher overall selectivity(80) is essential for prebiotic reactions. Indeed, reactant concentrations are often low and efficient reactions are therefore preferred.

1.4.2 Reactivity of acetylene

Although producing acetylene is expensive due to its high formation enthalpy of 226 kJ/mol, this same property makes it highly reactive. Acetylene's high reactivity allows it to react with even the most unreactive compounds, such as water. Using catalysts can make reactions happen efficiently even at temperatures below room temperature(81).

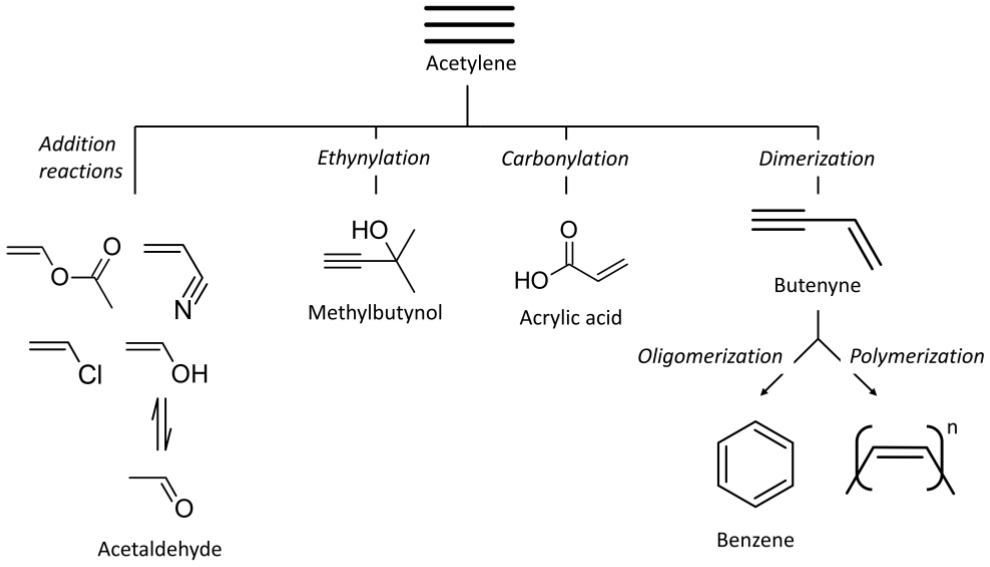

Figure 2: Reaction classes leading to industrially-used products derived from acetylene as a feedstock molecule.

The reactivity of acetylene greatly relies on the pH level of the reaction environment. Figure 2 illustrates that addition reactions are facilitated in acidic media, which was the preferred method for industrial-scale production of acetaldehyde through the hydration of acetylene(73). However, acidic media also has the drawback of causing polymerization, which then deactivates the catalyst used(74). Base-catalyzed reactions are more prevalent due to this inconvenience. Activation of acetylene via a base is easier than that of other hydrocarbons because its pKa is 25, making it more acidic than ethylene, which has a pKa of 44(82). This ease of deprotonation makes it a more efficient nucleophile and explains its potential for ethynylation reactions with carbonyl groups. Dimerization of acetylene under basic conditions, requiring a nucleophilic attack on acetylene by a second deprotonated acetylene (also called vinylation), also needs the presence of a metal catalyst to be efficient(83). Most prebiotic scenarios discussed by the scientific community today consider basic pH more probable for the origin of life(84, 85), which suits the pH-dependent reactivity of acetylene well.

Different forms of metal catalysts, including metal salts, dissolved ions, or metal complexes, dominate acetylene chemistry(86, 87). Such catalysts paved the way for more advanced chemical reactions like the carbonylation of acetylene via Reppe

chemistry(67). We previously noted that this is another significant pathway by which fatty acids can be produced under prebiotic conditions(66).

1.4.3 Carbonylation of acetylene via metal catalysis

As previously stated, acetylene production releases a significant quantity of carbon monoxide. In 1953, Walter Reppe utilized this fact to create highly unsaturated fatty acids by combining acetylene, carbon monoxide, and water in the presence of nickel carbonyl or nickel salts. The main product of this reaction is acrylic acid(67). This reaction mechanism is not limited to carbonylation only. The oxygen can be exchanged with sulfur or nitrogen in the respective reaction medium to form thio-acids or amides and their respective esters, depending on the reactant used.

The production of acrylic acid on an industrial scale relied on this technique as the primary method until it was replaced by propylene oxidation in the 1960s(77).

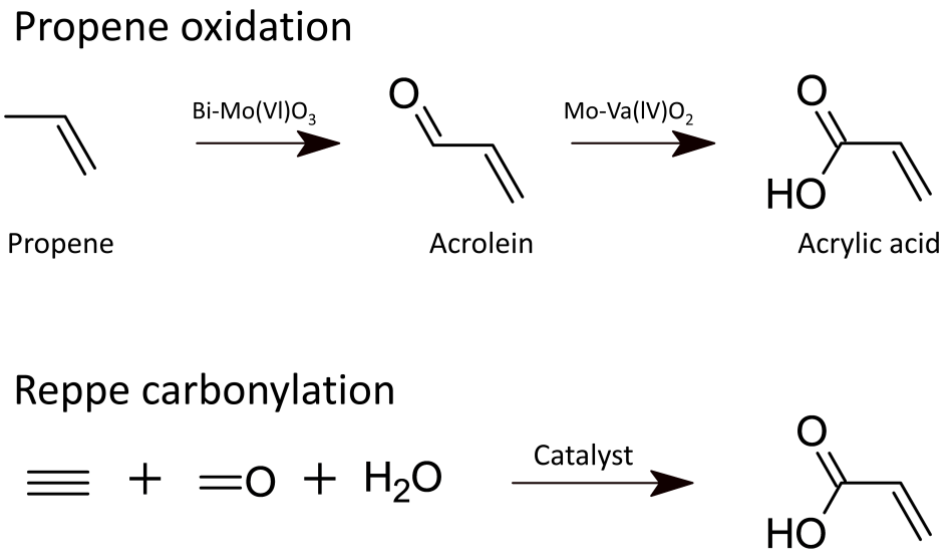

Figure 3: Transition metal-catalyzed synthesis routes to acrylic acid, the main product of acetylene and carbon monoxide under nickel sulfide-catalyzed prebiotic conditions.

1.4.4 Oligomerization and polymerization of acetylene: Forming new linear carbon bonds

Dimerization is the first step of oligomerization. The process of acetylene dimerization is closely linked to transition metals, indicating the natural affinity of acetylene for

metals and metal salts(83). When it comes to dimerization, the Nieuwland catalyst is utilized. This catalytic system consists of a copper chloride salt and either ammonium or potassium chloride(88). Here, the choice of the alkaline ion is important, as the reaction efficiency decreases if other counter ions are used. This type of chemistry was mainly used to industrially produce rubber polymers. It involved converting vinylacetylene, produced through acetylene dimerization, into chloroprene by adding hydrochloric acid to the dimerization product(89). However, in the 1960s, a more profitable process was introduced using butadiene as the starting material, replacing the previous method(90). The Nieuwland process has an interesting aspect that is useful for prebiotic chemistry. This catalytic system is one of the rare catalysts that can oligomerize acetylene in a linear way without the formation of cyclic species like benzene. Considering acetylene as a fundamental component in producing long-chain fatty acids is crucial. Biologically relevant fatty acids are linear and do not contain cycles. Studies on the production of fatty acids from acetylene using nickel sulfide salts have detected linear fatty acids(66). However, whether this catalytic system operates similarly to the Nieuwland system remains uncertain.

Notably, nickel catalysts are preferred for cyclization, which contradicts the hypothesis. Although the synthesis of benzene from acetylene has never been utilized industrially and has no significance in prebiotic chemistry, it is worth noting that it is a potential side reaction that commonly occurs. Similar statements can be made about its tetramer counterpart, cyclooctatetraene, commonly abbreviated COT.

1.4.5 Pyridine synthesis

Another class of compounds that are relevant to prebiotic scientists is nitrogen-containing heterocycles. Acetylene was considered to be used for pyridine synthesis on an industrial scale based on its effectiveness, but less expensive options have once again taken over this role. Acetylene is a very efficient reactant for pyridine synthesis and hydrogen cyanide or other nitriles(91). Hydrogen cyanide is a commonly used reactant in creating basic building blocks required for life(92, 93). The main use of hydrogen cyanide was the formation of nucleobases for DNA synthesis. It is intriguing to note that DNA is stabilized under acidic pH conditions through pyridine, as discovered by Portella in 2015(94). Pyridines do not naturally occur in extant

organisms. Their formation from acetylene can provide insights into how nitrogen can be introduced into larger cyclic oligomers formed from acetylene.

1.5 Acetylene in the universe

We must consider the potential presence of acetylene to investigate whether acetylene played a role in early metabolism or life processes. Acetylene is a rare gas in our atmosphere, at concentrations of 0.04 ppb(95). According to current knowledge, the conditions on early Earth likely differed from today's atmosphere(96). Acetylene in the atmosphere is the result of methane photolysis(97). Thus, it is consistently found in the atmosphere of planetary bodies that contain methane, and primitive Earth was such a planet. According to the hypothesis that the early Earth had a reducing atmosphere, it is conceivable that acetylene concentrations were higher than 5 ppm, as stated by Trainer et al. in 2004(98).

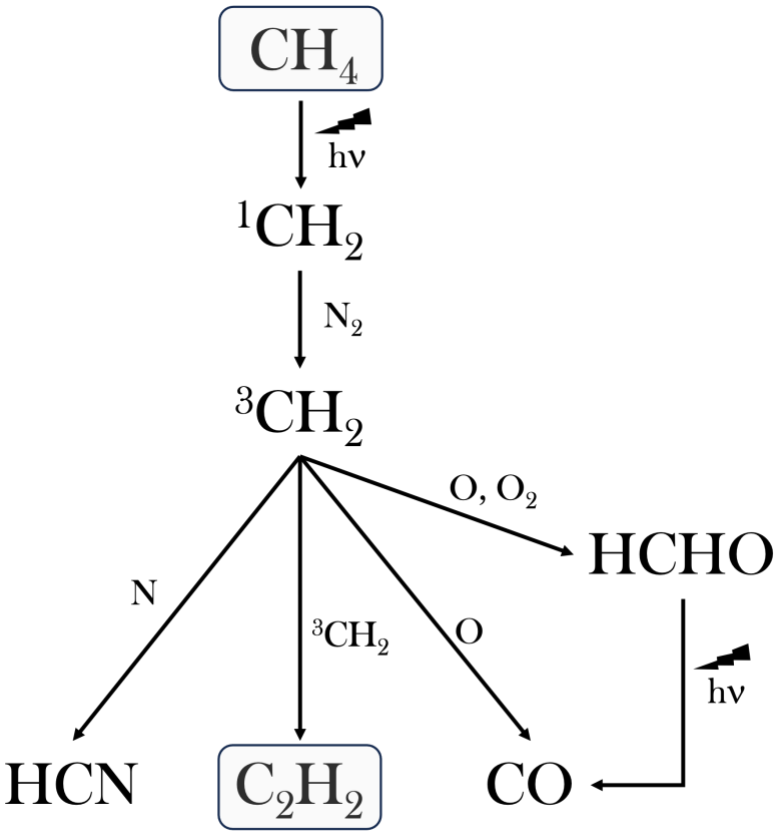

Figure 4: Hypothesized pathway from methane to acetylene catalyzed by irradiation of methane in the upper atmosphere of a primordial earth.

The potential role of acetylene in the origin of life is reinforced by its existence in the atmosphere of Jovian planets. The Jovian planets are called "giant planets" and consist of Saturn, Jupiter, Neptune, and Uranus. The amount of acetylene in the atmospheres of those planets reaches amounts of 4 ppm for Jupiter(99, 100), followed by 0.3 ppm for Saturn(101). Neptune(102) and Uranus(103) only show negligible amounts. Acetylene plays a crucial role in the formation of tholins in the atmosphere of certain planets like Titan. Tholins are large molecules with a high molecular weight of 8000 Dalton. They are responsible for giving Jupiter its distinct red color(104). Tholins have an interesting connection to the origin of life as they can serve as the only source of nutrition for various types of aerobic and anaerobic bacteria, as noted by Stoker(105). Scientists have proposed a process for tholin formation in the atmosphere of Titan, a fascinating moon of Saturn that contains 2-3.5 ppm of acetylene(104). Titan is a celestial object that has captured the attention of many due to its unique and distinct features. One of the most remarkable aspects of this moon is its atmosphere, which sets it apart from other moons that revolve around giant planets. Unlike its counterparts, Titan's atmosphere is not predominantly composed of hydrogen. This observation presents a fascinating opportunity to discover more about the composition and formation of celestial bodies. The atmosphere of Titan consists mainly of nitrogen gas(106) and is often seen as a "frozen" version of primitive Earth. Tholin formation on Titan is initiated by the irradiation of methane and nitrogen, which leads to acetylene, acetylene oligomers, hydrogen cyanide, and numerous radical species derived from those molecular entities. These compounds subsequently polymerize and recombine to form higher mass complex organic molecules and are further processed into large negatively charged mixed species broadly called tholins(104).

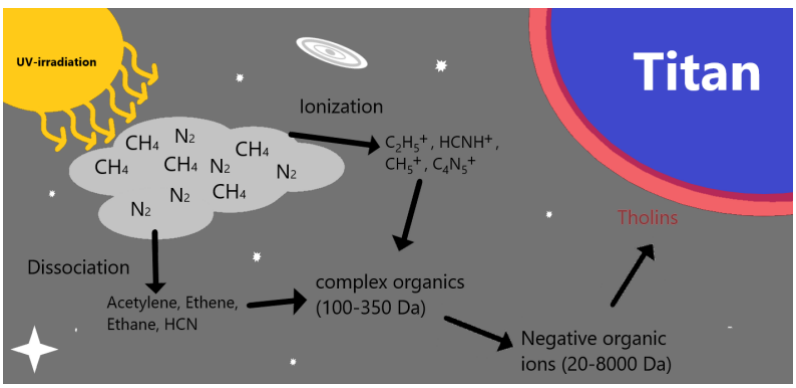

Figure 5: Formation of tholins in the atmosphere of Titan as proposed by Waite et al. (2007)(104).

Acetylene was a significant discovery during the Cassini-Huygens mission. This discovery provides valuable insights into the planet's chemical composition and highlights the potential for further exploration in the future.

While passing Enceladus, one of Saturn's moons, a cryovolcanic eruption occurred, causing a plume of water to shoot up into the atmosphere from the moon's lower layers. This plume contained significant amounts of methane and CO_2, along with acetylene and propane(107). It is unclear whether the detected acetylene originated from the moon or was created in the atmosphere by the irradiation of methane in the plume. However, this discovery validated that detectable amounts of acetylene likely exist on numerous planetary bodies throughout the universe.

Acetylene is among the numerous light organic compounds observed in cometary tails. The existence of acetylene in cometary material is significant because it is believed to have played a role in the creation of protoplanetary disks. Disk-like structures can be observed around young stars, made of gaseous and solid materials, and serve as the foundation for planet formation(108). During the initial stages of planetary formation, acetylene can be detected within these disks(109). The direct consequences of the presence of acetylene and the resulting diversity of organic compounds in those disks remain elusive and need further investigation.

1.6 Origins of enzymatic activity

Enzymes are an indispensable part of extant metabolisms(110). Enzymes in the present day comprise several protein subunits, which form a complex and weighty molecular structure. It is highly improbable that such a structure could have formed by mere chance. Electron-transfer enzymes, or oxidoreductases, are vital in the metabolic process(111). These enzymes facilitate the transfer of electrons from one molecule to another, essential for various metabolic reactions. In other words, oxidoreductases are crucial components that enable the body to produce and utilize energy efficiently. Most enzymes belonging to this class contain transition metals in their active centers(112). Iron is the prevalent active center among transition metals in this class, accounting for approximately 60%. Iron is predominantly present in the form of iron-sulfur clusters or heme, organic compounds containing iron essential for various metabolic processes in the body. Heme molecular components are used

across the Tree of Life to transfer single electrons without undergoing protonation. Heme-containing molecules such as cytochromes are often interspersed between electron carriers such as quinones that undergo protonation. The process exhibits a hopscotch-like pattern wherein protons are conveyed by a carrier and freed into a confined space while electrons are transported through the membrane to an oxidant. (i.e., the Q cycle)(113). One of the oldest pathways being considered is the Wood-Ljungdahl(114) or reductive acetyl-CoA pathway(115). This pathway relies heavily on the activity of the carbon monoxide dehydrogenase/acetyl CoA synthase enzyme. This nickel-containing enzyme shares a significant resemblance to the metal sulfide minerals believed to exist on early Earth.

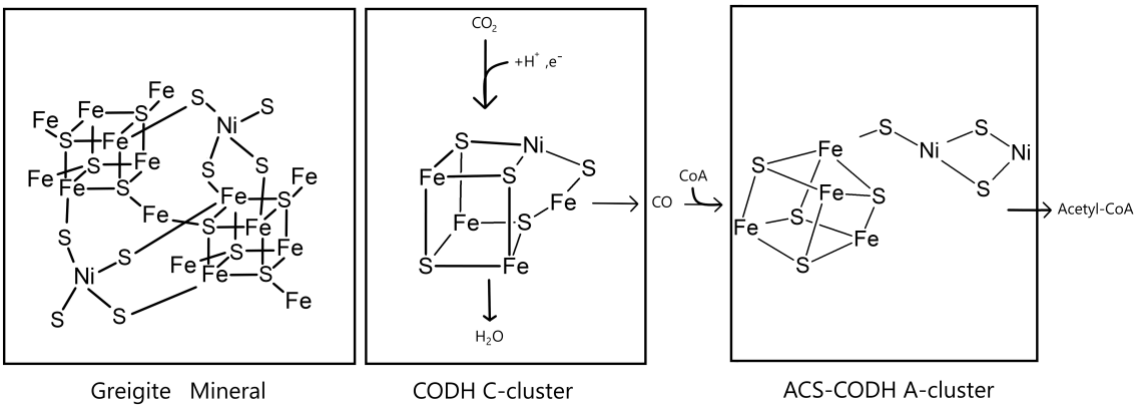

Figure 6: The structure of a halve cell of the iron-nickel mineral greigite and the active centers of ACS-CODH showing high structural and chemical similarities with the mineral.

A central component of this pathway is acetyl-CoA. This thioester is energy-rich and acts as an energy transporter. De Duve proposed the concept of the thioester world as a potential basis for life that does not require ATP(19). Thioesters have various uses beyond energy transfer. Fatty acid biosynthesis requires acetyl-CoA as an essential building block. Experiments by Huber and Wächtershäuser already demonstrated the formation of methyl thioesters if carbon monoxide is incubated in an oxygen-free system over water containing (Fe,Ni)sulfide and methyl mercaptan(116). Acetylene hydratase is an enzyme believed to have appeared very early(117) and uses an iron sulfide cluster. Acetylene hydratase requires one additional transition metal, namely tungsten. Tungsten is bound by two pterin units, forming a molybdopterin co-factor. Molybdopterin cofactors appear in multiple enzyme classes with either molybdopterin or tungsten as transition metals. There are several enzymes that contain molybdopterin, including carbon monoxide dehydrogenases, aldehyde oxidases, sulfite oxidases, and glyceraldehyde-3-phosphate ferredoxin

oxidoreductase. These enzymes have been previously discussed. It is imperative to note that the CODH species featuring a molybdopterin co-factor solely coexists with copper in anaerobic bacteria. Furthermore, these enzymes only facilitate carbon monoxide oxidation into carbon dioxide. In contrast to the previously mentioned nickel-containing CODH, which is only present in anaerobic bacteria, this enzyme also catalyzes the reverse reaction from carbon dioxide to highly reactive carbon monoxide. Acetylene hydratase is an interesting enzyme produced by *Pelobacter acetylenicus*(118). This enzyme catalyzes the hydration of acetylene to acetaldehyde used to form acetyl-CoA.

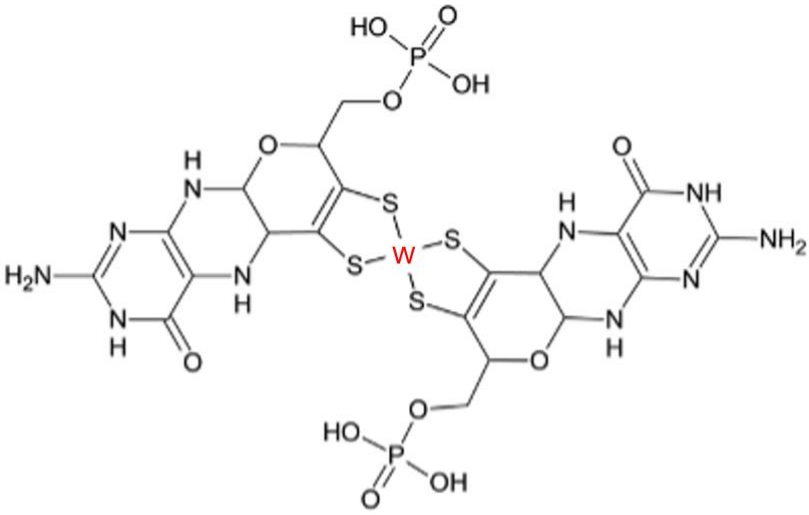

Molybdopterin cofactor as found in acetylene hydratase in *Pelobactor acetylenicus*

Figure 7: Structure of the molybdopterin cofactor found in acetylene hydratase in Pelobacter acetylenicus. The transition metal tungsten is highlighted in red.

Pyrococcus furiosus is a type of extremophile that belongs to the Archaea domain and is known for its ability to develop in extreme conditions. Specifically, this organism is often found in close proximity to hydrothermal vent formations on the ocean floor, where temperatures can reach up to 100°C. *Pyrococcus furiosus* has adapted to its environment and can carry out vital biological functions despite these harsh conditions. This species expresses an enzyme using acetaldehyde as a substrate. Acetaldehyde is turned into acetic acid via a molybdopterin cofactor(119). The recurring patterns, particularly using pterin-bound transition metals in enzyme co-factors, are fascinating. Further investigations are required to ascertain the probable roots of this pattern, as its origins are not as evident as those for NiCODH.

2. Methods

The complexity of the question surrounding the origin of life remains unresolved, particularly regarding the extent of chemical diversification required for its occurrence. Analyzing complex matrices is essential in the origin of life research field, but it can be challenging for analytical chemists. Many analytical techniques are available; each has its unique strengths. We will focus on two techniques that have shown a broad range of applications and are specifically useful for analyzing complex samples(120, 121). We will explain each technique and discuss its strengths and weaknesses. We will also highlight any biases and pitfalls associated with these techniques.

2.1 Nuclear magnetic resonance

The revolutionary technique of nuclear magnetic resonance, commonly abbreviated as NMR, was pioneered in the early 1950s. This novel methodology enables the detection of currents in a coil produced by the motion of nuclei within the coil. The motion frequency of the nuclei is closely connected to the chemical environment surrounding them(122). NMR facilitates the identification of molecules through the frequency spectrum detected. Initially, chemists used NMR to elucidate the molecular structure and concentration of compounds without requiring a reference standard. This focus changes to metabolomics(123, 124) and other untargeted applications(125, 126).

2.1.1 Physical principles

The basis of NMR spectroscopy is the detection of a current in a detection coil induced by the precession of nuclear spins in a homogenous magnetic field(127). Every nucleus has a spin associated with it. Spin is an intrinsic characteristic of a nucleus, like its mass or charge. The spins of nuclei vary depending on the isotope and can be whole integers, e.g., 0, 1, 5, or half integers, e.g., $^{1}/_{2}$, $^{3}/_{2}$, $^{5}/_{2}$. A spin other than 0 is required to receive a detectable NMR signal. In NMR spectroscopy, the proton (^{1}H) is

the most notable nucleus. ^{1}H has a spin of $^{1}/_{2}$ and an isotopic abundance of 99.985% for Hydrogen. The high sensitivity of this nucleus makes it ideal for NMR. As most organic molecules carry at least one hydrogen atom, NMR is well suited to study the evolution, transformation, and diversity of complex organic mixtures, including prebiotic setups. Hydrogen is a highly significant element to measure. Indeed, the field strength of NMR spectrometers is described by the resonance frequency of hydrogen at the specific field strength of the spectrometer instead of the actual field strength. This resonance frequency is called Lamor frequency. It is defined by the following equation:

$$\omega^0 = -\gamma B^0$$

The Lamor frequency ω^0 results from the negative product of the isotope-specific gyromagnetic ratio γ and the magnetic field B^0 (T). To produce a signal, the sample needs to be irradiated with this field-specific frequency to achieve excitation of the nuclei. Every isotope resonates at a different Lamor frequency, allowing for the selective excitation and detection of a single kind of isotope. This ability is especially useful for origin of life researchers, as different problems can be specifically addressed. If phosphorous is of interest, this nucleus can be detected alone, without interference from other elements contained in the system. Pasek successfully executed this method and analyzed different oxidation states of phosphates in a prebiotic setup(128). In another prebiotic experiment, NMR was used to measure the hetero atom in transforming apatite into fulgurite. The author conducted a stimulated lightning discharge experiment, which provided important insights into the fluor and phosphate chemical environment changes during the process(129).

When measuring NMR spectra, we need to consider two additional features of nuclei: chemical shift and relaxation.

- The chemical shift is the main information that can be gained from NMR measurements for most applications. The Lamor frequency only represents a theoretical resonance frequency for a specific isotope without considering its chemical environment. The chemical environment of an isotope shifts its resonance frequency away from the theoretical Lamor frequency. The absolute value of this chemical shift is expressed in Hz and is field strength-dependent. Therefore, the chemical shift in Hz

is not comparable between instruments of different field strengths. Normalization of this shift into a ppm scale solves this problem and is the generally accepted way of reporting NMR spectra. The ppm range of nuclei of the same isotope can vary significantly based on their chemical environment. For ^{1}H, a range between 0 to 11 ppm is observed for most samples. Exotic nuclei can become negative or present exceptional chemical shifts higher than 11. ^{13}C, on the other hand, shows shifts from 0 (carbon covalently bound to silicon) to 215 (ketones) or even 230 (thiocarbonyls). Other nuclei, like nitrogen, show ranges of a thousand ppm.

Chemical shifts identify functional groups of a purified compound or a mixture. Empirical data allowed us to attribute specific functional groups to chemical shifts since the earliest stages of NMR spectroscopy. Electron withdrawing groups increase the difference between the Lamor frequency and the observed resonance frequency, leading to higher ppm. It is currently only possible to calculate the exact chemical shifts for all isotopes to a limited extent. Especially hydrogen shifts can vary significantly from predicted values due to their extreme sensitivity to pH differences and intermolecular interactions. The knowledge about hydrogen shifts lets NMR-spectroscopists have an unbiased view of different hydrogen atoms in complex mixtures. The method accurately detects the primary functional groups present in a mixture. The previously unknown presence of carboxyl-rich alicyclic molecules was discovered in marine dissolved organic matter, a highly complex mixture of organic molecules(130).

- Another important factor to consider is relaxation. In NMR spectroscopy, we differentiate between two types of relaxation, spin-lattice relaxation (T1) and spin-spin relaxation (T2):

- **Spin-spin relaxation, or T2**, is the duration during which a signal can be detected. After irradiation of the sample, isotopes will start precession, generating a signal corresponding to a current in the detection coil. This precession is limited in time and will eventually cease due to the imperfection of the magnetic field. As of today, it is still impossible to create a completely homogenous magnetic field. Such minor imperfections lead to areas in the sample with a different apparent B^{0}, resulting in slightly different precession frequencies for the same nucleus in different areas of the measurement tube. This desynchronization or coherence decay of the

detected precession leads to a faster signal decay and broadening. The absence of field homogeneity is not the only factor influencing the coherence decay. In addition, every nucleus possesses an intrinsic spin-spin relaxation. This intrinsic relaxation is positively correlated with the size of the molecule. Macromolecules possess an intrinsically high coherence decay rate, so achieving the same peak widths for proteins as for small metabolites is impossible. Dissolved paramagnetic transition metal ions like nickel or iron represent another factor modulating the relaxation T2 time. Most routine analyses do not need to consider this factor, which has become important for complex samples mimicking prebiotic environments(131, 132). Indeed, metal ions interact with functional groups and lower the T2 time of all nuclei in their proximity already at low concentrations. In a controlled manner, this effect can identify nuclei in molecules that interact with metals. In an uncontrolled manner and at higher concentrations, such metals can degrade the spectral quality to such a degree that it hinders analysis. In such situations, additional sample preparation steps must be considered to remove interfering ions, for example, by precipitation of the paramagnetic element or by solid phase extraction methods.

- **Spin-lattice relaxation, or T1**, refers to the duration required for a nucleus to regain its capacity to generate a signal. The NMR signal is produced through the polarization of spins aligned with the magnetic field. When the sample is irradiated, the polarized magnetization changes direction to become perpendicular to the magnetic field. This leads to the precession. The flipped spins must re-align themselves (at least partially) with the magnetic field to re-generate a signal. The signal strength is related to the degree of the relaxation of nuclei after excitation. No magnetization occurs in the orthogonal plane when spins are fully aligned with the magnetic field. If NMR is used for quantification, T1 time requires special attention. As already mentioned, the intensity of a signal refers to the level of relaxation that a nucleus can attain between excitations. As a result, the area under the curve of a signal, used to quantify compounds, is also directly linked to T1. We will discuss the topic of quantification in more detail later.

2.1.2 Technical aspects of the NMR spectrometer

An NMR instrument or spectrometer has two primary components: the superconducting cryo-magnet and the probehead. The magnet consists of a metal alloy solenoid submerged in liquid helium. Those metal alloys, commonly made of niobium (Nb) and tin (Sn), manifest their superconducting nature at extremely low temperatures. A bath of liquid helium (4 K) is required to maintain the superconductivity of the magnet. The magnet runs nearly indefinitely after its initial charging with the current. It maintains a magnetic field with very low levels of fluctuations, which is necessary for exact and high-resolution measurements. The helium reservoir is placed in a liquid nitrogen reservoir (77 K) as helium is very volatile and would evaporate at room temperature. Even with the surrounding vacuum chambers, the two reservoirs gradually lose their cryogenic fluids and require regular refilling despite the countermeasures integrated into the instrument. How often the magnet needs to be refilled depends on its size and whether re-liquefiers are installed to capture and re-liquify evaporating gases onsite. If the magnets are not refilled properly because of carelessness or issues with delivering cryogenic liquid (as helium is becoming increasingly scarce), it can result in a phenomenon known as "quenching" of the magnet. If the helium level falls below a certain point, the solenoid will no longer remain superconductive and will start to resist the electrical current. This happens when the temperature around the solenoid rises above 4 K. If it encounters resistance, it can lead to intense heating and boiling of the liquid helium. Consequently, a significant quantity of helium gas is released into the room, presenting a significant risk of suffocation. In some cases, quenching also causes damage to the instrument, which may result in the loss of the entire instrument.

The probehead is the detector of the NMR spectrometer. The probehead contains a detection coil that can transmit and receive radiofrequency irradiation. The irradiation of the sample and detection of the emitted signal are central to the nuclear magnetic resonance technique and will be discussed in more detail later. The probehead is an exchangeable part of the spectrometer, with various specialized probeheads.

The main differences between the probeheads can be classified into spatial differences and transmission frequency differences.

- Probeheads differ spatially as they can fit different sample diameters. The wider the sample diameter, the more volume is in the detection area of the probehead, which increases signal strength. This is very advantageous if large quantities of samples are available, as one of the biggest problems for spectroscopists is the lack of sufficient sensitivity to maintain reasonable analysis times. On the other hand, smaller tubes are required if samples are limited to < 200 µl. Probeheads with a larger diameter (5–10 mm) can also measure tubes with a smaller diameter. Nevertheless, If the detection coil is positioned farther from the sample, the signal strength diminishes, leading to signal loss. An additional advantage of small diameters is the higher resolution that can be achieved. Creating a homogeneous magnetic field is easier when applied to a small area compared to a larger one. This approach translates into narrower peaks and, therefore, higher resolution.
- The probehead's ability to generate and detect specific frequencies is the second and most important factor to consider. Every NMR-active nucleus resonates at a different frequency. Probehead coils can be specific for one frequency or tunable to a wide range of frequencies (broadband coils). Probeheads usually contain two coils:
    - One coil is reserved for detecting and exciting hydrogen atoms, the most sensitive and widely used nucleus.
    - The second coil is either specialized for one nucleus (^{13}C in most cases) or consists of a broadband coil that can be tuned to nearly all nuclei.

  The arrangement of those coils can also be altered. Due to technical reasons, the first coil needs to be positioned closer to the sample. The second one is positioned around the first coil, forming a configuration of inner and outer coils. In the early days, the arrangement was nearly always a hydrogen coil on the outside. A second coil on the inside detected heteroatoms, as nuclei other than hydrogen are less sensitive. This arrangement was termed "ordinary" and describes broadband ordinary (BBO) probeheads. With the advent of metabolomics and the analysis of physiological samples, scientists became mainly interested in hydrogen-carrying molecules present at low concentrations. As a result, the opposite arrangement became popular, as the highest possible sensitivity was required, and the detection of non-hydrogen

nuclei was of lesser importance. This arrangement was therefore coined “inverse” and is found in Quadruple Resonance CryoProbe inverse (QCI) probeheads, for example.

Experienced spectroscopists can easily exchange probeheads in just a few minutes to rapidly adapt the NMR instrument to meet the sample requirements. Cryo-probeheads are an exception to this rule. These technically advanced probeheads possess higher sensitivity and signal-to-noise ratio. The detection coil of those probeheads is also cooled by helium and has, therefore, reduced electrical noise. Although such probeheads have several advantages over their room temperature counterparts, they also have some significant limitations. A scientifically irrelevant but financially draining aspect is the purchasing and maintenance costs of those probeheads. They require an additional module with a pump that produces a vacuum in the probehead and cools it down with helium gas. This fact also reduces their flexibility in daily use. Indeed, swapping the installed probehead with another one and cooling it down takes an entire day to complete.

It is worth mentioning an additional feature. A gas flow passes from the bottom of the instrument upwards through the bore. This gas flow achieves two tasks:

- The temperature of the probehead and sample is controlled by the gas that passes a heating coil installed in the probehead.
- The volume of gas blown through the bore also moves the sample from its position on the top of the probehead to the bore entrance at the top of the instrument, where the operator can remove and change it.

2.1.3 Quantification

NMR can quantify compounds in an absolute manner by comparing a signal belonging to the compound to the signal of an internal standard at a known concentration. This is unique because any compound can be used as an internal standard without calibration curves. The response of nuclei is absolute for NMR so that an excited hydrogen atom will generate the same signal intensity independently of the compound. When analyzing complex mixtures, using a reference standard for each compound of interest is impossible. This approach is required for quantifications with MS or UV/Vis.

Although NMR quantification has its benefits, it also has some potential drawbacks(133):

- It is necessary to integrate the entirety of the peak of interest without overlapping with other peaks to achieve a precision and accuracy better than +/- 2% of the measured value. As the mixture being analyzed becomes more complex, meeting this requirement becomes increasingly challenging. The NMR signals in a spectrum maintain a consistent shape due to the inherent properties of NMR. The NMR signal has a Lorentz-shaped appearance under ideal conditions. Due to technical imperfections, this signal shape becomes progressively convoluted and adopts a Gaussian shape. The resulting shape is then called Voigt shape or profile. This specific shape can be utilized to partially deconvolute overlapping peaks to enhance the quantification's precision eventually.
- Another crucial factor is understanding the T1 time. It was already discussed that the T1 time describes the time required by an excited nucleus to recover its magnetization in the direction of the magnetic field. Each nucleus that can be chemically differentiated has a unique T1 time.

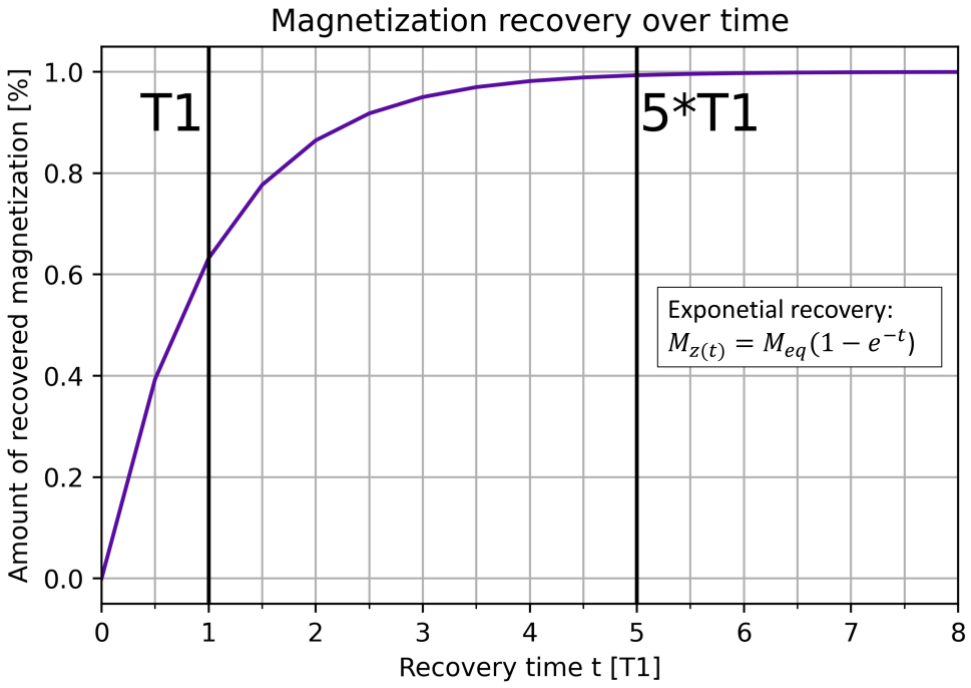

Figure 8: Theoretical amount of recovered magnetization in the z-direction after increasing amounts of recovery time incremented in T1.

Waiting for the T1 time is insufficient to obtain accurate quantitative measurements. Only 63% of the total magnetization is recovered after T1. A general rule of thumb recommends waiting 5 times the T1 to acquire the next transient of a spectrum. Five times T1 allows the magnetization to relax up to 99.3%. Every chemically different nucleus of the same isotope has a different inherent T1 time. Accordingly, measuring the T1 time for every signal is not feasible. Single T1 times can be determined via an inversion recovery approach. This approach is, however, very time-consuming, as total relaxation of the nucleus must be guaranteed to make the measurement accurate. One way to avoid this problem is by cautiously choosing a longer waiting time or recycling delay. For protons, 30-40 seconds can be considered sufficient to reach 99% of the recovery for nearly every chemical environment of the nucleus. In most cases, protons have a T1 time < 5-6 seconds. Finding reliable tables with specific T1 times for different protons can be challenging. Other nuclei like ^{13}C or ^{29}Si have much longer relaxation times, and quantitative measurements are rarely done. When a compound is highly concentrated, it becomes easier to measure and quantify, as the strong signal does not require the magnetization to be fully flipped by 90°. If a smaller flip angle is chosen (often 30° instead of 90°), the magnetization reaches the desired magnetization recovery of >99% much faster, and it becomes possible to quantify NMR-active heteroatoms once again. It is important to note that not all NMR experiments are quantitative in an absolute way. In 2D NMR experiments, numerous waiting times are inherent to the experiment. Therefore, signal responses of 2D experiments cannot be treated like signals from 1D experiments, as 2D experiments contain delays in modifying the signal response in various ways. It is sometimes necessary to use a 2D experiment with an enhanced resolution to accurately quantify the components in complex mixtures. Even though the advantage over other analytical techniques may be lost, it is possible to perform a quantification using an exact reference standard under these conditions.

2.1.4 Limitations and biases of NMR

NMR can detect all nuclei belonging to a chosen isotope in an absolute way and without bias. It is important to remember that not every compound in a mixture will contain NMR-active isotopes. Metabolomics is a research field that analyses complex mixtures and relies on NMR. If NMR is the only analysis method used, metabolites like oxalic acid (OA) may be overlooked. OA is the dicarboxylic acid with the shortest carbon chain (C2) and does not carry non-exchangeable hydrogens. OA is a crucial compound in the metabolism of amino acids and ascorbic acid. Furthermore, it can be easily detected in urine, a matrix heavily investigated using NMR. The urine OA concentration has an important prognostic value for detecting diseases like kidney stones(134). Urea is another compound measured in urine but is invisible to proton NMR. Urea is also discussed as a buildingblock for noncanonical nucleosides(135) and has a plethora of other applications in prebiotic chemistry(136, 137). Both mentioned compounds could easily be detected via ^{13}C-NMR. Unfortunately, large metabolomics studies with NMR exclusively rely on proton NMR because of the low sensitivity and the resulting long measurement times combined with the qualitative nature of ^{13}C-NMR.

Another NMR limitation is T2 shortening caused by paramagnetic components or impurities in a sample. In certain systems, selected signals may vanish without significantly impacting the residual spectrum(138). The extent of this signal deletion depends on the coordination strength of the paramagnetic metal. Addition of FeS to a mixture of Krebs-cycle intermediates showed the selective suppression of citrate, malate and fumarate(131). This effect is especially strong for organo-metal compounds with covalent bonds with paramagnetic transition metals.

When comparing NMR to mass spectrometry, sensitivity is a commonly mentioned limitation. While it is true that some compounds can be detected at picomolar concentrations when using mass spectrometers, there are also numerous counterexamples. In ESI-MS, certain compounds, especially hydrophobic substances, have a low ionization efficiency(139) which can make NMR a more sensitive technique in those cases. One benefit of NMR is that the signal response can be predicted. Suppose your system can detect a concentration of 10 µM of a compound. In that case, any compound with the same measured isotope at concentrations of 10 µM or

higher can be detected confidently. Thanks to advancements in cryo-probehead technology and ultra-high field spectrometers, the detection limit has been lowered to 1-10 µM. These levels can now be accurately detected within a reasonable analysis time.

2.2 Mass spectrometry

Mass spectrometry is another highly used analytical technique for analyzing complex mixtures(140). Mass spectrometry measures the mass-to-charge ratio (m/z) of the ionizable compounds present in a sample(141). The information gained from this technique can be of qualitative or quantitative nature if particular precautions are taken. Mass spectrometry can be performed by injecting a sample directly into the system, called direct infusion (DI), or hyphenated with a chromatographic system. Combining mass spectrometry with chromatographic systems is common. This method minimizes the impact of uncontrollable factors like ion suppression and ion clustering on the resulting spectra(142). Mass spectrometry instruments are based on different measurement principles(143), whereas NMR always measures the current induced in its detection coil. In this discussion, we will focus on two types of mass spectrometers that have been widely used in analyzing complex mixtures(144). These instruments have been featured in numerous publications and are well-regarded within the scientific community.

2.2.1 FT-ICR-MS

Fourier-transform-ion-cyclotron-resonance-mass spectrometers deliver the highest resolution of all available mass spectrometer architectures(145). It also shares multiple aspects with NMR spectrometers. The most obvious similarity is the cryo magnet providing the magnetic field necessary for FT-ICR-MS measurements. No other commercially available mass spectrometer architecture uses a cryo magnet. This magnetic field forces ionized compounds to orbit around the axis of the magnetic field direction. Multiple detection plates are placed around the orbit to detect this orbital motion(146). By measuring the frequency of ions orbiting, their mass can be determined. The cyclotron equation determines the mass:

$$\omega_c = \frac{qB}{m} <=> \frac{m}{q} = \frac{B}{\omega_c}$$

This equation allows us to determine the m/z ratio, as B, the field strength of the magnet is known, and the angular frequency ω_c is measured.

The most frequent method for conducting measurements on FT-ICR mass spectrometers is through direct infusion. This is due to the very low scan speed of the instrument (~1 second) required to reach the unrivaled resolution. The length of the acquired FID (free induction decay) is directly linked to the resolution(147), just like in NMR spectra. If hyphenated with a chromatographic system and scanned at a low frequency of 1 Hz, the resulting chromatograms would have limited data points. There is a risk of overlooking a peak because of elution between scans with this method and bad peak definition. Raising the scan rate may prevent this issue, resulting in a shorter FID and lower resolution. Under those conditions, FT-ICR-MS no longer holds any advantage over other types of mass spectrometers.

A second advantage of FT-ICR-MS over other mass spectrometers is the theoretically “infinite” sensitivity that can be achieved by accumulating scans. This aspect is shared with NMR spectroscopy. The accumulation of FIDs leads to a stronger buildup of the signal compared to noise, following the equation:

$$\left[\frac{S}{N}\right]_m = \sqrt{n}\left[\frac{S}{N}\right]_k$$

The actual signal of an ion will always be the same as opposed to the noise, which fluctuates around zero and will only increase by a factor of $\sqrt{n}$, with n being the ratio of m/k. Increasing the number of scans by 4 will increase S/N by 2. With sufficient scans, even a weak signal can be detected based on this concept. In most cases, this scenario is not realistic because very low concentrations would result in extremely long measurement times that are not practical.

2.2.2 LC-ToF-MS

Hyphenated mass spectrometry techniques are much more widespread than direct infusion(148). These approaches have multiple advantages over direct infusion. Unless UHR-mass spectrometers like FT-ICR-MS are being used, there is no advantage to choosing direct infusion over hyphenation with any type of separation other than the speed of analysis and less solvent consumption. Before injecting the sample into the mass spectrometer, it is beneficial to at least partially separate its chemical components. This approach helps to address two common issues in mass spectrometry, particularly in DI-MS:

- First, ion suppression happens during the co-elution of different compounds. It can lead to biased spectra, depending on the concentration and the presence or absence of compounds in a sample(149). Depending on the separation quality before injection, hyphenation can solve this problem. If all the compounds within a sample can be fully separated using the appropriate techniques, then ion suppression is negligible. Separating every compound in a complex biological or environmental sample is unrealistic in most situations. It is important to consider co-elution, as it cannot be completely avoided. Nevertheless, the issue remains significantly reduced with hyphenated separation since in DI-MS, every compound co-elutes, and ion suppression must be accepted as an essentially uncontrollable factor during the analysis.

- Second, ion-cluster or adduct formation(150). Despite the use of hyphenated ESI-MS, cluster formation cannot be eliminated. The eluents used in liquid chromatography already contain small ions from buffer salts, impurities, or added acids or bases. Those small ions co-elute permanently with the compounds contained in the sample and can form adducts. This is a predictable event that can be considered during data processing. The software for the mass spectrometer can identify specific mass differences provoked by adduct formation and flag or remove them. Non-hyphenated methods like DI-MS produce unpredictable clusters. As every compound elutes at the same time, it has the potential to form adducts or clusters with every other ionizable compound in the sample.

Using hyphenated methods has an advantage in allowing the automatic acquisition of MS2 fragment spectra for a significant portion of the identified masses. Fragment spectra deliver a whole new dimension of information otherwise absent in MS spectra. Pure MS^1 spectra provide information about the mass of compounds. UHR-spectrometers enable the direct assignment of elemental compositions in this manner. However, elemental compositions are not sufficient to identify functional groups. The function of a compound is determined to a large extent by its functional groups, hence the name. Fragmentation data offers further insights in this regard. In MS^2 spectra, specific functional groups can manifest themselves through the loss of specific masses or the appearance of new signals called diagnostic ions. Analyzing their fragmentation pattern makes it possible to classify compounds in samples. This research field was accelerated by the recent widespread use of bioinformatics and chemometrics, which attempt to completely characterize whole samples via a combination of MS^2 spectra and network approaches.

2.2.3 Limitations and biases of MS

The main bias of mass spectrometry was already mentioned and consisted mainly of the ionization bias. A mass spectrum usually only displays a specific portion of the sample. Multiple conditions must be fulfilled for a signal to appear in a mass spectrum. The first bias is always introduced through the choice of polarity. Ions can be positively (cations) or negatively (anions) charged. The spectrometer can only detect one polarity at a time. Not all compounds can ionize in both modes. Some compounds, like pure carboxylic acids, only ionize in negative mode. Amines ionize only in positive mode. Compounds like esters only ionize inefficiently in positive mode and are often completely missing. Every sample can be measured in both modes, doubling the analysis's time and cost and leading to more demanding data processing. Unfortunately, this solution does not address the issue of compounds that do not ionize at all. Ionization is also very dependent on the ionization technique used. ESI ionizes mainly polar compounds. APCI and APPI ionize apolar compounds. It is not practical to change the ionization source and test every sample in both ionization modes for studies that involve over 100 samples.

3. Research questions

3.1 General hypothesis

The in-depth investigation of the chemical reactivity and evolution of acetylene under prebiotic conditions is an important task, considering the presence of this gas in the atmospheres of Titan and Enceladus and its hypothesized existence on early Earth. There are already theoretical pathways described on Titan that lead from acetylene to acetaldehyde, which can be converted into alanine. However, the reactants involved in these pathways are less likely to have existed on early Earth. There is currently no experimental evidence to support the idea that the necessary reactants for an acetylene-based origin of life chemistry can be assessed under hydrothermal conditions.

Considering the dynamic nature of likely rapid conversions of reactants, it is a requirement to use advanced analytical techniques to provide a kinetic view of this conversion rather than investigating endpoints. Such an approach allows us to detect numerous parallel reaction products as well as their evolution towards end products. Related to the fate of acetylene, the initial interaction of reactants leading to intermediates and, finally, the conversion of acetylene into biomolecules must be considered. Moreover, advanced analytics would allow us to identify and quantify alterations of the described pathways.

The experimental setup needs to be analyzed untargeted to fully understand the range of possible outcomes from the combination of acetylene with prebiotically relevant reactants. This approach will expand the limited number of recently discovered reverse (r)TCA products and fatty acids. A comprehensive overview of all ionizable components in the system has the potential to reveal undiscovered reaction patterns, as it was previously shown for complex reaction mixtures like the Maillard reaction. Isotope labeling will be of utmost importance in this approach to distinguish products formed from acetylene alone and from acetylene together with other carbon sources.

Finally, the role of acetylene as a catalyst should be investigated, as acetylene is known to have a high affinity for transition metals and can, especially in combination with sulfur, lead to organo-metal complexes. Those organometal complexes could

then allow for a better understanding of the origin of organo-metal enzyme co-factor motifs.

Altogether, our general hypothesis is that acetylene is an ancestral C2 building block that leads to higher-order hydrocarbons alone or in combination with other carbon sources, in the presence of sulfur.

3.2 Specific objectives

To validate our general hypothesis, we will develop the following specific objectives:

1. To provide first kinetic evidence demonstrating the existence of a progressively increasing molecular complexity arising from a limited number of compounds. To achieve our objective, we will combine ^{13}C-labelling with untargeted ultrahigh-resolution mass spectrometry.

We postulate that this approach:

- will allow us to elucidate the molecular complexity of an early pre-metabolic system over time,
- will reveal the increasing diversity of functional groups in the investigated acetylene-containing reaction setup and
- detect reoccurring patterns in mass differences with the potential to represent chemical reactions.

2. To demonstrate the formation of acetaldehyde and a multitude of acetylene derivatives, we intend to describe the required conditions allowing the concentration of acetaldehyde:

- We will emphasize changes in the reaction path undertaken by aldehydes under early Earth conditions in a continuously changing system.
- Moreover, we will investigate the impact of the pH, allowing sufficient amounts to be yielded as a prerequisite for diversified chemical reactions.

3. To bridge the autonomous chemical pathways triggered by acetylene towards pre-enzymatic entities, we plan to identify enzymatic organo-metal motifs formed from acetylene in the presence of sulfur. In particular, we will investigate:

- the exact structure of organo-metal compounds found in the system,
- the time-dependent effect of those organo-metal complexes on the system and
- the potential of those compounds to be precursors for extant enzyme co-factors.

To achieve this aim, we will rely on ^{13}C-labelling with untargeted ultrahigh-resolution mass spectrometry and nuclear magnetic resonance, which will likely allow us to elucidate the molecular complexity of this early metabolic system emerging from acetylene.

3.3 Overview of this thesis

After an introduction to early Earth chemistry and the advanced analytical tools required to achieve our aims (**Chapter 3, Methods**), this thesis comprises three major result sections **(Chapter 4, Results**) that intend to provide answers to our general hypothesis by investigating detailed aspects of our specific objectives.

- **Paper 1** is entitled “Formation, stabilization, and fate of acetaldehyde and higher aldehydes in an autonomously changing prebiotic system emerging from acetylene”**.**
- **Paper 2** is entitled “C2-addition patterns emerging from acetylene and nickel sulfide in simulated prebiotic hydrothermal conditions”.
- **Paper 3** is entitled “Nickel-organo compounds as potential enzyme precursors under simulated early Earth conditions”.

The thesis will be finalized by an integrative discussion **(Chapter 5, Discussion),** followed by **Chapter 6, Conclusions**, including critical considerations and limitations of the study.

4. Results

Summary of contributed articles

A summary of all first-author publications that resulted from these doctoral studies is provided below, sorted by the research questions introduced in the section “Hypothesis and objectives.”

Formation, stabilization, and fate of acetaldehyde and higher aldehydes emerging from acetylene.

Aldehydes are crucial for the prebiotic synthesis of Life's essential building blocks, including amino acids, sugars, and nucleosides. Therefore, understanding how aldehydes formed under early earth conditions is vital. To investigate aldehyde formation, we simulated primordial early earth conditions, based on the metal-sulfur world theory, in an acetylene-rich atmosphere. Our results show that a pH-driven, self-regulating environment concentrates acetaldehyde and other higher molecular weight aldehydes. Acetaldehyde forms rapidly from acetylene over a nickel sulfide catalyst in water, followed by sequential reactions that increase the molecular diversity and complexity of the mixture. The evolution of this complex matrix leads to the auto-stabilization of newly synthesized aldehydes and alters the subsequent synthesis of relevant biomolecules, preventing uncontrolled polymerization. Our findings emphasize the influence of progressively generated compounds on reaction conditions and underscore the role of acetylene in forming essential building blocks for the emergence of terrestrial life.

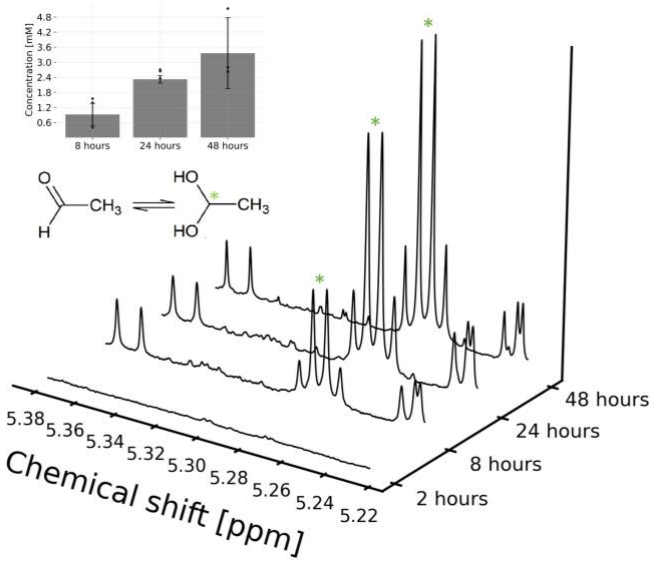

Figure 9: 1D-1H NMR spectra, zoomed-in on the diol-hydrogen of acetaldehyde (green asterisk), at different time points. A bar plot shows the quantified absolute yield of acetaldehyde in the mixture.

Candidate's contributions: P. Diederich designed the research, performed all analytical experiments, processed all the MS and NMR data, and analyzed all the data. P. Diederich prepared all the figures and wrote and revised the manuscript.

C2-addition patterns emerging from acetylene and nickel sulfide in simulated prebiotic hydrothermal volcanic conditions

We analyzed the chemical evolution of a complex prebiotic mixture containing acetylene, carbon monoxide, and nickel sulfide using mass spectrometry. Isotopic ^{13}C-labeling allowed us to identify multiple reaction products, including diverse CHO and CHOS compounds. Molecules belonging to the same chemical spaces showed varying degrees of ^{13}C labeling and differences in saturation levels, enabling more robust functional group characterization. We detected a characteristic C2-addition pattern in all compound classes, along with a high diversity of thio acids, reminiscent of extant microbial C2-metabolism. We analyzed the mixture over time using a molecular network, revealing the behavior of sulfur in the system. Early-formed compounds contained more sulfur atoms than later-emerging compounds. Our results provide insight into the elusive role of sulfur dynamics in the emergence of life and show the progressively increasing molecular complexity arising from a limited number of compounds.

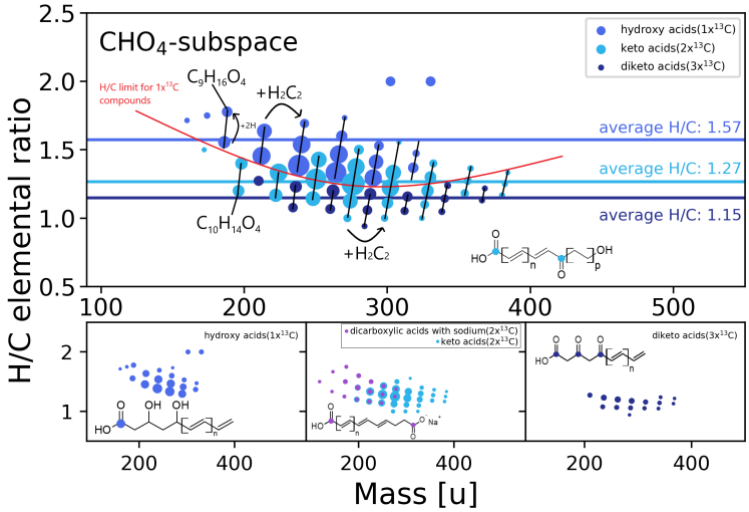

Figure 10: ^{13}C-labeled elemental compositions of the CHO_4-subspace highlighting the C2-addition pattern found in all identified compound classes.

Candidate's contributions: P. Diederich designed the research, performed all analytical experiments, processed all the MS and NMR data, and analyzed all the data. P. Diederich prepared all the figures (except figures 5 and 6) and wrote and revised the manuscript.

Nickel-organo compounds as potential enzyme precursors under simulated early Earth conditions.

For this study, we used a prebiotically-inspired experimental environment that contained acetylene and mimicked volcanic hydrothermal conditions to investigate the efficient and spontaneous self-assembly of organo-metal complexes. We identified the simplest bis(dithiolene)nickel complex, $(C_2H_2S_2)_2Ni$, using various techniques such as UV/Vis spectroscopy, mass spectrometry, nuclear magnetic resonance, and capillary electrophoresis. We then studied the temporal evolution of this Ni-containing compound and its possible function. We used a simulated early Earth atmosphere by isolating the main bis(dithiolene)nickel species from the primordial experimental setup. Our approach allowed us to uncover the significant diversity of organo-nickel compositions by identifying 156 elemental annotations. One intriguing finding was the formation of acetaldehyde through the subsequent degradation of these organo-metal complexes. This is reminiscent of the ability of *Pelobacter acetylenicus* to ferment acetylene to acetaldehyde via its bis(dithiolene)-containing enzyme acetylene hydratase. Our findings provide a mechanistic characterization of the role of nickel sulfide in catalyzing the formation of acetaldehyde. This fundamental pre-metabolic reaction could play the role of a primitive enzyme precursor of the enzymatic acetylene metabolism of *Pelobacter acetylenicus* and further strengthen the role of acetylene in the origin of life.

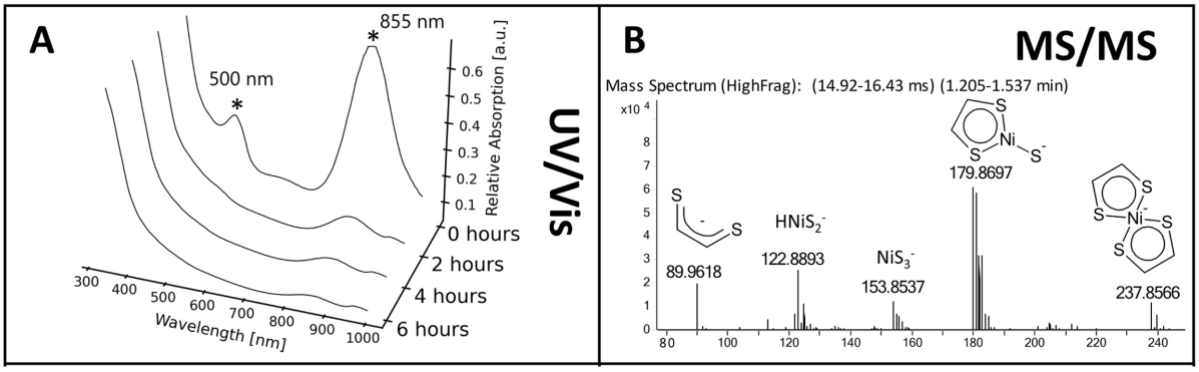

Figure 11: (A) UV/Vis spectrum of the prebiotic mixture after two hours, incubated at room temperature for various amounts of time. (B) MS/MS spectrum of the identified nickel bis(dithiolene) complex.

Candidate's contributions: P. Diederich designed the research, performed all analytical experiments, processed all the MS and NMR data, and analyzed all the data. P. Diederich prepared all the figures and wrote and revised the manuscript.

5. Discussion and Conclusion

Advances in the origin of life research have allowed scientists to address progressively more complex questions. Pathways leading to the synthesis of all small building blocks under arguably prebiotic conditions have been proposed in the past(10). Sugars, nucleic acids, amino acids, and fatty acids can be synthesized under multiple prebiotic conditions, as shown in the introduction (**Chapter 1**). The diversity of the suggested synthesis pathways also partially highlights the ambiguity of prebiotic formation pathways. This ambiguity justifies the continued search for new prebiotic pathways from less investigated educts.

On the other hand, recent progress in analytical technologies enables us to go beyond synthesizing a limited number of biologically relevant building blocks. New research emerges showing the impact of mixtures on the progress of synthesis routes(151). Vahab showed a reduction of the emerging complexity if more reactants were used in the synthesis(152). This was an unexpected result, considering the theoretical increase in possible reaction permutations. Generally, a large part of prebiotic chemistry was performed in chemically “pure” environments with a very limited number of reactants. The environment on prebiotic Earth was likely not a chemically “pure” environment but a complex mixture of organic compounds(11). Future investigations must focus on the impact of the growing complexity of prebiotic reaction systems to understand how pathways are shaped by the evolving mixture.

A second emerging research field is catalysis. Prebiotic reactions need to be efficient as concentrations are often low. Catalysts are investigated for this purpose, as they lower the required energy for reactions to proceed. Catalysts can be of organic or inorganic origin. Organic catalysts are of interest, as they are formed from the organic feedstock molecules that are also useful for the synthesis of the building blocks themselves. A particularly interesting organo-catalyst system was shown by Closs,

who developed different organo-catalysts. Depending on the chemical environment, these catalysts continuously changed the output of produced compounds(153). Organo-catalysts are also the core of auto-catalytical reactions(154). On the other hand, there are inorganic catalysts derived from transition metals. Those metals show a broad range of redox potentials and are prebiotically plausible, as they are contained in minerals(155). Iron was heavily investigated for its role as an oxidating agent and is essential in a proposed prebiotic reverse tricarboxylic acid (rTCA) cycle(156). The most interesting aspect of those inorganic catalysts is their similarity to active sites of extant enzymes. Iron-nickel cluster motifs exist in enzymes and minerals and were shown to catalyze similar reactions(156). The detailed investigation of metal-binding motifs in contemporary enzymes could provide further clues for the discovery of inorganic or organometallic catalysts with autonomous catalytic functions, even without a protein scaffold.

Through investigating the role of acetylene in the origin of life, it has been discovered that this gas has multiple previously underestimated purposes. Examining the pathways this molecule took under volcanic hydrothermal conditions revealed that there are still more potential uses for this gas to be explored. Previous literature described that acetylene reacts with carbon monoxide, water, and nickel sulfide to form unsaturated fatty acids(66). While this compound class is significant(59), it is not the only essential compound class required for life as we know it today(10).

First, we elucidated a pathway for acetylene to generate a large diversity of aldehydes. These aldehydes were time-dependently converted into amino acids or α-hydroxy acids. We incorporated the already-known formation of acids and the resulting lower pH into our investigation. This effect demonstrated the influence of the complex mixture forming in parallel on the described aldehyde formation pathway. Indeed, we eventually discovered a system that autonomously transitioned from producing amino acids to producing α-hydroxy acids. These essential biomolecules are well known to be indispensable for the function of extant organisms. It is important to mention that not every formation pathway is influenced to the same extent. Products originating from acetaldehyde were transformed into another compound class. The formation of acetaldehyde from acetylene only changed in its efficiency of the conversion and resulted in higher yields. Those yields originate also partially from a stabilization of acetaldehyde in the more acidic pH. The change in the chemical environment through

the complex mixture, therefore, had a second effect countering the often-occurring uncontrolled polymerization of acetaldehyde, resulting in tar formation, mentioned as a limiting factor in other aldehyde-dependent pathways, like the formose reaction for sugar synthesis. Considering the whole complexity of an observed reaction system and its evolution is inevitable to assess its potential for the origin of life.

This targeted and quantitative look at the evolution of acetylene and its products gave acetylene more relevance in the origin-of-life field. So far, acetylene has rarely been mentioned as a prebiotic chemistry reactant(68). The use of untargeted techniques to analyze complex mixtures revealed the presence of numerous unknown molecules in this setup. This approach provides an even more comprehensive understanding of the situation required to investigate the underlying system fully. It allows the detection of around 3000 distinct elemental compositions from the CHO and CHOS space in the investigated setup.

This level of molecular diversity was impossible to investigate with the techniques used in our initial study. Our initial method of using NMR as a detection method was unbiased towards hydrogen-bearing organic molecules but less sensitive, which resulted in a less clear understanding of the extent of complexity. Especially the recognition of sulfur-bearing compounds was mainly achieved with FT-ICR-MS. Sulfur is a nucleus that possesses an isotope with an NMR-active nucleus. However, the T2 time of this nucleus is so short that its measurement is impossible in solution NMR. Still, the chemical shift of hydrogen and carbon atoms in close vicinity of sulfur are influenced and shifted. However, the shift caused by sulfur in the chemical environment of hydrogen and carbon remains inconclusive.

As shown during the investigation of the fate of aldehydes in the hydrothermal acetylene system, identifying the sulfur-bearing 4-oxobutane-2-sulfonic acid required the synthesis of the exact compound in combination with mass spectrometric measurements to confirm its identity. The system was analyzed at different time points to investigate the behavior and temporal evolution of 2300 sulfur compounds. An untargeted examination of this system clearly revealed C2-addition patterns reinforced by stable isotope labeling.

Stable isotope labeling already allowed for robust conclusions on the exact origin of carbon in our first investigation, where it was necessary to differentiate between two separate pathways leading to formic acid. Using ^{13}C labeling, we could use our knowledge to categorize the overwhelming number of elemental compositions into functional classes. The targeted and untargeted investigations complemented each other, highlighting the strengths of both approaches.

The targeted approach with NMR easily described the diversity and quantity of aldehydes in the system over time, which was impossible with FT-ICR-MS for two reasons:

- The aldehyde group has poor ionization ability. Deprotonation of the aldehyde functional group is rather difficult compared to a carboxylic acid and lowers, therefore, the ionization efficiency. This observation alone, however, would not exclude the possibility of detecting pure aldehydes. We demonstrated that the acetaldehyde concentration reaches 4 mM, which could compensate for the low ionization efficiency in favorable situations.
- The excitation bandwidth of FT-ICR-MS excludes the detection of acetaldehyde with FT-ICR-MS. Small m/z ratios need much higher frequencies to be excited because FT-ICR-MS has to excite molecules with a frequency equal to their orbiting frequency. The instrument's radiofrequency generator has a limit on the highest frequency it can produce, so it is technically unfeasible to measure m/z ratios below 100 m/z. Acetaldehyde has a mass of 44.05 g/mol, which lies far below this technical limitation. Most compounds described in our first investigation were only detectable with NMR because of their low molecular weight (e.g., acetic acid, formic acid). In our initial investigation, we utilized a different MS archetype, specifically ToF-MS, to decrease the limit of detectable masses. This enabled us to detect alanine using LC-ToF-MS successfully. However, this has the disadvantage of reducing the resolution.

On the other hand, analysis with FT-ICR-MS allows superior resolution. This approach allowed us to describe the molecules from 120 m/z to 550 m/z in much greater qualitative detail than with NMR. Our research discovered that the fatty acid and hydroxy acid compound classes initially identified using NMR or GC-MS

existed in even greater diversity at higher masses. The detected compounds initially allowed a better qualitative characterization of the formed compounds. Additionally, we were able to propose hypotheses on how larger molecules may have developed from the smaller molecules identified in a targeted configuration. The untargeted investigation revealed the presence of thio acids arising solely from acetylene carbon. We observed that acetylene is mainly converted into acetaldehyde, which grows via aldol condensation. One of our tempting hypotheses is that these hydrocarbons could be oxidized to form thio acids(157). This oxidation would happen via the geminal hydroxy-thiol form of acetaldehyde conditioned by hydrogen sulfide in the system.

This oxidation would link the results from our first investigation with a key finding of the second investigation. By combining the information from the two different approaches, it is possible to connect and better understand the results from each method.

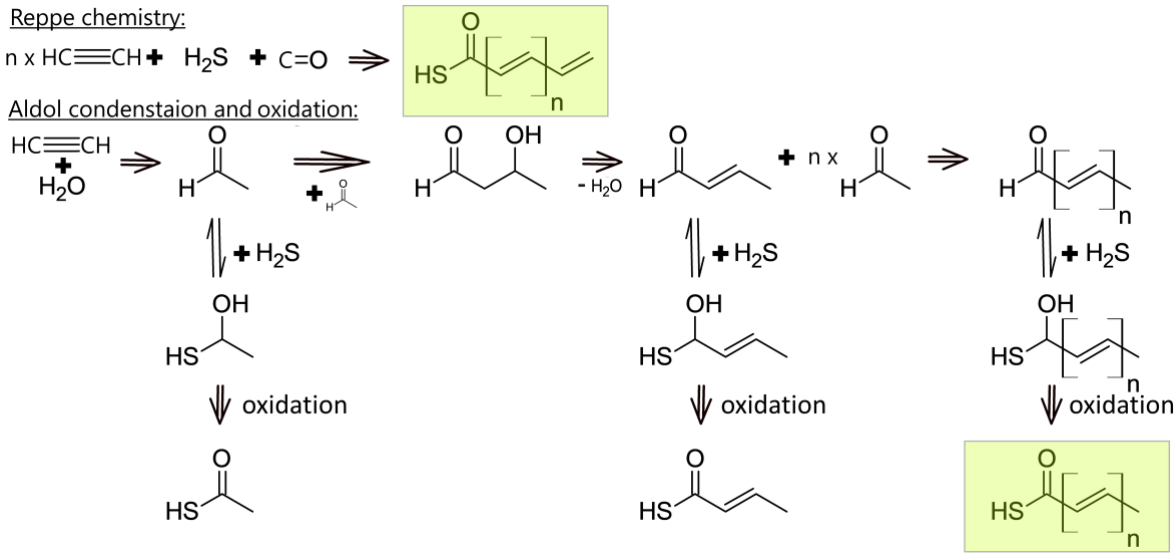

Figure 12: Two pathways leading to thio acids. One via the Reppe chemistry route and a second via an aldol condensation route as a possible explanation of the observed masses in the untargeted FT-ICR-MS approach, originating from compounds detected with the targeted quantitative NMR approach. Higher thio acids are marked with a green background.

Our last investigation focused on the enzyme that allows *Pelobacter acetylenicus* to thrive solely on acetylene(118). Acetylene hydratase enables this microorganism to convert acetylene into acetaldehyde. The conversion of acetylene into aldehyde was already the result of our first investigation. A highly abundant signal with an elemental

composition fitting an organo-nickel complex at early time points of our temporal analysis of this system led to the discovery of nickel-bis(dithiolene). The formation of this specific transition-metal complex in water was interesting in two ways:

- The isolated complex was only soluble in water at higher temperatures (>50°C) and transformed quickly into acetaldehyde and formic acid. In our initial investigation, we discovered one potential pathway that allowed the production of acetaldehyde using nickel sulfide.
- In addition to the elucidation of this formation pathway, the complex showed a strong similarity to the co-factor of acetylene hydratase. Molybdopterin contains a bis(dithiolene) motif(118, 158). The only difference is the transition metal found in the extant co-enzyme. Such pterin co-factors contain either tungsten or molybdopterin(158). In our case, the transition metal is nickel.

Nonetheless, the formed complex still originated from the same reactant, namely acetylene, and resulted in the same product, acetaldehyde. The additional strong structural similarity to the pterin co-factor further strengthens the relevance of this complex as a precursor of extant co-factor motifs.

The third investigation ties in seamlessly with the first two, as the mechanism described clarifies the formation of acetaldehyde discussed in the second investigation. The relevance of the first investigation stems from the discovered C2-addition patterns. *Pelobacter acetylenicus* transforms acetylene into acetaldehyde to further metabolize it into acetyl-CoA. Acetyl-CoA is then used to fuel its metabolism and especially to synthesize fatty acids in a C2-addition manner.

Altogether, figure 13 provides an overview showing how our main publications are interconnected to proceed from a gas, water, and nickel-sulfide mixture to a potential vesicle-containing machinery able to produce a proto-metabolism.

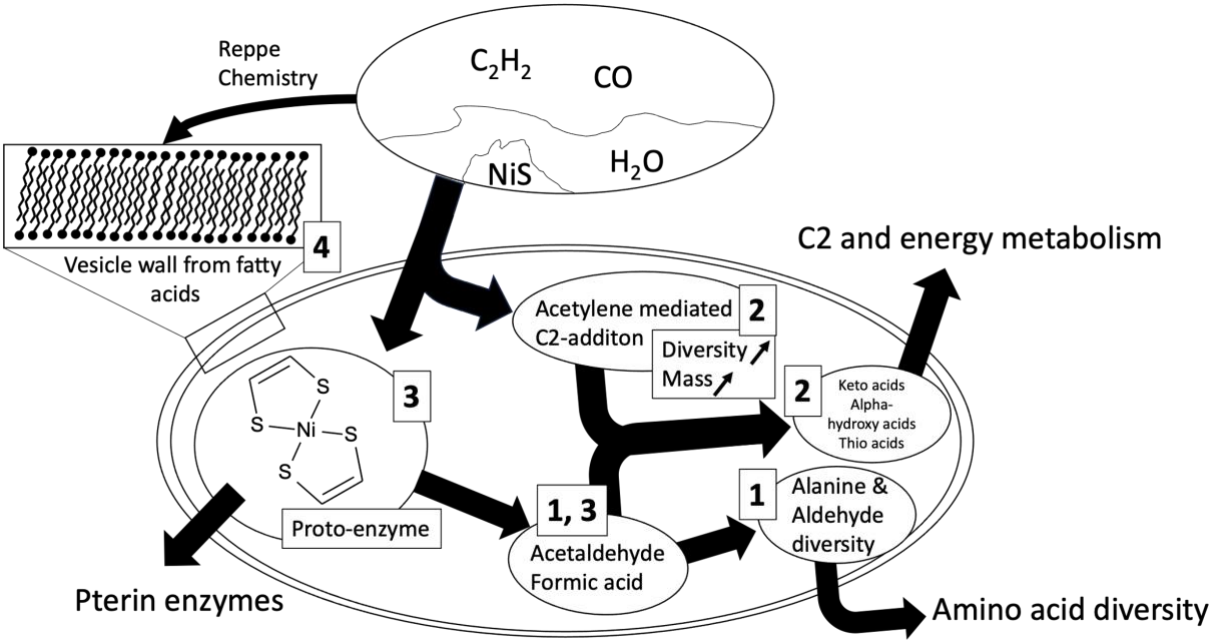

*Figure 13: Overview figure showing how all publications are connected to proceed from a gas, water, and nickel-sulfide mixture to a potential vesicle-containing machinery that produces a proto-metabolism. The number **one** represents findings from the first investigation, the number **two** from the second, the number **three** from the third, and the number **4** from the co-authored publication(159).*

Our study attempted to analyze the underlying system comprehensively. With the analytical techniques available today, a completely unbiased description is impossible. The investigation based on a combination of NMR and mass spectrometry eliminated some of the biases of both techniques. Despite our efforts, our methods were unable to detect certain biologically significant molecules that have a low mass and no non-exchangeable hydrogens, such as oxalate.

Another limitation is the lack of quantitative data for a large number of described compounds, especially during the investigation of the complexity of the system. There is currently no practical solution to this problem due to the lack of absolute quantification in mass spectrometry. The absence of reference standards, in combination with unpredictable ion suppression effects, is the main bottleneck that prevents quantification. Additionally, for most detected annotations, the exact structure remains unknown or at least highly ambiguous, which would prevent quantification via a reference standard even if they were available.

Nonetheless, the amount of reliable and unambiguous information that could be gained with this approach demonstrates that it is possible to advance knowledge in a field at the edge of analytical possibilities. We show that the overwhelming complexity emerging from systems mimicking prebiotic conditions can be tamed to some degree with the most advanced analytical systems available today.

Further insights can be gained through stronger integration of chromatography. We refrained from using chromatography for all FT-ICR-MS-related investigations, as it would have entailed an unacceptable reduction of resolution in the mass spectra. The newest FT-ICR-MS instruments, however, have a faster scan rate. This enhanced scan rate will allow future investigations to take advantage of the numerous benefits of separation prior to the injection into the mass analyzer. The knowledge of the retention time itself carries information about the interaction of the detected compounds with the stationary phase of the column material. In the case of reverse-phase (RP) chromatography with C-18 columns, this retention time strongly correlates with the hydrophobicity of the compounds. A separation of compound classes could be attempted with this knowledge alone, as elemental annotations belonging to either esters or carboxylic acids could be categorized more reliably. This process can be

facilitated because esters have a higher level of hydrophobicity than carboxylic acids, especially if chain lengths are low (short-chain fatty acids), with direct relevance for metabolic pathways like the TCA cycle(160).

This study laid the foundation for future investigations based on our hydrothermal acetylene-containing system. The emerging chemical space of CHO and CHOS compounds was described to a large extent and allows the introduction of further additional elements known to be required for the emergence of life, including nitrogen and phosphorous. We have already investigated the influence of nitrogen reactants on the evolution of aldehydes in the system. This was far from comprehensive, and further investigations of heterocycle formation, for example, would be very interesting, as they could potentially lead to purine and pyrimidine synthesis. Phosphorous is another indispensable element, as it is a prerequisite for energy transfer. Phosphorous was not investigated in this study, but the discovery of a nickel complex with electron-transportation properties calls for the introduction of phosphorous.

The discovered nickel complex is an interesting candidate to investigate further and develop additional hypotheses. This study did not achieve the exchange of nickel with tungsten or molybdenum. It is crucial to conduct additional research to explore options for facilitating this exchange to approach a prebiotically synthesized co-factor even more akin to pterins. Additionally, ways to derivatize this complex further and grow it in mass would be relevant to reach higher similarity to extant pterin co-factors. This approach would require the addition of nitrogen into the system to allow the formation of the structure of the extant co-factor (Figure 5).

7. Appendix Chapter 4

7.1.1 Appendix Paper 1

communications chemistry

ARTICLE

https://doi.org/10.1038/s42004-023-00833-5 OPEN

Formation, stabilization and fate of acetaldehyde and higher aldehydes in an autonomously changing prebiotic system emerging from acetylene

Philippe Diederich[1], Thomas Geisberger[2], Yingfei Yan[1], Christian Seitz[2], Alexander Ruf[3,4], Claudia Huber[2], Norbert Hertkorn[1] & Philippe Schmitt-Kopplin[1,5,6]✉

Many essential building blocks of life, including amino acids, sugars, and nucleosides, require aldehydes for prebiotic synthesis. Pathways for their formation under early earth conditions are therefore of great importance. We investigated the formation of aldehydes by an experimental simulation of primordial early earth conditions, in line with the metal-sulfur world theory in an acetylene-containing atmosphere. We describe a pH-driven, intrinsically autoregulatory environment that concentrates acetaldehyde and other higher molecular weight aldehydes. We demonstrate that acetaldehyde is rapidly formed from acetylene over a nickel sulfide catalyst in an aqueous solution, followed by sequential reactions progressively increasing the molecular diversity and complexity of the reaction mixture. Interestingly, through inherent pH changes, the evolution of this complex matrix leads to auto-stabilization of de novo synthesized aldehydes and alters the subsequent synthesis of relevant biomolecules rather than yielding uncontrolled polymerization products. Our results emphasize the impact of progressively generated compounds on the overall reaction conditions and strengthen the role of acetylene in forming essential building blocks that are fundamental for the emergence of terrestrial life.

[1] Helmholtz Munich, Research Unit Analytical BioGeoChemistry, Neuherberg, Germany. [2] Technical University of Munich Structural Membrane Biochemistry, BNMRZ, Lichtenbergstr 4, 85748 Garching, Germany. [3] Excellence Cluster ORIGINS, Boltzmannstraße 2, 85748 Garching, Germany. [4] Faculty of Physics, LMU Munich, Schellingstraße 4, 80799 Munich, Germany. [5] Technical University of Munich, Analytische Lebensmittel Chemie; Maximus-von-Forum 2, 85354 Freising, Germany. [6] Center for Astrochemical Studies, Max Planck Institute for Extraterrestrial Physics, Gießebachstraße 1, 85748 Garching bei München, Germany. ✉email: schmitt-kopplin@helmholtz-muenchen.de

Acetylene is a gaseous compound that was most likely available in the early Earth´s atmosphere and throughout the universe as it was formed through the photolysis of methane[1,2]. Spectroscopic measurements of astrophysical objects like Titan and Jupiter revealed acetylene as a part of their atmosphere[3]. Hypothetical scenarios for its role in prebiotic chemistry have already been discussed in the literature and mentioned routes to polycyclic aromatic hydrocarbons[4] and other biomolecules[5] under extraterrestrial conditions. At the same time, acetylene has been an often-used educt for numerous chemical reactions since the earliest stages of organic synthesis. After the discovery of acetylene hydration by Mikhail Kucherov in 1881[6], acetylene became the main precursor for acetaldehyde production until modern industrial chemistry introduced the Wacker process[7]. Compounds carrying an aldehyde functional group are frequent educts in primordial synthesis pathways (and in chemical synthesis in general) as they are easily transformed into several coveted functional groups to fuel the origin of life[8]. The reactions of aldehydes are well characterized in the literature, making them an attractive basis for new reaction hypotheses[9]. Previous publications already reported the formation of acetaldehyde and various other aldehydes under extraterrestrial conditions, as extraterrestrial samples contain a large variety of organic compounds covering a broad chemical space[10] whereas cometary ice contains acetaldehyde as a product of small building blocks and UV-radiation[11,12]. Ketones and aldehydes became part of systematic, targeted analytical screening in extraterrestrial materials (meteorites and return mission samples), underlining the importance of these compounds as essential reaction partners in synthesizing life-relevant molecules[13–16]. Despite the extraterrestrial hypothesis of aldehyde origins, the synthesis and accumulation of such precursors on early Earth remain largely unclear. In addition, the high reactivity of aldehydes leads to concentration issues and may prevent the accumulation of sufficient amounts of aldehydes that would allow specific reactions. Prebiotically relevant synthesis pathways, starting from aldehydes as biological building blocks, play a crucial role in understanding the origin of life. Synthesis of numerous necessary small building blocks of life has been demonstrated under varying levels of primordial plausibility[17]. As varying amounts of comparable chemical entities were also discovered in extraterrestrial materials such as meteorites or real samples from asteroid sample return missions[18–21], the aim of this paper was a demonstration of a potentially universal, auto-regulatory, up-scalable synthesis of aldehydes explaining the occurrence of aldehydes under both Early Earth and extraterrestrial conditions.

The “metal-sulfur world” represents a prebiotically plausible hypothesis describing a reduced chemical environment allowing the emergence of life[22]. The investigation of this environment started with Wächtershäuser et al. with the incubation of CO and H_2S in the presence of different metal-sulfur catalysts like FeS and NiS, which eventually resulted in activated acetic acid as an early analog of acetyl-CoA, hinting at a primitive form of the citric acid cycle[23].

Recent work hypothesized acetylene as a precursor for reactions leading to relevant biomolecules, including unsaturated fatty acids and thiophens[24,25]. Until now, aldehydes were an unknown part of this hypothetical prebiotic environment, even though the potential relevance of acetaldehyde in the context of the metal sulfur world theory was already mentioned in a previous work[24].

Here we provide experimental proof for the formation of acetaldehyde and a multitude of follow-up products. At the same time, we describe a pH-driven, intrinsic autoregulatory environment that concentrates acetaldehyde and changes the reaction path undertaken by aldehydes, fully compatible with early earth conditions and yielding sufficient amounts allowing for diversified detectable chemical reactions.

Results

Nickel sulfide catalyzes acetaldehyde formation. To investigate the formation of acetaldehyde, we incubated a gaseous mixture of carbon monoxide and acetylene over water containing a nickel sulfide catalyst in an oxygen-free environment. This experimental setup was inspired by the acetylene metabolism of the anaerobic extant *Pelobacter acetylenicus* utilizing a tungstopterin enzyme to convert acetylene to acetaldehyde[26]. We determined the concentration of acetaldehyde via nuclear magnetic resonance spectroscopy (NMR) after different incubation periods (Fig. 1). The concentration of acetaldehyde showed a steady increase over two days, suggesting a higher conversion of acetylene to acetaldehyde compared to the reaction rate of acetaldehyde to later reaction products. Acetaldehyde reached a concentration of 3.3 mM after 48 h, representing a conversion of about 1% of the total available acetylene. Acetaldehyde could already be detected after 8 h of incubation, demonstrating the conversion efficiency with the used catalyst. Acetaldehyde results most likely from the hydration of acetylene followed by tautomerization of hydroxyethanal to acetaldehyde, analogous to the mercury salt catalyzed synthesis described by Kutscheroff in 1881. In this aqueous environment, acetaldehyde was detected as a mixture of the free aldehyde and its hydrate with a pH-dependent ratio. This hydration is, in our case, catalyzed by nickel sulfide, mimicking a mineral surface, as experiments without catalyst only resulted in trace amounts of acetaldehyde (<40 µM). Experiments with low concentrations of free nickel ions (4 µM), simulating the effect of dissolved NiS, didn’t lead to higher amounts of acetaldehyde compared to the experiments without NiS. However, experiments with trace amounts of sulfide (10 µM) lead to low but quantifiable acetaldehyde yields, suggesting a parallel pathway catalyzed by sulfide ions alone. This experiment led to concentrations of 360 µM of acetaldehyde, 10% of the yield with NiS (Supplementary Fig. 1). We performed additional experiments with FeS and NiS/FeS (1:1), as nickel sulfide is most often found in conjunction with iron sulfide in Nature. The setup with FeS alone did not show any detectable amount of free acetaldehyde nor the hydrate. The NiS/FeS setup produced acetaldehyde in the same concentration range as NiS alone (2.5 mM) (Supplementary Fig. 2), highlighting the importance of nickel sulfide in iron-nickel-sulfide minerals.

Increased aldehyde diversity through aldol condensation. We detected trans-but-2-enal as the direct aldol condensation product of acetaldehyde, showing the feasibility of this type of reaction in the complex system, without interference from other matrix components. The aldol condensation and numerous other reactions drive the diversification of aldehydes in the explored system and generate a diverse aldehyde mixture (Fig. 2). The extensively investigated formose reaction generates a similar diversity of aldehydes through aldol condensation, starting with formaldehyde, leading to highly hydroxylated products, resulting in carbohydrates[27]. In contrast to the formose reaction, the condensation of acetaldehyde leads to highly reactive α,β-unsaturated aldehydes[28]. These aldehydes carry one double bond conjugated to the aldehyde group giving both the carbonyl carbon and the β-carbon an electrophilic character. This character allows nucleophiles to be added to the molecule. One of these potential nucleophiles is sulfur which will be discussed later. However, the aldol condensation reaction also carries the risk of rapid polymerization under favorable pH conditions. It leads to large, water-insoluble compounds, hereby removing the aldehydes from the reaction medium. The complex matrix of our system contains a large diversity of water-soluble aldehydes.

The numerous proton NMR resonances between 9.1 and 10 ppm reflect the diversity of aldehydes formed under these

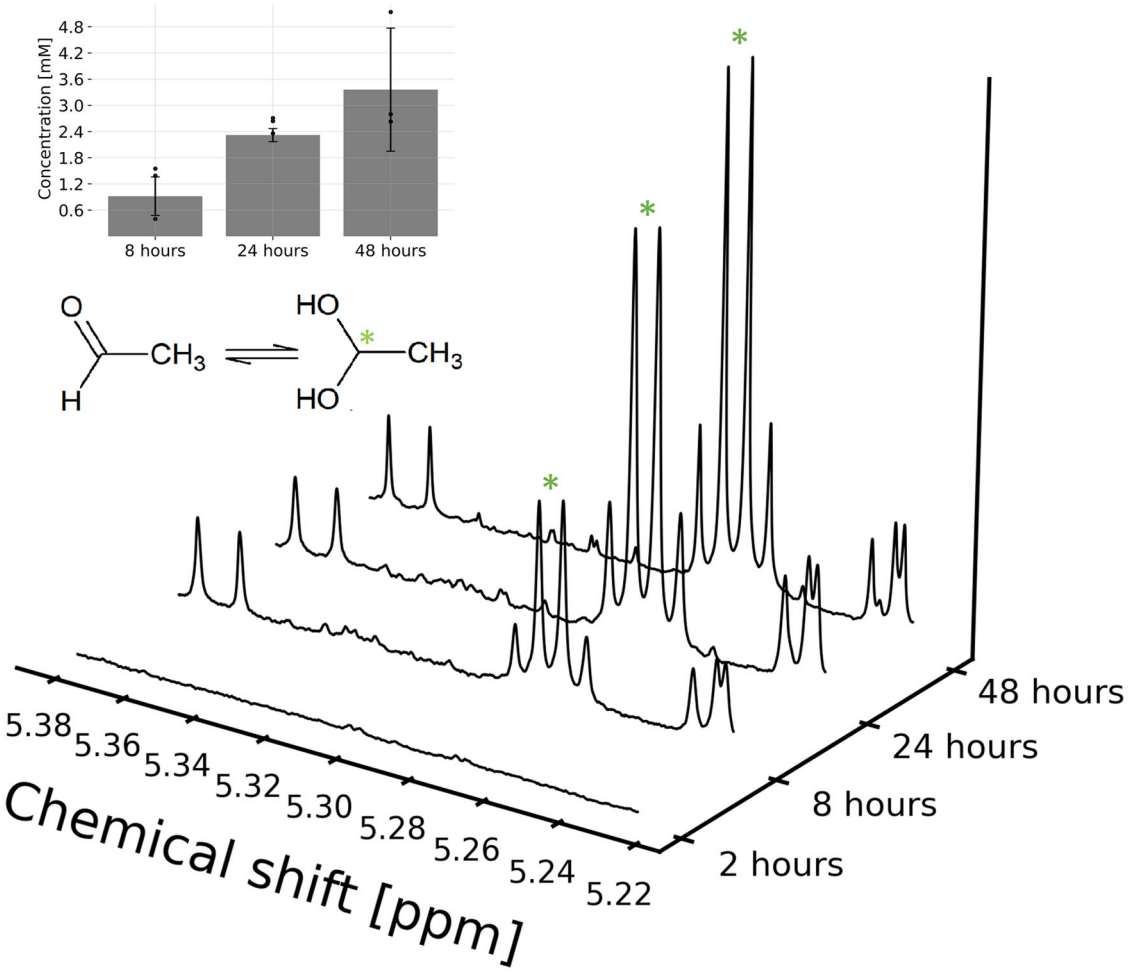

Fig. 1 Quantification of acetaldehyde over time. 1D-^{1}H spectrum showing the hydrogen signal of the single hydrogen connected to the carbon carrying the diol functionality (marked with a green asterisk). Spectra for four time points are shown. The bar plot shows the measured average concentration of acetaldehyde in the aqueous mixture over time, with error bars representing the standard deviation and black dots for individual data points.

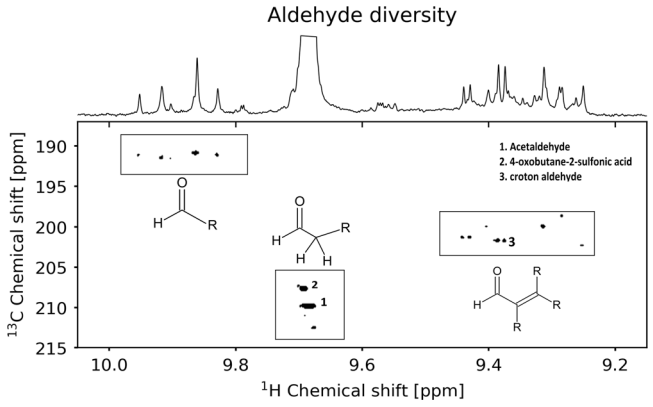

Fig. 2 Aldehyde diversity formed after 7 days in an alkaline setup. The ^{1}H,^{13}C HSQC shows three different groups (marked with a black frame) of signals sharing similar hydrogen and carbon shifts, suggesting chemical similarity of the aldehyde group. The acetaldehyde signal is cut to allow magnification of the other aldehydes.

conditions. The observed clustering in the ^{1}H,^{13}C-HSQC experiment (an experiment that links hydrogen atom shifts to the carbon atom shift directly attached to the hydrogen atom) suggests a rough classification into three chemically similar aldehyde groups: α,β-unsaturated aldehydes (doublets 9.1–9.5 ppm), acetaldehyde (quartet 9.68 ppm), aliphatic aldehydes (multiplets 9.55–9.65 ppm) and aldehydes attached to an olefinic carbon without hydrogen or heteroatom, but not necessarily aromatic (singlets 9.75–10 ppm).

We further performed isotope-labeled experiments to clarify the origin of acetaldehyde in the investigated system and to confirm the hypothesized reactions. ^{13}C-labeled acetylene experiments demonstrate acetylene as the sole origin of the detected aldehyde functional group. The absence of $^{1}J_{CH}$ coupling in the ^{1}H 1D NMR spectrum during ^{13}C-labelling of carbon monoxide provides strong evidence for this hypothesis (Supplementary Fig. 3). Carbon monoxide does not react to detectable amounts of aldehydes under these conditions. Experiments with acetylene alone also produced acetaldehyde (Supplementary Fig. 4), excluding a relevant catalytical role of carbon monoxide in this reaction in form of nickel carbonyl for example.

Increase in aldehyde diversity through Michael addition reactions with sulfur and formation of sulfuric acids. The overall complexity emerging out of the investigated system was already demonstrated by Fourier transform ion cyclotron resonance mass spectrometry measurements, showing an, until then, to the best of our knowledge unreported chemical space defined by sulfur[29]. These measurements revealed 2332 individual elemental compositions divided into 575 formulas consisting of only carbon, hydrogen, and oxygen and 1757 formulas with sulfur as an

additional element. These results call for further characterization of the formed compounds and evaluation of their relevance to the origin of life.

The α,β-unsaturated functionality of the condensation products drives further diversification of aldehydes contained in the mixture by sequential aldol condensation and additions to the double bond by Michael addition reactions. Especially hydrogen sulfide and other thiols act as good nucleophiles and form new carbon-sulfur bonds. The sulfur in the investigated system originates from the NiS catalyst, as it is the only source of sulfur in the system. Sulfide addition is often observed in our system to be followed by the oxidation of sulfur to form a sulfonic acid group, shown through 4-oxobutane-2-sulfonic acid, which can be found in amounts comparable to acetaldehyde (half of the acetaldehyde concentration). More than 250 possibly sulfonated compounds could be detected by LC-MS, even though it remains unknown if all derive from Michael additions to α,β-unsaturated aldehydes (Supplementary Table 4). With the new knowledge of the existence of those sulfonic acids, a part of the sulfur compounds detected by FT-ICR-MS can be attributed to this compound class.

Stabilization of aldehydes via intrinsic environmental pH changes. pH is a key parameter with a substantial impact on the reactivity of aldehydes. The pH of the investigated system evolves, starting at an alkaline pH of 12 and changing to a nearly neutral pH (7.6 ± 0.5 s.d.) *via* the formation of a large variety of carboxylic and sulfonic acids (Supplementary Table 1). The formation of highly unsaturated carboxylic acids has been described in a previous paper[24]. The chemistry leading to those carboxylic acids was already described by Walter Reppe in 1953[30]. The formation of these carboxylic acids requires carbon monoxide, also added to the gas phase of the experimental setup. However, smaller carboxylic acids like formic acid and acetic acid were also formed to some degree from acetylene alone. Formic acid was potentially formed through cleavage of the triple bond in acetylene by a so far unknown mechanism. This reaction usually requires strong oxidative conditions not present in the investigated setup[31]. This hypothesis was drawn from the observation of formic acid in setups with acetylene alone and the coexistence of labeled and unlabeled formic acids, in setups including labeled acetylene and unlabeled carbon monoxide (Supplementary Fig. 5). Acetic acid is observed and originates from acetylene alone[32]. We consider that the disproportionation of acetaldehyde provides the acetic acid to a certain extent, as ethanol is also detected in this prebiotic experiment. Acetaldehyde disproportionates into acetic acid and ethanol under all tested pH conditions. Lower pH (<8 after 7 days of incubation) enabled the stabilization of the observed aldehydes and slowed aldol condensation. The concentration of acetaldehyde was found to be 2.5 mM on average after 7 days. Experiments with added formic acid (pH 3) showed a significantly increased acetaldehyde yield (up to 40 mM, Supplementary Table 1). Further experiments with a standard acetaldehyde solution alone showed the compounds near inert behavior under acidic conditions. An incubation of acetaldehyde at 105 °C for one day in formic acid containing water (pH 4) did not lead to detectable reaction products besides a small amount of butenal (Supplementary Fig. 6). Morooka et al. reported the formation of lactic acid from formic acid and acetaldehyde under acidic conditions in subcritical water at 200–250 °C[33]. Even though both compounds were present in the mixture, lactic acid could not be detected under the much milder conditions utilized in this setup. Lower pH slows down the aldol condensation and inhibits rapid polymerization of the acetaldehyde, making it available for other reactions that are essential to the origin of life, depending on the prevailing pH.

pH-dependent fate of the aldehydes: alkaline conditions. To test the feasibility of a Strecker-type reaction in this complex mixture, we added potassium cyanide (KCN) and ammonium chloride (NH_4Cl) to the alkaline setup. We detected the formation of alanine (180 µM, 0.02% yield based on ammonium chloride) in the resulting incubation mixture after 7 days. Alanine is the Strecker reaction product of acetaldehyde with potassium cyanide and ammonium chloride. The Strecker reaction is considered a likely reaction for forming amino acids under origin of life conditions[34]. Incubation of the same setup under acidic conditions (pH 3) leads to a mixture of acetaldehyde (27 mM) and 2-hydroxy propanenitrile (10.2 mM) but no alanine, showing the stabilization of the produced acetaldehyde and pH dependence of the fate of the formed aldehydes. The introduction of additional ammonia alkalinized the reaction mixture (pH 12), allowing the detection of intermediate products, namely 1-aminoethane-1-ol and 2-amino propanennitrile of the Strecker reaction from acetaldehyde to alanine in this chemically diverse environment (Fig. 3). These results support the hypothesis that the Strecker reaction is the main pathway leading to amino acid synthesis under these conditions from aldehydes. Alanine was additionally confirmed by LC-MS analysis. (Supplementary Table 3).

pH-dependent fate of the aldehydes: acidic conditions. Acidic conditions, occurring naturally through the generation of carboxylic and sulfonic acids, change the reaction pathway of aldehydes. A strong indicator of this behavior is the intermediate product 2-hydroxypropanenitrile, detected in the already mentioned setup acidified with formic acid. Formic acid was used for acidification as it is generated naturally in the investigated system. The acidified system should be thought of as a system that has already produced many carboxylic and sulfonic acids. The result is the conversion of acetaldehyde to an α-hydroxycarboxylic acid, namely lactic acid, instead of alanine via the hydrolysis of the cyanide group of the now prominent 2-hydroxypropanenitrile (Fig. 4, i). This pathway leading to lactic acid requires less harsh thermal conditions than the pathway starting from formic acid and acetaldehyde at 200–250 °C described by Morooka et al.[33]. It occurs naturally over time through the generation of carboxylic and sulfonic acids. To further validate the importance of acidic pH conditions, the pH of the acidified setup was further lowered with sulfonic acid to pH 1. After incubation, we observed a

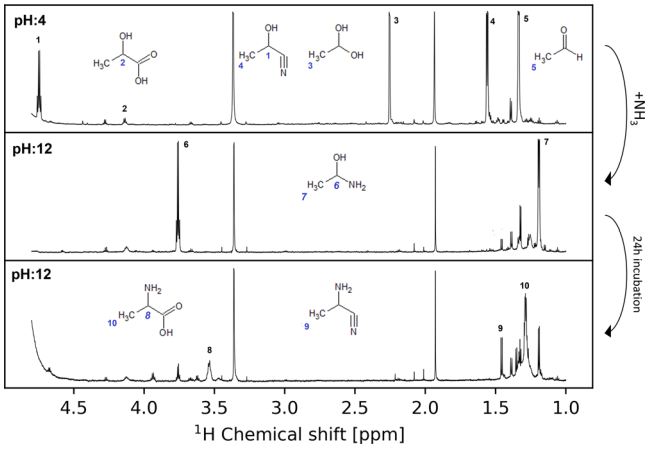

Fig. 3 Investigation of the reactions of acetaldehyde under different pH conditions. The pH of an acidified setup was readjusted to alkaline conditions to observe the behavior of acetaldehyde. Blue numbers indicate detected hydrogen atoms and black numbers the corresponding resonance in the hydrogen spectrum.

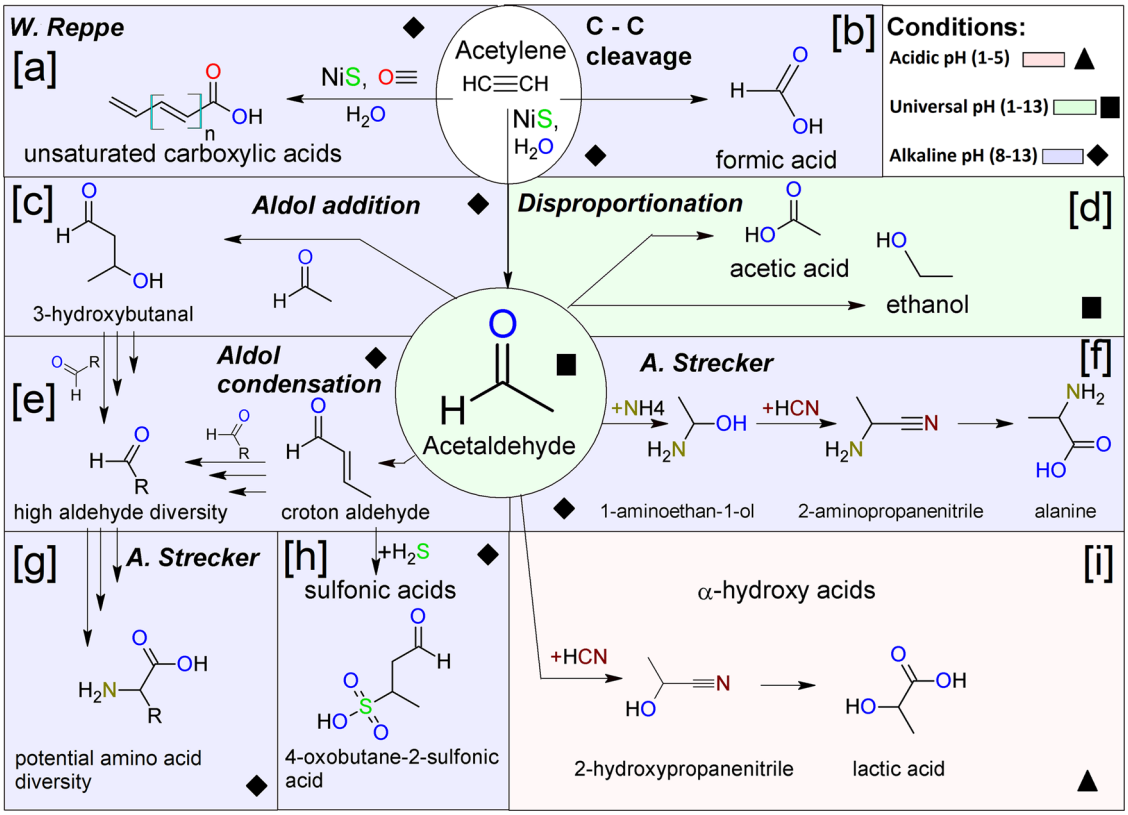

Fig. 4 Reaction diagram showing all discussed reactions and detected compounds under different pH conditions. Background color and shapes indicate the pH conditions the compounds were detected at. The different panels show suggested formation pathways for the different compounds. Conversion of acetylene to unsaturated carboxylic acids via Reppe chemistry (**a**), conversion of acetylene into formic acid via an unkown pathway (**b**), condensation of acetaldehyde (c + e), dispropotionation of acetaldehyde leading to acetic acid and ethanol (**d**), Strecker reaction (f + g), michael addition followed by oxidation resulting in sulfonic acid (**h**), lactic acid formation (**i**).

further increase in lactic acid concentration. α-hydroxy acids are known to promote peptide bond formation during dry-down reactions[35].

An observed side effect of the lower pH is a higher percentage of dissolved NiS in the aqueous phase. This can be seen by the strong line broadening in the 1D-^{1}H NMR spectra of the acidified solutions. The paramagnetic nickel in the solution leads to this effect. Carboxylic acids are strongly affected by a higher percentage of NiS, as they seem to coordinate with the Ni^{2+} in solution. At an acidic pH, the measurement became impossible without additional precipitation of the nickel ions with a sodium phosphate solution.

Discussion

Our findings show an efficient and prebiotically relevant pathway to acetaldehyde and higher condensation products starting from a simple gaseous mixture of acetylene and carbon monoxide over NiS containing water under hydrothermal conditions. The mixture evolves by changing its pH in the first step by forming a multitude of carboxylic and sulfonic acids, which then, in a second step, changes the reaction pathway undertaken by the newly formed aldehydes. The aldehydes are later stabilized by the lowered pH of the complex mixture of carboxylic and sulfonic acids. Therefore, they stay available for further non-polymerization reactions even under high temperatures.

The first aldehyde formed in our experimental system, acetaldehyde, is described in the literature as required for multiple building blocks, including a path for synthesizing deoxyribonucleosides utilizing acetaldehyde as a critical educt[36]. Converting the aldehyde group into an amino acid group via the Strecker reaction is a more straightforward idea. The conditions of this primordial setup allow an expedient synthesis of amino acids, witnessed by the presence of alanine, readily formed *via* the Strecker reaction. The high diversity in aldehydes present in this system has therefore, the potential to form a diverse set of amino acids. The slow acidification of the environment by the carboxylic acids leads to favorable conditions for the Strecker reaction. We observe a transition from a basic pH, required for the nucleophilic addition of ammonia to the aldehyde group, to a more acidic pH that facilitates the imine formation and the hydrolysis of the α-aminonitrile.

Further acidification of the matrix leads to the detection of 2-hydroxy propanenitrile and lactic acid. These conditions suggest a pathway leading to α-hydroxycarboxylic acids via the hydrolysis of the nitrile group, analogous to the hydrolysis during the Strecker reaction[37]. The presence of the hydroxy group in alpha position enables this reaction only in an aged system that has already accumulated sufficient acids or lowered its pH in a different way. The positive impact of α-hydroxycarboxylic acids on peptide-bond formation during dry-down reactions is an interesting effect in a system that evolves from an amino acid-producing system to an α-hydroxycarboxylic acid producing system. The acidified environment also showed a higher concentration of dissolved nickel ions.

The α,β-unsaturated nature of a part of the formed aldehydes facilitates the functionalization of the formed compounds, as the addition of sulfur shows. The carbon-sulfur bond formation is a sought-after reaction in the field of the origin of life[38,39]. Early papers suggest a thioacid/thioester-based metabolism as a precursor to extant phosphate-based metabolic pathways[40,41]. The

presence of sulfonic acids was also detected in the Murchison meteorite, even though a direct relevance for the origin-of-life remained uncommented[42]. Recent reports show the increased importance of sulfur functional groups, especially thiols, as precursors of protopeptides[43] and organocatalysts[44].

Future investigations could focus on a pH swing back to alkaline conditions due to external events. This alkalization would create starting conditions with much higher acetaldehyde concentrations, leading to stronger polymerization and higher-weight aldehydes. If the polymerization is stopped quickly enough by the formation of acids, this would change product distribution to potentially higher mass amino acids and sulfonic acids.

Conclusion

Acetylene, a prominent molecule in the universe[45], reported on the poles of Jupiter[46], and supposed to be abundant on early Earth[47], shows great potential as a precursor for primordial building blocks and reaction matrix modification. This paper sheds light on a possible pathway to acetaldehyde in a primordial setup aligned with the idea of a metal-sulfur world. The rapid diversification of acetaldehyde into a large variety of aldehydes and the transformation of acetaldehyde into alanine shows the potential to produce amino acids from acetylene gas in a one-pot experiment. Additionally, through the parallel formation of carboxylic acids and the efficient generation of sulfonic acids *via* Michael addition reactions, the environment intrinsically changes over time, especially the pH. This alteration changes the prevailing conditions to such an extent that the reactions involving the formed aldehydes shifted from an amino acid-producing system to an α-hydroxycarboxylic acid-producing system. Considering this change in reaction conditions, provoked by intrinsic, de novo compound synthesis within the same setup allowed us to demonstrate how this system autonomously changes its chemical output without any external input.

Materials and methods

Chemicals. A D_2O sodium phosphate (for analysis, Merck KGaA) buffer (1.5 M) was prepared with added sodium trimethylsilylpropanoate (2 mM) (98 atom %D, Aldrich) as the internal standard. The pH of this buffer was adjusted to 7 with sodium hydroxide. This solution was used to reference and quantify signals in 1D-^{1}H NMR experiments. Ammonia solution in water (25% ammonia, Lichropur Merck KGaA), Sulfuric acid (95–98%, Sigma-Aldrich), Acetaldehyde standard (ReagentPlus, >99.0%, Sigma-Aldrich)), Lactic acid standard (>99.0%, Sigma-Aldrich).

Nitrogen-free bottles: setup S1. A 125 ml glass serum bottle was charged with 1.0 mM $NiSO_4$ • 6 H_2O (99%, Aldrich) and sealed with a silicon stopper. Three times the bottle was evacuated and filled with argon, finally ending in a deaerated state. Subsequently, the bottle was filled with 8.5 ml argon-saturated water, with 1.0 mL argon-saturated 1 M Na_2S (solid Na_2S: 99.99%, Sigma-Aldrich) solution with 0.5 mL 1 M NaOH solution and finally with 60 ml CO (2.44 mmol) and 60 ml (2.53 mmol) acetylene (acetone free), using gastight syringes for the injections. Reactions were carried out at 105 °C. After a reaction time of up to 7 days, the reaction mixture was allowed to cool down.

Acetylene and CO were replaced by argon in a blank run with otherwise identical composition.

Nitrogen-free bottles: setup S1*. A 125 ml glass serum bottle was charged with 1.0 mM $NiSO_4$ • 6 H_2O (99%, Aldrich), 50 µl of formic acid and sealed with a silicon stopper. The bottle was evacuated Three times and filled with argon, finally ending in a deaerated state. Subsequently, the bottle was filled with 8.5 ml argon-saturated water, with 1.0 mL argon-saturated 1 M Na_2S (solid Na_2S: 99.99%, Sigma-Aldrich) solution with 0.5 mL 1 M NaOH solution and finally with 60 ml CO (2.44 mmol) and 60 ml (2.53 mmol) acetylene (acetone free), using gastight syringes for the injections. Reactions were carried out at 105 °C. After a reaction time of up to 7 days, the reaction mixture was allowed to cool down.

Nitrogen-free ^{13}C bottles setup. To confirm the hypothesized reactions, ^{13}CO or $^{13}C_2$-acetylene were used in representative experiments. Whereas ^{13}CO (Cambridge Isotopes Laboratories Inc. (Tewksbury, MA, USA) could be used directly, ^{13}C-acetylene had to be set free from Ethinyl-$^{13}C_2$-trimethylsilan (90 atom % ^{13}C, Sigma-Aldrich). To release the $^{13}C_2$acetylene from its silylated form, a glass serum bottle was charged with the stoichiometric amount of tetrabutylammonium fluoride (TBAF) (≥97.0%, SigmaAldrich). The bottle was sealed with a silicon stopper. The bottle was evacuated three times and flushed with argon, finally ending in a deaerated state. The $^{13}C_2$-acetylene was transferred into the bottle using a gastight syringe. TBAF and $^{13}C_2$-acetylene amounts were calculated to produce a slight overpressure in the serum bottle.

Nitrogen-containing bottles: S2 setup. A 125 ml glass serum bottle was charged with 1.0 mM $NiSO_4$ • 6 H_2O (99%, Aldrich), 1.0 mmol NH_4Cl (>99.5% Sigma-Aldrich) and 1.0 mmol KCN (>98.0 % Sigma-Aldrich) resulting in starting molarities of 100 mM for each nitrogen containing compound. and sealed with a silicon stopper. Three times the bottle was evacuated and filled with argon, finally ending in a deaerated state. Subsequently, the bottle was filled with 8.5 ml argon-saturated water, with 1.0 mL argon-saturated 1 M Na_2S (solid Na_2S: 99.99%, Sigma-Aldrich) solution with 0.5 mL 1 M NaOH solution and finally with 60 ml CO (2.44 mmol) and 60 ml (2.53 mmol) acetylene (acetone free), using gastight syringes for the injections. Reactions were carried out at 105 °C. After a reaction time of up to 7 days, the reaction mixture was allowed to cool down.

Nitrogen-containing bottles: S2*. A 125 ml glass serum bottle was charged with 1.0 mM $NiSO_4$ • 6 H_2O (99%, Aldrich), 50 µl of formic acid, 1.0 mmol NH_4Cl (> 99.5% Sigma-Aldrich) and 1.0 mmol KCN (>98.0% Sigma-Aldrich) resulting in starting molarities of 100 mM for each nitrogen containing compound and sealed with a silicon stopper. Three times the bottle was evacuated and filled with argon, finally ending in a deaerated state. Subsequently, the bottle was filled with 8.5 ml argon-saturated water, with 1.0 mL argon-saturated 1 M Na_2S (solid Na_2S: 99.99%, Sigma-Aldrich) solution with 0.5 mL 1 M NaOH solution and finally with 60 ml CO (2.44 mmol) and 60 ml (2.53 mmol) acetylene (acetone free), using gastight syringes for the injections. Reactions were carried out at 105 °C. After a reaction time of up to 7 days, the reaction mixture was allowed to cool down.

NMR spectroscopy. All NMR experiments were carried out on an 800 MHz Bruker AVANCE III spectrometer equipped with a 5 mm QCI-probe head at 300 K.

Quantification of acetaldehyde. 1D-^{1}H spectra were acquired for triplicates of bottles incubated for 8 h, 24 h, and 48 h. 150 µl supernatant of each centrifuged sample was spiked with 50 µl D_2O buffer. The pulse program consisted of a simple 90° pulse followed by acquisition. 64 scans were acquired for each sample with a relaxation delay of 16 s and an acquisition time of 4 s. On-resonance pre-saturation was used during the relaxation delay to suppress the water signal. The optimized 90° pulse had a duration of 12.75 µs. Quantification was done by comparing the sum of the integrals after baseline correction of the hydrate single hydrogen signal and the acetaldehyde methyl hydrogens signal added together to the TSP internal reference integral. The average for every time point was calculated. The acquired FID was apodized with an exponential function (LB = 0.3), and Fourier transformed.

Aldehyde complexity. A bottle incubated for 7 days was used to prepare the sample. 180 µl of the sample were spiked with 20 µl of D_2O buffer.

1D-^{1}H spectrum was acquired using a 1D version of the nuclear Overhauser effect (NOE) experiment with on-resonance pre-saturation of the water signal during the relaxation delay of 6 s (s) and mixing time of 20 ms. 256 scans were acquired. HSQC spectrum was recorded with a phase-sensitive version using Echo/AntiechoTPPI gradient selection (hsqcetgpprsisp2.2), decoupling during acquisition, and onresonance pre-saturation during the relaxation delay (1.5 s). 197 increments were acquired with 800 transients each. The spectral width was set to 15 ppm in the F2 dimension and 40 ppm in the F1 dimension, with an offset of 200 ppm in the F1 dimension. The FID of the F2 dimension was apodized with a sine function (SSB = 2), and the F1 Dimension with a squared sine function (SSB = 3).

Alanine and lactic acid formation experiments. To observe the formation of alanine from acetaldehyde in the investigated system, bottle setup S2* was used as it showed a high amount of acetaldehyde due to the acidic conditions. 2 µl of ammonia solution (25%) was added to 200 µl of S2* solution contained in a 3 mm NMR tube with a final concentration of 140 mM. This reaction mixture was measured *via* NMR. A first 1D-^{1}H spectrum was acquired immediately after the addition and a second after a 24 h incubation at 100 °C. Spectra were acquired with a simple 90-degree pulse (13.75 us) and on-resonance pre-saturation during the relaxation delay. Eight scans were acquired for each sample with a 4-second acquisition time and a relaxation delay of 16 s to allow for quantitative information.

The same experiment was repeated with sulfuric acid instead of ammonia to further prove the origin of lactic acid in this specific experimental setup.

Acquisition parameters for NMR experiments with the purpose of compound identification or spectra not shown in the main text can be found in Supplementary Table 2. LC-MS parameters can be found in Supplementary Methods page S14.

pH-Measurement. The pH of the solutions was determined with a Metrohm Ecotrode Gel pH-Electrode (Mettler Toledo, Gießen, Germany) and checked with VWR chemicals Dosatest pH test strips pH 0-14 (VWR International, Radnor, Pennsylvania, USA).

Data availability

The authors declare that [the/all other] data supporting the findings of this study are available within the paper [and its supplementary information files]. Further data that support the findings of this study are available from the corresponding author upon reasonable request. All NMR spectra can be found in Supplementary Data 1

Received: 27 September 2022; Accepted: 7 February 2023;
Published online: 22 February 2023

References

1. Acetylene as Fast Food. Implications for development of life on anoxic primordial earth and in the outer solar system. *Astrobiology* **8**, 45–58 (2008).
2. Trainer, M. G. et al. Haze aerosols in the atmosphere of early earth: manna from heaven. *Astrobiology* **4**, 409–419 (2004).
3. Niemann, H. B. et al. The abundances of constituents of Titan's atmosphere from the GCMS instrument on the Huygens probe. *Nature* **438**, 779–784 (2005).
4. Menor-Salván, C., Ruiz-Bermejo, M., Osuna-Esteban, S., Muñoz-Caro, G. & Veintemillas-Verdaguer, S. Synthesis of polycyclic aromatic hydrocarbons and acetylene polymers in ice: a prebiotic scenario. *Chem. Biodivers.* **5**, 2729–2739 (2008).
5. Abbas, O. & Schulze-Makuch, D. Acetylene-based pathways for prebiotic evolution on Titan. *Exo-Astrobiology* **518**, 345–348 (2002).
6. Kutscheroff, M. Ueber eine neue methode direkter addition von wasser (hydratation) an die kohlenwasserstoffe der acetylenreihe. *Ber. der Dtsch. Chemischen Ges.* **14**, 1540–1542 (1881).
7. Keith, J. A. & Henry, P. M. The mechanism of the wacker reaction: a tale of two hydroxypalladations. *Angew. Chem. Int. Ed.* **48**, 9038–9049 (2009).
8. Muchowska, K. B., Varma, S. J. & Moran, J. Synthesis and breakdown of universal metabolic precursors promoted by iron. *Nature* **569**, 104–107 (2019).
9. Murray, B. A. Reactions of Aldehydes and Ketones and Their Derivatives. In: *Organic Reaction Mechanisms · 2015* (2019).
10. Schmitt-Kopplin, P. et al. High molecular diversity of extraterrestrial organic matter in Murchison meteorite revealed 40 years after its fall. *Proc. Natl Acad. Sci.* **107**, 2763–2768 (2010).
11. Marcellus, P. D. et al. Aldehydes and sugars from evolved precometary ice analogs: Importance of ices in astrochemical and prebiotic evolution. *Proc. Natl Acad. Sci.* **112**, 965–970 (2015).
12. Martín-Doménech, R., Öberg, K. I. & Rajappan, M. Formation of NH2CHO and CH3CHO upon UV photoprocessing of interstellar ice analogs. *Astrophys. J.* **894**, 98. (2020).
13. Aponte, J. C., Whitaker, D., Powner, M. W., Elsila, J. E. & Dworkin, J. P. Analyses of aliphatic aldehydes and ketones in carbonaceous chondrites. *ACS Earth Space Chem.* **3**, 463–472 (2019).
14. Simkus, D. N., Aponte, J. C., Hilts, R. W., Elsila, J. E. & Herd, C. D. K. Compound-specific carbon isotope compositions of aldehydes and ketones in the Murchison meteorite. *Meteorit. Planet. Sci.* **54**, 142–156 (2019).
15. Jungclaus, G. A., Yuen, G. U., Moore, C. B. & Lawless, J. G. Evidence for the presence of low molecular weight alcohols and carbonyl compounds in the murchison meteorite†. *Meteoritics* **11**, 231–237 (1976).
16. Peltzer, E. T., Bada, J. L., Schlesinger, G. & Miller, S. L. The chemical conditions on the parent body of the murchison meteorite: some conclusions based on amino, hydroxy and dicarboxylic acids. *Adv. Space Res.* **4**, 69–74 (1984).
17. Kitadai, N. & Maruyama, S. Origins of building blocks of life: a review. *Geosci. Front.* **9**, 1117–1153 (2018).
18. Burton, A. S., Stern, J. C., Elsila, J. E., Glavin, D. P. & Dworkin, J. P. Understanding prebiotic chemistry through the analysis of extraterrestrial amino acids and nucleobases in meteorites. *Chem. Soc. Rev.* **41**, 5459–5472 (2012).
19. Oba, Y. et al. Identifying the wide diversity of extraterrestrial purine and pyrimidine nucleobases in carbonaceous meteorites. *Nat. Commun.* **13**, 2008 (2022).
20. Meinert, C. et al. Ribose and related sugars from ultraviolet irradiation of interstellar ice analogs. *Science* **352**, 208–212 (2016).
21. Ruf, A. et al. The challenging detection of nucleobases from pre-accretional astrophysical ice analogs. *Astrophys. J.* **887**, L31 (2019).
22. Wächtershäuser, G. Before enzymes and templates: theory of surface metabolism. *Microbiol. Rev.* **52**, 452–484 (1988).
23. Huber, C. & Wächtershäuser, G. Activated acetic acid by carbon fixation on (Fe,Ni)S under primordial conditions. *Science* **276**, 245–247 (1997).
24. Scheidler, C., Sobotta, J., Eisenreich, W., Wächtershäuser, G. & Huber, C. Unsaturated C3,5,7,9-monocarboxylic acids by aqueous, one-pot carbon fixation: possible relevance for the origin of life. *Sci. Rep.* **6**, 27595 (2016).
25. Geisberger, T., Sobotta, J., Eisenreich, W. & Huber, C. Formation of thiophene under simulated volcanic hydrothermal conditions on earth—implications for early life on extraterrestrial planets? *Life* **11**, 149 (2021).
26. Schink, B. Fermentation of acetylene by an obligate anaerobe, pelobacter acetylenicus sp. nov. *Arch. Microbiol.* **142**, 295–301 (1985).
27. Breslow, R. On the mechanism of the formose reaction. *Tetrahedron Lett.* **1**, 22–26 (1959).
28. Nielsen, A. T., Houlihan, W. J. The Aldol Condensation. In: *Organic Reactions*.
29. Geisberger, T. et al. Evolutionary steps in the analytics of primordial metabolic evolution. *Life* **9**, 50 (2019).
30. Reppe, W. Carbonylierung I. Über die Umsetzung von Acetylen mit Kohlenoxyd und Verbindungen mit reaktionsfähigen Wasserstoffatomen Synthesen α,β-ungesättigter Carbonsäuren und ihrer Derivate. *Justus Liebigs Ann. der Chem.* **582**, 1–37 (1953).
31. Cremer, D., Crehuet, R. & Anglada, J. The ozonolysis of acetylenea quantum chemical investigation. *J. Am. Chem. Soc.* **123**, 6127–6141 (2001).
32. Sobotta, J. et al. A possible primordial acetyleno/carboxydotrophic core metabolism. *Life* **10**, 35 (2020).
33. Morooka, S., Matubayasi, N. & Nakahara, M. Hydrothermal C−C bond formation and disproportionation of acetaldehyde with formic acid. *J. Phys. Chem. A* **112**, 6950–6959 (2008).
34. Masamba, W. Petasis vs. strecker amino acid synthesis: convergence, divergence and opportunities in organic synthesis. *Molecules* **26**, 1707 (2021).
35. Frenkel-Pinter, M., Sargon, A. B., Glass, J. B., Hud, N. V. & Williams, L. D. Transition metals enhance prebiotic depsipeptide oligomerization reactions involving histidine. *RSC Adv.* **11**, 3534–3538 (2021).
36. Teichert, J. S., Kruse, F. M. & Trapp, O. Direct prebiotic pathway to DNA nucleosides. *Angew. Chem. Int. Ed.* **58**, 9944–9947 (2019).
37. Strecker, A. Ueber die künstliche Bildung der Milchsäure und einen neuen, dem Glycocoll homologen Körper. *Justus Liebigs Ann. der Chem.* **75**, 27–45 (1850).
38. Goldford, J. E., Hartman, H., Smith, T. F. & Segrè, D. Remnants of an ancient metabolism without phosphate. *Cell* **168**, 1126–1134.e1129 (2017).
39. Ruf, A. et al. Sulfur ion irradiation experiments simulating space weathering of Solar System body surfaces. *A&A* **655**, A74 (2021).
40. Wächtershäuser, G. Evolution of the first metabolic cycles. *Proc. Natl Acad. Sci.* **87**, 200–204 (1990).
41. de Duve, C. *Blueprint for a cell: the nature and origin of life*. N. Patterson (1991).
42. Cooper, G. W., Onwo, W. M. & Cronin, J. R. Alkyl phosphonic acids and sulfonic acids in the Murchison meteorite. *Geochimica et. Cosmochimica Acta* **56**, 4109–4115 (1992).
43. Frenkel-Pinter, M. et al. Thioesters provide a plausible prebiotic path to proto-peptides. *Nat. Commun.* **13**, 2569 (2022).
44. Closs, A. C., Bechtel, M. & Trapp, O. Dynamic exchange of substituents in a prebiotic organocatalyst: initial steps towards an evolutionary system. *Angew. Chem. Int. Ed.* **61**, e202112563 (2022).
45. Cable, M. L., Vu, T. H., Maynard-Casely, H. E., Choukroun, M. & Hodyss, R. The acetylene-ammonia co-crystal on titan. *ACS Earth Space Chem.* **2**, 366–375 (2018).
46. Melin, H., Fletcher, L. N., Irwin, P. G. J. & Edgington, S. G. Jupiter in the ultraviolet: acetylene and ethane abundances in the stratosphere of Jupiter from cassini observations between 0.15 and 0.19 μm. *Astronomical J.* **159**, 291 (2020).
47. Rimmer, P. B. & Shorttle, O. Origin of life's building blocks in carbon- and nitrogen-rich surface hydrothermal vents. *Life* **9**, 12 (2019).

Acknowledgements

This research was funded by the Deutsche Forschungsgemeinschaft (DFG, German Research Foundation) – Project-ID 364653263 – TRR 235 (CRC 235). CS and CH thank the Hans-Fischer-Gesellschaft (D-Munich) for financial support. Furthermore, funded by the Deutsche Forschungsgemeinschaft (DFG, German Research Foundation) under Germany´s Excellence Strategy - EXC 2094 - 390783311 (A.R.).

Author contributions

P.D. conceived and designed the analysis, collected the data, performed experiments, performed data analysis, and wrote the manuscript. T.G., C.S., and C.H. contributed analysis tools. T.G. and C.S. performed experiments. C.H. edited the manuscript. Y.Y. collected data and performed analysis. A.R. edited the manuscript. N.H. co-supervised

the project and edited the manuscript. P.S.K. provided funding, conceived the analysis, co-supervised the project, wrote and edited the manuscript.

Funding

Open Access funding enabled and organized by Projekt DEAL.

Competing interests

The authors declare no competing interests.

Additional information

Supplementary information The online version contains supplementary material available at https://doi.org/10.1038/s42004-023-00833-5.

Correspondence and requests for materials should be addressed to Philippe Schmitt-Kopplin.

Peer review information *Communications Chemistry* thanks Matthew Pasek, Moran Frenkel-Pinter and the other, anonymous, reviewer for their contribution to the peer review of this work.

Reprints and permission information is available at http://www.nature.com/reprints

Publisher's note Springer Nature remains neutral with regard to jurisdictional claims in published maps and institutional affiliations.

7.1.2 Appendix Supplementary 1

Supplementary Information

Formation, stabilization, and fate of acetaldehyde and higher aldehydes in an autonomously changing prebiotic system emerging from acetylene

Philippe Diederich [a], Thomas Geisberger [b], Yingfei Yan [a], Christian Seitz [b], Alexander Ruf [c,d], Claudia Huber [b], Norbert Hertkorn[a], Philippe Schmitt-Kopplin [a, e, f*]

[a] Helmholtz Munich, Research Unit Analytical BioGeoChemistry, Neuherberg, Germany.
[b] Technical University of Munich Structural Membrane Biochemistry, BNMRZ, Munich, Germany
[c] Excellence Cluster ORIGINS, Boltzmannstraße 2, 85748 Garching, Germany
[d] LMU Munich, Faculty of Physics, Schellingstraße 4, 80799 Munich, Germany

[e] Technical University of Munich, Analytische Lebensmittel Chemie; Maximus-von-Forum 2, 85354 Freising, Germany.

[f]Max Planck Institute for Extraterrestrial Physics, Center for Astrochemical Studies, Gießebachstraße 1, 85748 Garching bei München, Germany.

[*]Corresponding author: Research Unit Analytical BioGeoChemistry, Helmholtz Zentrum München–German Research Center for Environmental Health, Neuherberg, Germany

Email: schmitt-kopplin@helmholtz-muenchen.de

Supplementary methods

Experiments with trace amounts of dissolved ions

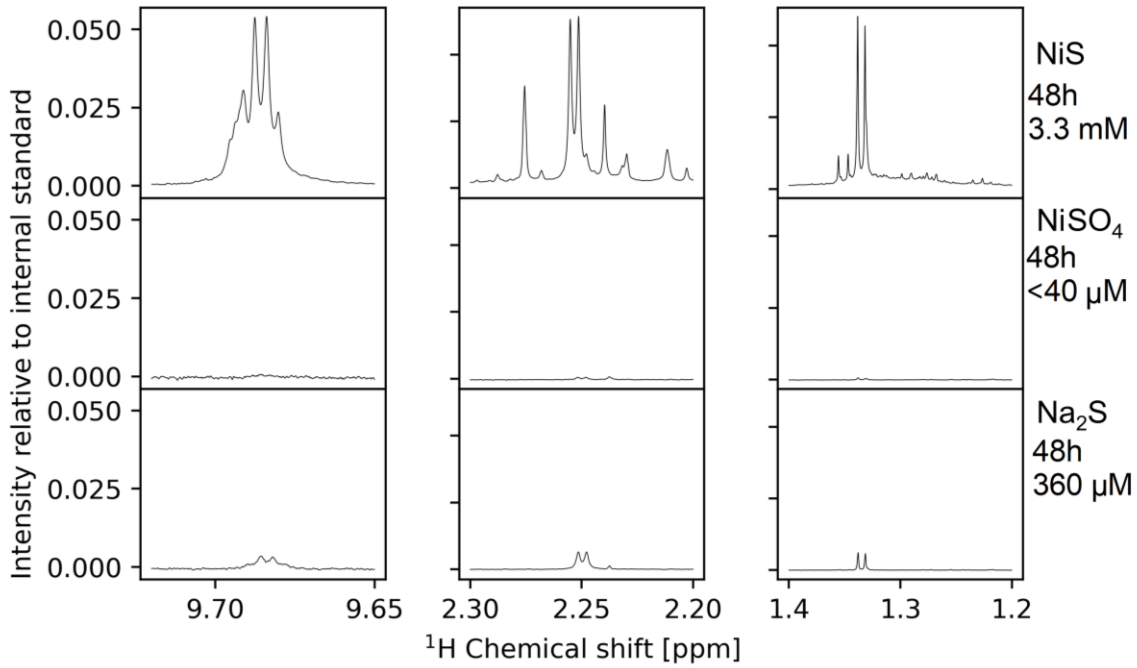

Supplementary Figure 1: 1D-^{1}H NMR spectra comparing the acetaldehyde yield of identical setups differing only in the potential catalyst. The NMR signals of the aldehyde hydrogen signal (column on the left), the methyl hydrogen of acetaldehyde (column in the middle), and the methyl hydrogen of the hydrate form of acetaldehyde (right column) are shown. The annotation on the right-hand side indicates the added catalyst, the incubation time, and the resulting yield in acetaldehyde.

Control bottles: setup S3_Supplement

A 125 ml glass serum bottle was charged with 1 mg $NiSO_4$ • 6 H_2O (99%, Aldrich) for the trace nickel experiment and with 10 µl of argon-saturated 1M Na_2S (solid Na_2S: 99.99%, Sigma-Aldrich) solution for the trace sulphide experiment. and sealed with a silicon stopper. Three times the bottle was evacuated and filled with argon, finally ending in a deaerated state. Subsequently, the bottle was filled with argon-saturated water (calculated for the end volume of 5 ml) with 1.0 mL 1M NaOH solution and finally with 60 ml CO (2.44 mmol) and 60 ml (2.53 mmol) acetylene (acetone free), using gastight syringes for the injections. Reactions were carried out at 105 °C. After a reaction time of up to 7 days, the reaction mixture was allowed to cool down. Acetylene and CO were replaced by argon in a blank run with otherwise identical composition.

Experiments with FiS and NiS/FeS

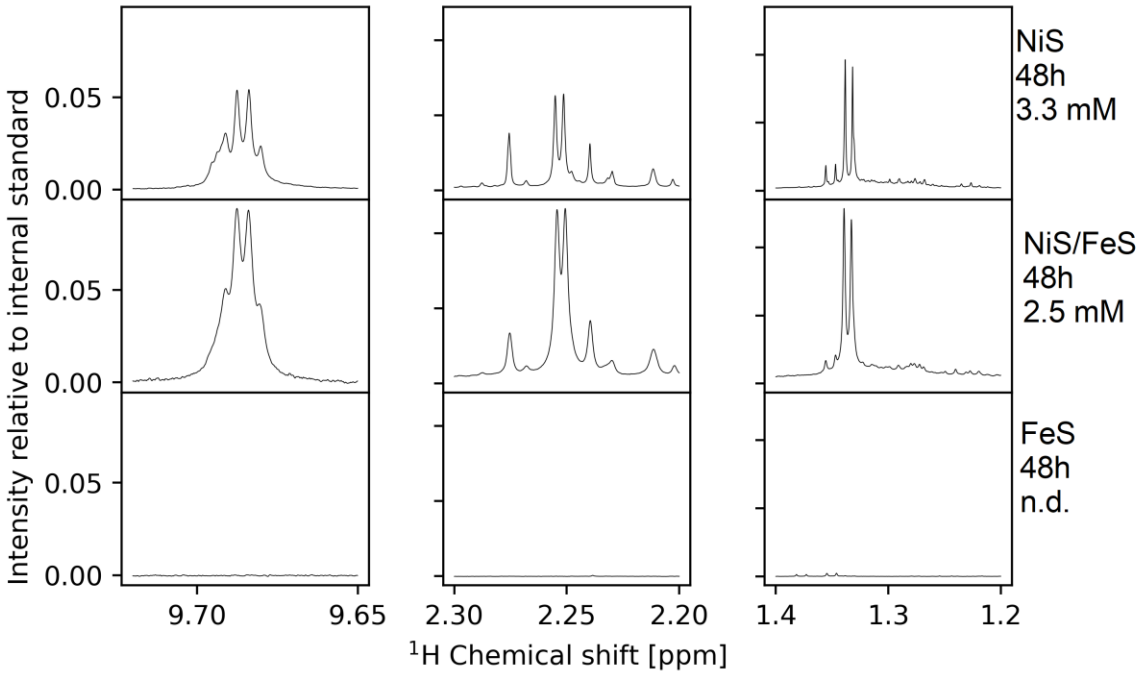

Supplementary Figure 2: Comparative acetaldehyde formation in setups with different catalyst compositions. The NMR signals of the aldehyde hydrogen signal (column on the left), the methyl hydrogen of acetaldehyde (column in the middle), and the methyl hydrogen of the hydrate form of acetaldehyde (right column) are shown. The annotation on the right-hand side indicates the added catalyst, the incubation time, and the resulting yield in acetaldehyde. The seemingly higher intensity in the NiS/FeS setup than the NiS setup stems purely from the broadened linewidth in the NiS/FeS setup and is an artifact of the processing. The concentrations derived from the peak integrals show the correct result.

Control bottles: setup S4_Supplement

A 125 ml glass serum bottle was charged with 131 mg $NiSO_4$ • 6 H_2O (99%, Aldrich) and 139 mg $FeSO_4$ • 7 H_2O (99%, Aldrich) for the NiS/FeS experiment and with 278 mg $FeSO_4$ • 7 H_2O (99%, Aldrich) for the FeS-only experiment. and sealed with a silicon stopper. Three times the bottle was evacuated and filled with argon, finally ending in a deaerated state. Subsequently, the bottle was filled with argon-saturated water (calculated for the end volume of 5 ml) with 1.0 mL argon-saturated 1M Na_2S (solid Na_2S: 99.99%, Sigma-Aldrich) solution with 1.0 mL 1M NaOH solution and finally with 60 ml CO (2.44 mmol) and 60 ml (2.53 mmol) acetylene (acetone free), using gastight syringes for the injections. Reactions were carried out at 105 °C. After a reaction time of up to 7 days, the reaction mixture was allowed to cool down. Acetylene and CO were replaced by argon in a blank run with otherwise identical composition.

Unlabelled versus labelled experiments

^{13}C labelling leads to additional splitting in 1D-^{1}H NMR spectra because of the NMR activity of this isotope. $^{1}J_{CH}$-couplings between the detected hydrogen signal and the ^{13}C-atom are 120-180 Hz. The absence of such a coupling in ^{13}CO-labelled experiments establishes acetylene as the origin of all detected aldehydes. On the other hand, experiments with ^{13}C-labelled acetylene showed the mentioned $^{1}J_{CH}$-splittings. $^{1}J_{CH}$ and $^{2}J_{CH}$ couplings were clearly observed.

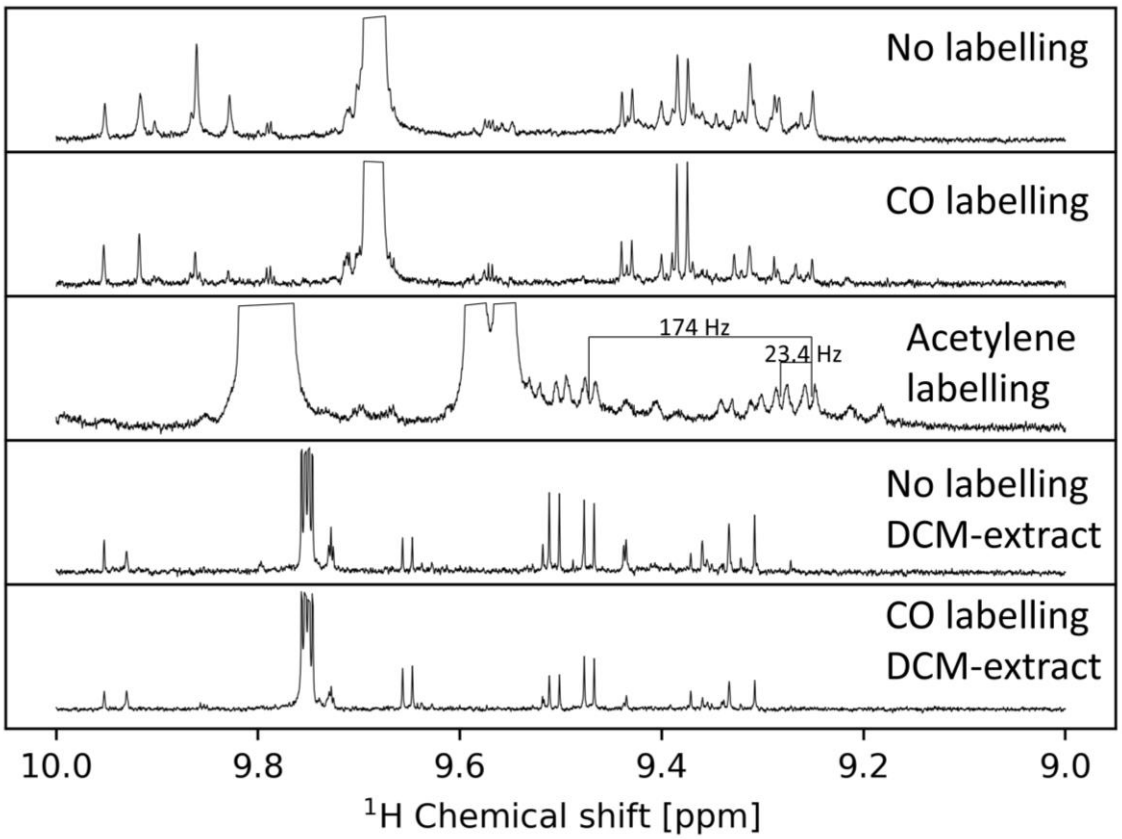

Supplementary Figure 3: 1D- ^{1}H NMR spectra of the aldehyde region for labelled and unlabelled samples. Additional couplings through ^{13}C labelling are added for the direct aldol condensation product of acetaldehyde, crotonaldehyde.

Acetaldehyde from acetylene alone

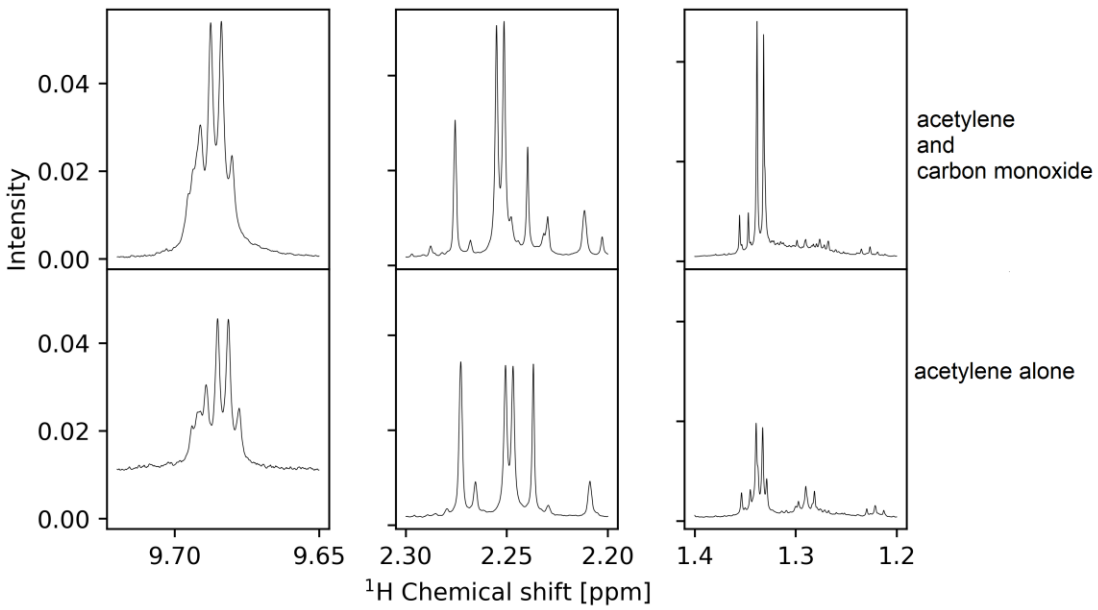

Supplementary Figure 4: Comparative acetaldehyde formation in setups with (top) and without (bottom) carbon monoxide. The NMR signals of the aldehyde hydrogen signal (column on the left), the methyl hydrogen of acetaldehyde (column in the middle), and the methyl hydrogen of the hydrate form of acetaldehyde (right column) are shown. The annotation on the right-hand side indicates the added catalyst, the incubation time, and the resulting yield in acetaldehyde.

Formic acid from acetylene

Based on the same principle, namely the splitting of the hydrogen signal, the origin of formic acid could be traced back partially to acetylene. Experiments with solely acetylene also produced formic acid.

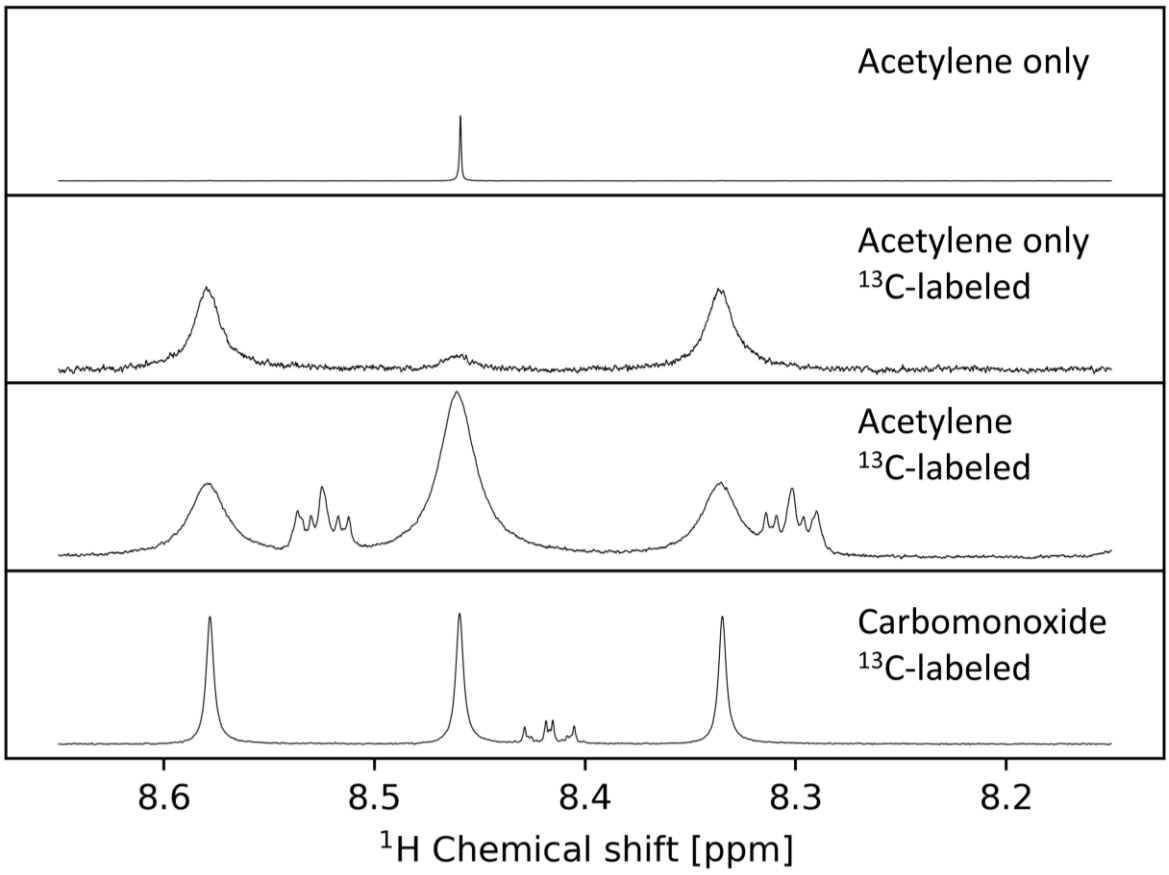

Supplementary Figure 5: 1D-1H NMR spectra of setups with varying ^{13}C labels showing the origin of formic acid.

pH influence on the reactivity of acetaldehyde

Prove of a strongly decreased aldol condensation of acetaldehyde under the exact reaction conditions. Acetaldehyde (300mM) was reacted in water containing NiS as a catalyst. The reaction time was 25 hours at 100°C. Acidification of the pH 4 reaction was achieved by adding formic acid to the water. The alkaline reaction also contained formic acid and was adjusted to pH 11 with sodium hydroxide. Both spectra are normalised to the TSP (0.2 mM) signal at 0 ppm. The acidified reaction only shows the first aldol condensation product but-2-enal. The alkaline reaction shows a much higher aldehyde diversity and greater complexity in general.

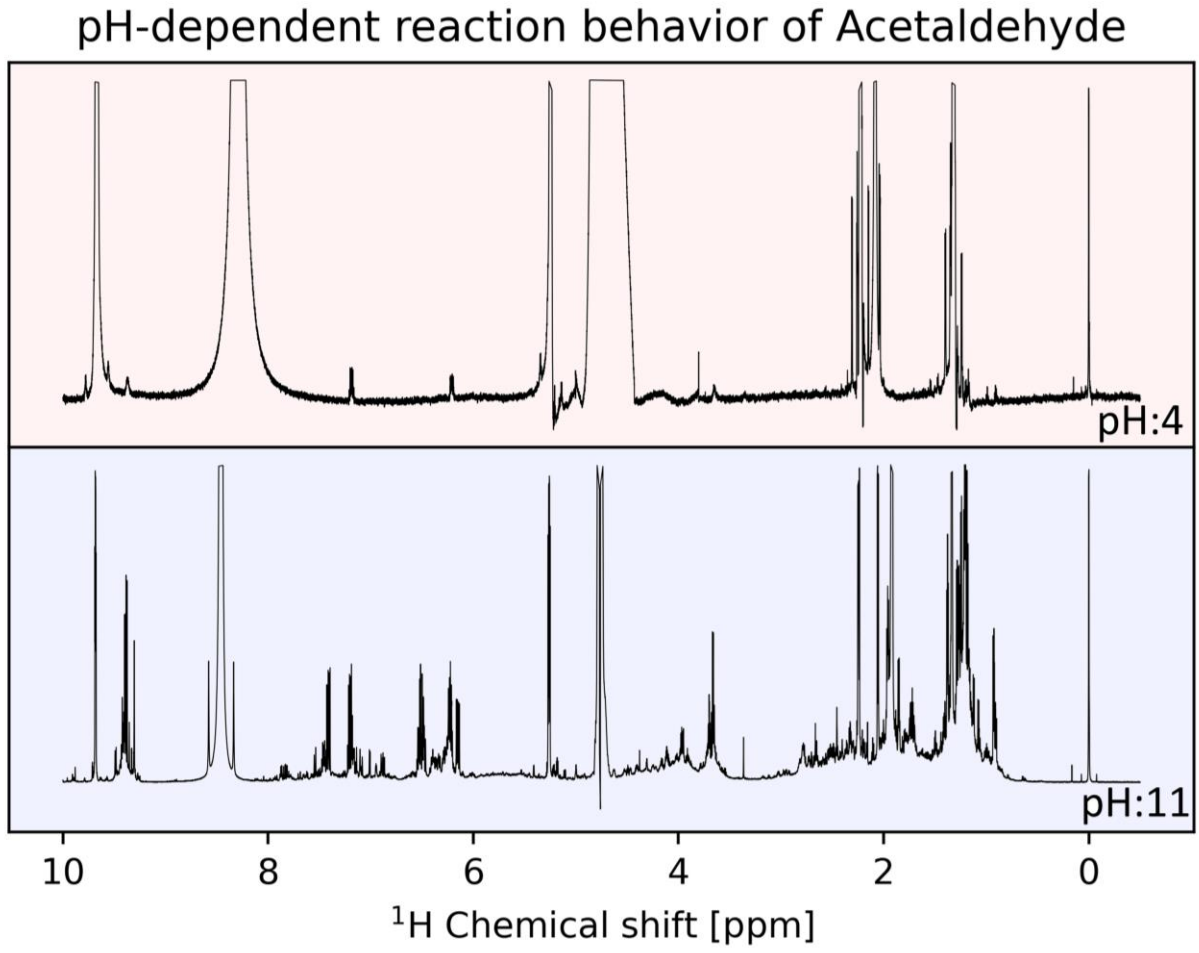

Supplementary Figure 6: 1D-1H NMR spectra of the same concentration of acetaldehyde standard in water over an NiS catalyst, spiked with formic acid at different pH. Samples were incubated for 24 hours at 378K.

Identification of 4-oxobutan-2-sulfonic acid

To prove the annotation of the ^{1}H-signals (9.69(dd), 3.55(ddd), 2.96(ddd), 2.72 (ddd), 1.35 (d)) with the structure of 4-oxobutan-2-sulfonic acid, a synthesis following the hypothesised formation route was performed. Acetaldehyde (5 mM) was reacted with a Na_2S-solution (10 mM in the reaction mixture) in water. After 60 minutes at 100°C, the annotated signals could be detected in a 1D-^{1}H spectrum. This reaction solution was then diluted in methanol and analysed at two different concentrations with an FT-ICR-MS showing a peak at m/z 151.00700 with an intensity correlating with the different concentration levels and not found in the blank. The high mass accuracy of FT-ICR-MS allowed for the direct annotation of the elemental composition, namely $C_4H_7O_4S^-$ as negative ionization mode was used for the detection of sulfonic acid. The exact elemental composition together with the connectivity and shift information of the NMR measurement made the identification of the compound possible.

Oxobutanesulfonic acid (hydrate): NMR (800 MHz, H2O/D2O): δ 5.22 (dd, J=4.95 Hz, 6.78 Hz, 1H), δ 3.02 (ddq, J=9.3 Hz, 4.64 Hz, 6.9 Hz, 1H), δ 2.17 (ddd, J =4.65 Hz, 6.9 Hz, 14 Hz, 1H), δ 1.75 (ddd, J = 4.96 Hz, 9.03 Hz, 14 Hz, 1H), 1.33 (d, J= 6.9 Hz, 3H), ^{13}C-^{1}H NMR (200MHz/800MHz, H2O/D2O): δ 92, 55, 42, 17.5.

Oxobutanesulfonic acid: NMR (800 MHz, H2O/D2O): δ 9.69 (dd, 1H), δ 3.54 (m, width=42 Hz, 1H), δ 2.96(ddd, J = 1.96 Hz, 6.45 Hz, 17.7 Hz, 1H), δ 2.72 (m, , width=40 Hz, 1H), 1.35 (d, J= 6.92 Hz, 3H), ^{13}C-^{1}H NMR (200MHz/800MHz, H2O/D2O): δ 207, 53, 43, 17; FT-ICR-MS (*m/z*): [M]- calcd. For $C_4H_7O_4S$, 151.00705; found, 151.00700.

Compound identification and quantification

The hydrogen and carbon shifts of all mentioned compounds are reported in the table below. The different methods of identification are noted in the column “Identification”. Standard means identification by spiking a standard into the mixture to observe an increase of the compound signal. For some compounds with very characteristic NMR shifts and high probability to be formed or unstable compounds only the NMR shifts are reported. Identification of 4-oxobutan-2-sulfonic acid was already described above. Signals used for quantification are also reported together with possible interferences leading to higher quantification error.

Compound	Identification	^{1}H-shift (ppm)	13C-shift (ppm)	Quantified signals	Interference
Acetaldehyde	Standard	9.68(q), 2.25(d)	33, 209.9	2.25 (d)	/
Acetaldehyde (hydrate)	Standard	5.26(q), 1.33(d)	26, 93	5.26(q)	Solvent suppression
Acrylic acid	Standard	6.14(dd), 6.03(dd), 5.66(dd)	125.5, 135.7, 177	6.14(dd), 6.03(dd), 5.66(dd)	/
Oxobutanesulfonic acid	1H/13C shift LC-MS mass + fragmentation FT-MS elemental composition	9.69(dd), 3.55(ddd), 2.96(ddd), 2.72 (ddd), 1.35 (d)	17, 43, 53, 207.6	/	/
Oxobutanesulfonic acid (hydrate)	1H/13C shift	5.22(dd), 3.02(m), 2.17(ddd), 1.75 (ddd), 1.33(d)	17.5, 42, 55, 92	5.22(dd)	Solvent suppression
Crotonaldehyde	1H/13C shift	9.38, 7.2,	201.69,	9.38(d)	/

		6.23, 2.05			
Alanine	Standard	1.25-1.48 (d), 3.6-3.8(q) strong pH dependency	23, 53, 178	1.48 (d)	Slight overlap
Lactic acid	Standard	4.13(q), 1.33(d)	/	4.13	/
Aminoethanol	1H/13C shift	1.194, 3.758	22.0, 66.8	1.194	/
Formic acid	Standard	8.46(s)	174	8.46	/
Acetic acid	1H/13C shift	1.97(s)	26, 184	1.97	/
Ethanol	1H shift	1.19(t), 3.66(q)	/	3.66	low S/N
Hydroxypropannitrile	1H/13C shift	1.569(d), 4.75(q)	23, 59, 123	1.57	/

Bottle setup	pH	Incubation time	Acetaldehyde (mM)	Acetaldehyde (hydrate) (mM)	Acrylic acid (mM)	Croton- aldehyde (mM)
S1	11	8 hours	0.16/0.48/0.45	0.24/0.91/1.10	0.46/0.28/0.20	nd
S1	10	24 hours	0.85/0.99/0.99	1.51/1.65/1.72	0.75/0.73/0.72	nd
S1	8	48 hours	2.07/1.03/1.14	3.07/1.60/1.66	0.766/0.88/0.93	0.04/qualitative
S1	7.6	7 days	1.08/1.01/1.22	1.24/1.19/1.32	0.60/0.57/0.46	qualitative
S1*	3	7days	18/19/18	19/22/21	nd	nd
S2	8	7 days	0.33/0.30/0.32	0.41/0.57/0.58	2.24/0.97/1.01	nd
S2*	3	7 days	11/13/13	13/16/17	nd	nd
Bottle	**pH**	**Incubation**	**Lactic acid (mM)**	**Aminoethanol (mM)**	**Formic acid (mM)**	**Acetic acid (mM)**
S1	11	8 hours	nd	nd	4.55/2.81/2.92	0.948/0.536/0.6
S1	10	24 hours	nd	nd	8.75/8.52/8.28	0.72/0.64/0.72
S1	8	48 hours	nd	nd	7.20/10.72/8.98	0.92/0.79/0.79
S1	7.6	7 days	nd	nd	8.48/9.36/11.7	1.02/0.98/1.032
S1*	3	7days	nd	nd	Not quantified	2.07/1.89
S2	8	7 days	nd	nd	3.17/2.00/2.01	0.50/0.33/0.31
S2*	3	7 days	0.16/0.17/0.17	nd	Not quantified	1.03/0.95
Bottle	**pH**	**Incubation**	**Alanine (mM)**	**Ethanol (mM)**	**2-hydroxypropannitrile (mM)**	**Oxobutanesulfonic acid (hydrate) (mM)**
S1	11	8 hours	nd	qualitative	nd	0.16/0.39/0.33
S1	10	24 hours	nd	qualitative	nd	0.64/0.62/0.70
S1	8	48 hours	nd	qualitative	nd	1.15/0.46/0.68
S1	7.6	7 days	nd	0.02/0.01/0.01	nd	0.6/0.57/0.58
S1*	3	7days	nd	0.59/0.43	nd	nd
S2	8	7 days	0.18/0.29/0.28	qualitative	nd	qualitative
S2*	3	7 days	nd	0.265/0.288	14.71/8.14/8.02	nd

Supplementary table 1: Concentration values of reported compounds for every replicate of the various setups. "nd" for not detected.

NMR experiment parameters for identification

Setup	Experiment	Spectral width (F2)	Spectral width (F1)	Number of scans	Increments	Relaxation delay (s)	Acquisition time (s)	Mixing time (ms)	1J coupling
S1	TOCSY	12 ppm	12 ppm	8	857	1.5	1	70	/
S1	HSQC	14 ppm	245 ppm	800	249	1.75	0.25	/	145
S2	TOCSY	11 ppm	11 ppm	16	1024	0.5	1.5	80	/
S2	HSQC-TOCSY	10 ppm	190 ppm	320	438	1.5	0.25	70	145
S2	HMBC	11 ppm	240 ppm	1280	137	0.5	1.5	/	145
S2*	HSQC	12 ppm	190 ppm	24	59	1.75	0.25	/	145
S2*	HMBC	12 ppm	230 ppm	256	39	0.5	1	/	145

Supplementary table 2: NMR experiment parameters for various spectra

LC-MS parameters

Materials

L-alanine (99%), acetonitrile and methanol (both LC-MS grade) were purchased from Merck (Darmstadt, Germany). Formic acid (98%, for mass spectrometry) was obtained from Honeywell Fluka (North Carolina, USA). Ammonium formate (10 M in water) was ordered from Sigma Aldrich (Steinheim, Germany). Purified water (18.2 MΩ) was from a Milli-Q integral system (Billerica, MA, USA). ESI-L low concentration tuning mix was supplied by Agilent (Santa Clara, CA, USA).

HILIC-MS/MS analysis

Samples were diluted 1:5 (*v*/*v*) with methanol, and analyzed by UPLC system (Waters Acquity, Milford, MA, USA) coupled to a Quadrupole time-of-flight (QTOF) mass spectrometer (MS) (Bruker maXis, Bremen, Germany). A hydrophilic interaction liquid chromatography (HILIC) column ZIC-cHILIC (100 x 2.1 mm, 3 µm, Merck, Darmstadt, Germany) was used at flow rate of 0.5 mL/min under 40 °C for chromatographic separation. 5:95 (*v*/*v*) acetonitrile:water and 95:5 (*v*/*v*) acetonitrile:water, both with 5 mM ammonium formate and 0.1% formic acid, were used as eluent A and B, respectively. The gradient was: 0 min, 99.9% B; 2 min, 99.9% B; 13 min, 56% B; 14 min, 30% B; 14.1 min, 10 %B; 16 min, 10 %B; 16.1 min, 99.9 %B. The column was equilibrated at 99.9 %B for 3 min after each injection and 5 µL was injected for each sample.

The MS was operated in both positive and negative ionization mode with mass range from m/z 50 to m/z 1500. MS settings were: nebulizer pressure 2 bar, capillary voltage 4500 V for positive mode and 4000 V for negative mode, dry gas 10 L/min with temperature 200 °C. Data were obtained with an acquisition rate of 5 Hz in data-dependent mode. MS/MS spectra were triggered for the three highest MS1 ions in each precursor scan with collision energy of 20 eV. Diluted ESI-L tuning mix (1:4 (*v*/*v*) with 75:25 (*v*/*v*) acetonitrile:water) was analyzed from 0.1 to 0.3 minutes in each measurement for internal recalibration.

Data processing

Raw HILIC-MS/MS data were calibrated and converted to mzXML format by Bruker DataAnalysis 5.0 software (Bremen, Germany). The data processing, including peak

picking, peak alignment and correspondence, feature annotation, and data cleaning were done using in-house script based on XCMS and CAMERA packages in R[1, 2]. The fragmentation pattern, characterized by fragment ions of HSO_3^- (*m/z* 80.9641), $SO_3^{\bullet-}$ radicals (*m/z* 79.9573), $HSO4^-$ (*m/z* 96.9590), and neutral losses of H_2SO_3(81.9725 Da), SO_3(79.9568 Da), H_2SO_4(97.9674 Da) for sulfonic acids in negative ionization mode, were summarized and used for searching compounds containing the sulfonic acid group[3, 4]. The consensus MS/MS spectra were screened with an error of 0.005 Da and features with MS/MS spectra containing at least $HSO3^-$ fragments were kept as candidates. The formula of potential sulfonic acids was calculated by SIRIUS software based on MS/MS spectra [5]. The calculated formula with explained intensity > 0.6 and absolute ppm error < 10 were kept.

Alanine identified in the alkaline setup by LC-MS/MS							
Metabolite Name	**Molecular formula**	**RT**	**m/z**	**Theoretical m/z[1]**	**Error (ppm)**	**Ionization mode**	**Confidence Level[2]**
Alanine	C3H7O2N	8,24	90,0544	90,0550	6,10	positive	Level 2
Alanine	C3H7O2N	8,31	88,0395	88,0393	2,21	negative	Level 2
1: The theoretical m/z was calculated as $[M+H]^+$ for positive mode and $[M-H]^-$ for negative mode 2: The amino acids were identified by comparing to the reference standards analyzed with the same LC-MS/MS method. The identification level was assigned following the Metabolomics Standards Initiative [1]: Level 1: retention time difference < 0.2 min, error of m/z < 10 ppm, MS/MS spectra (main fragment ions matching within 0.01 Da) Level 2: retention time difference < 0.2 min, error of m/z < 10 ppm							
[1] Sumner L W, Amberg A, Barrett D, et al. Proposed minimum reporting standards for chemical analysis[J]. Metabolomics, 2007, 3(3): 211-221.							

Supplementray table 3 Identification of alanine via LC-MS/MS

Molecular formulas showing fragment characteristic for sulfonic acids

m/z	Retention time (min.)	Molecular formula	Adduct	Fragment HSO3-	Fragment SO3-	Neutral loss H2SO3	Neutral loss SO3	Theoretical m/z	Error (ppm)
106,9799	4,95	C2H4O3S	[M - H]-	Yes	Yes	NO	NO	106,9797	1,48
126,9515	3,91	CH4O3S2	[M - H]-	Yes	Yes	NO	NO	126,9518	-2,46
138,9519	0,58	C2H4O3S2	[M - H]-	Yes	Yes	NO	NO	138,9518	0,63
139,006	5,57	C3H8O4S	[M - H]-	Yes	Yes	NO	NO	139,0060	0,32
140,9671	3,45	C2H6O3S2	[M - H]-	Yes	Yes	NO	Yes	140,9675	-2,57
150,9697	8,72	C3H4O5S	[M - H]-	Yes	Yes	NO	NO	150,9696	0,86
151,006	4,97	C4H8O4S	[M - H]-	Yes	Yes	NO	NO	151,0060	0,29
151,0061	4,40	C4H8O4S	[M - H]-	Yes	Yes	NO	NO	151,0060	0,95
152,9859	8,12	C3H6O5S	[M - H]-	Yes	Yes	Yes	NO	152,9852	4,44
154,9468	0,94	C2H4O4S2	[M - H]-	Yes	Yes	NO	NO	154,9467	0,47
154,9837	3,14	C3H8O3S2	[M - H]-	Yes	Yes	NO	Yes	154,9831	3,79
161,0271	4,35	C6H10O3S	[M - H]-	Yes	Yes	NO	NO	161,0267	2,54
165,0217	4,72	C5H10O4S	[M - H]-	Yes	Yes	NO	NO	165,0216	0,57
166,9473	1,29	C3H4O4S2	[M - H]-	Yes	NO	NO	Yes	166,9467	3,44
166,983	4,26	C4H8O3S2	[M - H]-	Yes	Yes	NO	NO	166,9831	-0,67
166,9831	12,82	C4H8O3S2	[M - H]-	Yes	Yes	NO	NO	166,9831	-0,07
167,0009	4,64	C4H8O5S	[M - H]-	Yes	Yes	NO	NO	167,0009	0,18

167,0011	7,89	C4H8O5S	[M - H]-	Yes	Yes	Yes	NO	167,0009	1,37
168,9988	2,87	C4H10O3S2	[M - H]-	Yes	Yes	NO	NO	168,9988	0,22
170,9238	6,89	C2H4O3S3	[M - H]-	Yes	Yes	NO	NO	170,9239	-0,48
170,9415	8,30	C2H4O5S2	[M - H]-	Yes	NO	Yes	Yes	170,9416	-0,83
170,9421	10,25	C2H4O5S2	[M - H]-	Yes	Yes	NO	NO	170,9416	2,68
174,919	2,51	CH4O4S3	[M - H]-	Yes	Yes	NO	NO	174,9188	1,16
175,0057	5,12	C6H8O4S	[M - H]-	Yes	Yes	NO	NO	175,0060	-1,46
177,0218	5,28	C6H10O4S	[M - H]-	Yes	Yes	NO	NO	177,0216	1,10
179,0373	4,53	C6H12O4S	[M - H]-	Yes	Yes	NO	NO	179,0373	0,25
180,9799	6,16	C4H6O6S	[M - H]-	Yes	Yes	Yes	Yes	180,9801	-1,30
180,9801	10,00	C4H6O6S	[M - H]-	Yes	Yes	NO	NO	180,9801	-0,19
180,9801	9,77	C4H6O6S	[M - H]-	Yes	Yes	NO	NO	180,9801	-0,19
181,0168	5,67	C5H10O5S	[M - H]-	Yes	Yes	NO	NO	181,0165	1,54
184,9572	7,24	C3H6O5S2	[M - H]-	Yes	NO	NO	Yes	184,9573	-0,49
188,9517	9,91	C2H6O6S2	[M - H]-	Yes	Yes	Yes	NO	188,9522	-2,68
189,0212	5,02	C7H10O4S	[M - H]-	Yes	Yes	Yes	NO	189,0216	-2,15
190,8959	1,92	CH4O3S4	[M - H]-	Yes	Yes	NO	Yes	190,8960	-0,28
190,9137	9,81	CH4O5S3	[M - H]-	Yes	NO	NO	NO	190,9137	-0,06
191,0002	5,34	C6H8O5S	[M - H]-	Yes	Yes	NO	NO	191,0009	-3,51
191,0013	8,04	C6H8O5S	[M - H]-	Yes	Yes	NO	NO	191,0009	2,25

191,0374	4,36	C7H12O4S	[M - H]-	Yes	Yes	NO	NO	191,0373	0,75
192,9986	4,21	C6H10O3S2	[M - H]-	Yes	Yes	NO	NO	192,9988	-0,84
193,0164	4,34	C6H10O5S	[M - H]-	Yes	Yes	NO	NO	193,0165	-0,62
193,0171	8,03	C6H10O5S	[M - H]-	Yes	Yes	NO	NO	193,0165	3,00
194,924	9,18	C4H4O3S3	[M - H]-	Yes	Yes	NO	Yes	194,9239	0,60
194,9415	5,72	C4H4O5S2	[M - H]-	Yes	Yes	NO	NO	194,9416	-0,72
194,9956	8,05	C5H8O6S	[M - H]-	Yes	NO	NO	NO	194,9958	-0,95
194,9959	9,64	C5H8O6S	[M - H]-	Yes	Yes	Yes	NO	194,9958	0,59
195,0319	6,04	C6H12O5S	[M - H]-	Yes	Yes	NO	NO	195,0322	-1,39
195,0323	5,49	C6H12O5S	[M - H]-	Yes	Yes	NO	NO	195,0322	0,66
195,0324	3,24	C6H12O5S	[M - H]-	Yes	Yes	NO	NO	195,0322	1,18
196,9394	4,00	C4H6O3S3	[M - H]-	Yes	Yes	NO	Yes	196,9395	-0,67
196,9567	3,50	C4H6O5S2	[M - H]-	Yes	NO	NO	NO	196,9573	-3,00
196,9751	9,69	C4H6O7S	[M - H]-	Yes	Yes	NO	NO	196,9750	0,26
197,0117	8,40	C5H10O6S	[M - H]-	Yes	Yes	Yes	NO	197,0114	1,34
197,0477	6,97	C6H14O5S	[M - H]-	Yes	Yes	NO	NO	197,0478	-0,61
198,0179	8,46	C5H11O6S	[M - H]-	Yes	Yes	NO	NO	198,0193	-6,87
198,9552	2,01	C4H8O3S3	[M - H]-	Yes	Yes	NO	Yes	198,9552	0,09
198,9729	5,42	C4H8O5S2	[M - H]-	Yes	NO	Yes	Yes	198,9729	-0,21
198,9731	3,03	C4H8O5S2	[M - H]-	Yes	Yes	NO	NO	198,9729	0,80

198,9731	2,60	C4H8O5S2	[M - H]-	Yes	Yes	NO	NO	198,9729	0,80
200,88	10,57	C2H2O3S4	[M - H]-	Yes	Yes	NO	NO	200,8803	-1,51
200,8804	11,56	C2H2O3S4	[M - H]-	Yes	Yes	NO	NO	200,8803	0,48
201,0217	4,37	C8H10O4S	[M - H]-	Yes	NO	NO	NO	201,0216	0,47
202,8962	4,54	C2H4O3S4	[M - H]-	Yes	Yes	NO	NO	202,8960	1,22
202,9136	8,81	C2H4O5S3	[M - H]-	Yes	Yes	NO	Yes	202,9137	-0,55
202,9136	13,21	C2H4O5S3	[M - H]-	Yes	Yes	NO	NO	202,9137	-0,55
202,9136	7,01	C2H4O5S3	[M - H]-	Yes	Yes	NO	Yes	202,9137	-0,55
203,0366	4,63	C8H12O4S	[M - H]-	Yes	Yes	NO	NO	203,0373	-3,23
204,9113	1,63	CH2O8S2	[M - H]-	Yes	Yes	NO	NO	204,9107	2,76
204,9299	9,43	C2H6O5S3	[M - H]-	Yes	Yes	NO	NO	204,9294	2,63
205,0165	8,40	C7H10O5S	[M - H]-	Yes	NO	NO	NO	205,0165	-0,10
205,0166	4,02	C7H10O5S	[M - H]-	Yes	Yes	NO	NO	205,0165	0,39
205,0167	3,78	C7H10O5S	[M - H]-	Yes	NO	NO	NO	205,0165	0,87
205,0533	4,16	C8H14O4S	[M - H]-	Yes	Yes	NO	NO	205,0529	1,92
206,9957	9,66	C6H8O6S	[M - H]-	Yes	Yes	Yes	NO	206,9958	-0,41
206,9958	5,12	C6H8O6S	[M - H]-	Yes	Yes	NO	NO	206,9958	0,07
207,032	3,28	C7H12O5S	[M - H]-	Yes	NO	NO	NO	207,0322	-0,82
207,0321	5,85	C7H12O5S	[M - H]-	Yes	Yes	Yes	NO	207,0322	-0,34
209,0475	5,41	C7H14O5S	[M - H]-	Yes	NO	NO	NO	209,0478	-1,53

209,0476	5,17	C7H14O5S	[M - H]-	Yes	NO	NO	NO	209,0478	-1,06
210,9723	2,72	C5H8O5S2	[M - H]-	Yes	NO	NO	NO	210,9729	-3,04
210,9729	3,04	C5H8O5S2	[M - H]-	Yes	Yes	NO	Yes	210,9729	-0,20
210,9731	7,23	C5H8O5S2	[M - H]-	Yes	Yes	NO	NO	210,9729	0,75
210,9895	4,02	C5H8O7S	[M - H]-	Yes	NO	NO	NO	210,9907	-5,69
211,0094	4,71	C6H12O4S2	[M - H]-	Yes	Yes	NO	NO	211,0093	0,35
212,9854	12,03	C8H6O5S	[M - H]-	Yes	NO	NO	NO	212,9852	0,84
212,9882	10,12	C5H10O5S2	[M - H]-	Yes	Yes	NO	NO	212,9886	-1,84
212,9883	7,59	C5H10O5S2	[M - H]-	Yes	NO	NO	NO	212,9886	-1,37
215,0018	11,64	C8H8O5S	[M - H]-	Yes	NO	NO	NO	215,0009	4,32
216,9296	5,13	C3H6O5S3	[M - H]-	Yes	Yes	NO	Yes	216,9294	1,10
217,0528	4,45	C9H14O4S	[M - H]-	Yes	Yes	NO	NO	217,0529	-0,49
219,0141	4,31	C8H12O3S2	[M - H]-	Yes	Yes	NO	NO	219,0144	-1,43
219,0325	5,63	C8H12O5S	[M - H]-	Yes	NO	NO	NO	219,0322	1,50
220,924	8,98	CH2O11S	[M - H]-	Yes	Yes	NO	Yes	220,9234	2,68
221,0116	4,74	C7H10O6S	[M - H]-	Yes	Yes	NO	Yes	221,0114	0,75
221,0473	4,79	C8H14O5S	[M - H]-	Yes	Yes	NO	NO	221,0478	-2,36
221,0475	4,16	C8H14O5S	[M - H]-	Yes	Yes	NO	NO	221,0478	-1,45
221,0482	5,15	C8H14O5S	[M - H]-	Yes	Yes	NO	NO	221,0478	1,72
223,0267	5,92	C7H12O6S	[M - H]-	Yes	Yes	NO	Yes	223,0271	-1,73

223,0267	5,34	C7H12O6S	[M - H]-	Yes	NO	NO	NO	223,0271	-1,73
223,0269	6,41	C7H12O6S	[M - H]-	Yes	NO	NO	NO	223,0271	-0,83
223,0273	4,49	C7H12O6S	[M - H]-	Yes	Yes	NO	NO	223,0271	0,96
223,0628	5,22	C8H16O5S	[M - H]-	Yes	Yes	NO	NO	223,0635	-3,01
226,8959	2,04	C4H4O3S4	[M - H]-	Yes	Yes	NO	Yes	226,8960	-0,23
226,9136	9,56	C4H4O5S3	[M - H]-	Yes	NO	NO	NO	226,9137	-0,49
226,9311	10,14	C4H4O7S2	[M - H]-	Yes	NO	NO	Yes	226,9315	-1,63
227,0044	6,60	C6H12O5S2	[M - H]-	Yes	NO	NO	NO	227,0042	0,70
227,0219	8,37	C6H12O7S	[M - H]-	Yes	NO	NO	NO	227,0220	-0,44
228,9112	12,65	C4H6O3S4	[M - H]-	Yes	Yes	NO	NO	228,9116	-1,76
228,9112	12,00	C4H6O3S4	[M - H]-	Yes	Yes	NO	NO	228,9116	-1,76
228,9288	5,43	C4H6O5S3	[M - H]-	Yes	NO	NO	NO	228,9294	-2,45
228,9833	6,39	C5H10O6S2	[M - H]-	Yes	NO	NO	Yes	228,9835	-0,90
230,9447	4,79	C4H8O5S3	[M - H]-	Yes	Yes	NO	NO	230,9450	-1,35
231,0325	3,06	C9H12O5S	[M - H]-	Yes	Yes	NO	NO	231,0322	1,43
231,0686	4,10	C10H16O4S	[M - H]-	Yes	Yes	NO	NO	231,0686	0,19
233,0479	5,36	C9H14O5S	[M - H]-	Yes	Yes	NO	NO	233,0478	0,34
234,8682	3,12	C2H4O3S5	[M - H]-	Yes	NO	NO	NO	234,8680	0,75
234,8852	8,13	C2H4O5S4	[M - H]-	Yes	Yes	NO	Yes	234,8858	-2,48
234,8854	7,02	C2H4O5S4	[M - H]-	Yes	Yes	NO	Yes	234,8858	-1,63

234,9902	9,59	C7H8O7S	[M - H]-	Yes	Yes	Yes	NO	234,9907	-2,13
235,0093	4,61	C8H12O4S2	[M - H]-	Yes	Yes	NO	NO	235,0093	-0,11
235,0095	4,96	C8H12O4S2	[M - H]-	Yes	Yes	NO	NO	235,0093	0,74
235,0268	9,50	C8H12O6S	[M - H]-	Yes	Yes	NO	NO	235,0271	-1,21
235,0269	4,57	C8H12O6S	[M - H]-	Yes	Yes	NO	Yes	235,0271	-0,79
235,0271	6,21	C8H12O6S	[M - H]-	Yes	NO	NO	NO	235,0271	0,06
235,0271	6,02	C8H12O6S	[M - H]-	Yes	NO	NO	NO	235,0271	0,06
236,9874	3,04	C7H10O5S2	[M - H]-	Yes	NO	NO	Yes	236,9886	-5,03
237,0426	6,40	C8H14O6S	[M - H]-	Yes	Yes	Yes	NO	237,0427	-0,57
238,9498	4,16	C6H8O4S3	[M - H]-	Yes	Yes	Yes	Yes	238,9501	-1,24
239,0042	6,06	C7H12O5S2	[M - H]-	Yes	Yes	NO	NO	239,0042	-0,17
239,0209	6,57	C7H12O7S	[M - H]-	Yes	Yes	NO	NO	239,0220	-4,60
239,0582	5,13	C8H16O6S	[M - H]-	Yes	NO	NO	NO	239,0584	-0,78
239,0583	5,46	C8H16O6S	[M - H]-	Yes	Yes	NO	NO	239,0584	-0,36
242,9451	5,70	C5H8O5S3	[M - H]-	Yes	Yes	NO	Yes	242,9450	0,36
242,9814	3,76	C6H12O4S3	[M - H]-	Yes	Yes	NO	Yes	242,9814	0,01
244,9604	4,61	C5H10O5S3	[M - H]-	Yes	Yes	NO	NO	244,9607	-1,07
244,9606	6,11	C5H10O5S3	[M - H]-	Yes	NO	NO	NO	244,9607	-0,25
246,9398	9,14	C4H8O6S3	[M - H]-	Yes	Yes	Yes	NO	246,9399	-0,51
247,0266	8,09	C9H12O6S	[M - H]-	Yes	NO	NO	NO	247,0271	-1,96

247,0636	5,20	C10H16O5S	[M - H]-	Yes	NO	NO	NO	247,0635	0,52
247,0641	4,82	C10H16O5S	[M - H]-	Yes	Yes	NO	NO	247,0635	2,55
248,9016	4,72	C3H6O5S4	[M - H]-	Yes	Yes	NO	Yes	248,9014	0,67
249,0426	6,47	C9H14O6S	[M - H]-	Yes	Yes	Yes	NO	249,0427	-0,54
249,0426	5,87	C9H14O6S	[M - H]-	Yes	NO	Yes	NO	249,0427	-0,54
249,043	9,28	C9H14O6S	[M - H]-	Yes	Yes	NO	NO	249,0427	1,06
250,8806	6,95	C2H4O6S4	[M - H]-	Yes	Yes	NO	Yes	250,8807	-0,39
251,0582	5,47	C9H16O6S	[M - H]-	Yes	NO	Yes	NO	251,0584	-0,74
251,0585	6,13	C9H16O6S	[M - H]-	Yes	Yes	Yes	NO	251,0584	0,46
252,9115	1,66	C6H6O3S4	[M - H]-	Yes	NO	NO	Yes	252,9116	-0,41
252,9653	4,23	C7H10O4S3	[M - H]-	Yes	Yes	NO	Yes	252,9657	-1,77
253,0012	8,90	C7H10O8S	[M - H]-	Yes	Yes	NO	NO	253,0013	-0,25
253,0016	8,48	C7H10O8S	[M - H]-	Yes	NO	NO	Yes	253,0013	1,33
254,9991	6,13	C7H12O6S2	[M - H]-	Yes	NO	NO	NO	254,9992	-0,22
255,0168	8,53	C7H12O8S	[M - H]-	Yes	NO	NO	NO	255,0169	-0,45
256,9421	3,96	C5H6O8S2	[M - H]-	Yes	Yes	NO	NO	256,9420	0,25
256,9778	8,65	C6H10O7S2	[M - H]-	Yes	Yes	NO	NO	256,9784	-2,41
256,9786	8,90	C6H10O7S2	[M - H]-	Yes	Yes	Yes	NO	256,9784	0,70
258,9939	4,97	C6H12O7S2	[M - H]-	Yes	Yes	NO	NO	258,9941	-0,66
258,9942	9,37	C6H12O7S2	[M - H]-	Yes	Yes	Yes	NO	258,9941	0,50

259,0632	4,83	C11H16O5S	[M - H]-	Yes	Yes	NO	NO	259,0635	-1,05
260,9009	1,27	C4H6O5S4	[M - H]-	Yes	Yes	NO	Yes	260,9014	-2,04
260,9019	2,11	C4H6O5S4	[M - H]-	Yes	Yes	NO	NO	260,9014	1,79
260,9734	10,73	C5H10O8S2	[M - H]-	Yes	NO	Yes	NO	260,9733	0,25
261,0095	10,10	C6H14O7S2	[M - H]-	Yes	NO	NO	NO	261,0097	-0,85
261,025	2,66	C10H14O4S2	[M - H]-	Yes	NO	NO	NO	261,0250	0,09
261,0251	4,05	C10H14O4S2	[M - H]-	Yes	Yes	NO	NO	261,0250	0,47
261,0421	7,04	C10H14O6S	[M - H]-	Yes	Yes	NO	NO	261,0427	-2,43
261,0428	5,86	C10H14O6S	[M - H]-	Yes	NO	Yes	NO	261,0427	0,25
261,0786	4,64	C11H18O5S	[M - H]-	Yes	Yes	NO	NO	261,0791	-2,00
263,0217	8,84	C9H12O7S	[M - H]-	Yes	NO	Yes	NO	263,0220	-1,14
263,0404	4,29	C10H16O4S2	[M - H]-	Yes	Yes	Yes	NO	263,0406	-0,86
263,041	2,30	C10H16O4S2	[M - H]-	Yes	NO	NO	NO	263,0406	1,42
264,9836	4,50	C8H10O6S2	[M - H]-	Yes	Yes	NO	Yes	264,9835	0,35
265,0015	9,26	C8H10O8S	[M - H]-	Yes	Yes	Yes	NO	265,0013	0,89
265,0197	6,29	C9H14O5S2	[M - H]-	Yes	NO	NO	NO	265,0199	-0,72
265,0371	6,20	C9H14O7S	[M - H]-	Yes	NO	NO	NO	265,0377	-2,08
265,0371	5,33	C9H14O7S	[M - H]-	Yes	NO	NO	NO	265,0377	-2,08
266,9805	4,13	C8H12O4S3	[M - H]-	Yes	Yes	NO	Yes	266,9814	-3,36
268,9071	3,66	C6H6O4S4	[M - H]-	Yes	Yes	NO	Yes	268,9065	2,16

268,9782	8,74	C7H10O7S2	[M - H]-	Yes	Yes	Yes	Yes	268,9784	-0,82
268,9786	9,37	C7H10O7S2	[M - H]-	Yes	Yes	Yes	Yes	268,9784	0,67
269,0324	9,21	C8H14O8S	[M - H]-	Yes	Yes	NO	NO	269,0326	-0,61
270,976	5,34	C7H12O5S3	[M - H]-	Yes	NO	NO	NO	270,9763	-1,15
270,976	3,72	C7H12O5S3	[M - H]-	Yes	NO	NO	NO	270,9763	-1,15
270,9938	9,47	C7H12O7S2	[M - H]-	Yes	Yes	Yes	NO	270,9941	-1,00
270,9941	8,11	C7H12O7S2	[M - H]-	Yes	NO	NO	NO	270,9941	0,11
273,0097	9,29	C7H14O7S2	[M - H]-	Yes	NO	Yes	NO	273,0097	-0,08
274,9712	4,78	C6H12O6S3	[M - H]-	Yes	NO	NO	NO	274,9712	-0,10
274,9888	10,57	C6H12O8S2	[M - H]-	Yes	NO	NO	NO	274,9890	-0,67
275,0583	3,01	C11H16O6S	[M - H]-	Yes	NO	Yes	NO	275,0584	-0,31
275,0589	5,49	C11H16O6S	[M - H]-	Yes	NO	NO	NO	275,0584	1,87
277,0202	4,86	C10H14O5S2	[M - H]-	Yes	NO	NO	NO	277,0199	1,11
277,0733	5,72	C11H18O6S	[M - H]-	Yes	NO	NO	NO	277,0740	-2,65
277,0736	5,33	C11H18O6S	[M - H]-	Yes	NO	Yes	NO	277,0740	-1,57
277,0738	6,09	C11H18O6S	[M - H]-	Yes	NO	NO	NO	277,0740	-0,85
278,9999	4,86	C9H12O6S2	[M - H]-	Yes	NO	NO	NO	278,9992	2,67
280,9429	3,85	C7H6O8S2	[M - H]-	Yes	Yes	NO	NO	280,9420	3,08
282,8526	6,81	C2H4O6S5	[M - H]-	Yes	Yes	NO	NO	282,8528	-0,59
282,9761	4,77	C8H12O5S3	[M - H]-	Yes	Yes	NO	NO	282,9763	-0,75

285,0093	9,70	C8H14O7S2	[M - H]-	Yes	NO	NO	NO	285,0097	-1,48
285,0099	8,05	C8H14O7S2	[M - H]-	Yes	NO	NO	NO	285,0097	0,63
285,0427	5,43	C12H14O6S	[M - H]-	Yes	NO	NO	NO	285,0427	-0,12
287,0251	9,14	C8H16O7S2	[M - H]-	Yes	Yes	Yes	NO	287,0254	-0,94
287,0586	6,13	C12H16O6S	[M - H]-	Yes	NO	Yes	NO	287,0584	0,75
288,9674	12,17	C6H10O9S2	[M - H]-	Yes	NO	Yes	NO	288,9682	-2,94
288,9678	10,38	C6H10O9S2	[M - H]-	Yes	NO	NO	Yes	288,9682	-1,56
289,0557	4,74	C15H14O4S	[M - H]-	Yes	Yes	NO	NO	289,0529	9,67
290,9989	5,81	C10H12O6S2	[M - H]-	Yes	NO	Yes	NO	290,9992	-0,88
293,0132	6,53	C13H10O6S	[M - H]-	Yes	NO	NO	NO	293,0114	6,02
293,0141	5,92	C10H14O6S2	[M - H]-	Yes	NO	NO	NO	293,0148	-2,41
294,9424	1,34	C5H12O6S4	[M - H]-	Yes	Yes	NO	NO	294,9433	-3,04
296,9554	5,43	C8H10O6S3	[M - H]-	Yes	NO	NO	NO	296,9556	-0,59
297,0098	9,34	C9H14O7S2	[M - H]-	Yes	Yes	Yes	Yes	297,0097	0,27
297,0272	9,14	C9H14O9S	[M - H]-	Yes	NO	NO	NO	297,0275	-0,94
297,0798	4,47	C14H18O5S	[M - H]-	Yes	Yes	NO	NO	297,0791	2,29
303,0893	5,36	C13H20O6S	[M - H]-	Yes	NO	Yes	NO	303,0897	-1,27
304,945	11,60	C6H10O8S3	[M - H]-	Yes	NO	NO	NO	304,9454	-1,33
306,8523	7,10	C4H4O6S5	[M - H]-	Yes	NO	NO	Yes	306,8528	-1,52
306,9788	8,13	C6H12O10S2	[M - H]-	Yes	NO	NO	NO	306,9788	-0,05

308,8673	7,10	C4H6O6S5	[M - H]-	Yes	NO	NO	NO	308,8684	-3,62
308,868	6,81	C4H6O6S5	[M - H]-	Yes	NO	NO	Yes	308,8684	-1,35
313,0039	9,01	C9H14O8S2	[M - H]-	Yes	Yes	Yes	NO	313,0046	-2,35
313,0562	3,82	C14H18O4S2	[M - H]-	Yes	Yes	NO	NO	313,0563	-0,25
314,9836	12,16	C8H12O9S2	[M - H]-	Yes	NO	Yes	NO	314,9839	-0,95
315,0203	9,43	C9H16O8S2	[M - H]-	Yes	NO	Yes	NO	315,0203	0,05
316,9984	10,06	C8H14O9S2	[M - H]-	Yes	NO	Yes	NO	316,9995	-3,63
319,0304	5,73	C12H16O6S2	[M - H]-	Yes	NO	NO	NO	319,0305	-0,18
320,9761	10,15	C7H14O8S3	[M - H]-	Yes	NO	Yes	NO	320,9767	-1,89
322,9703	5,83	C10H12O6S3	[M - H]-	Yes	Yes	NO	NO	322,9712	-2,87
324,8627	10,25	C4H6O7S5	[M - H]-	Yes	NO	NO	NO	324,8633	-1,95
325,002	10,09	C13H10O8S	[M - H]-	Yes	Yes	Yes	NO	325,0013	2,26
326,8789	11,89	C3H4O12S3	[M - H]-	Yes	NO	NO	NO	326,8781	2,40
328,9991	10,65	C9H14O9S2	[M - H]-	Yes	NO	NO	Yes	328,9995	-1,37
329,0356	9,72	C13H14O8S	[M - H]-	Yes	NO	Yes	Yes	329,0326	9,23
331,0151	10,08	C9H16O9S2	[M - H]-	Yes	NO	Yes	NO	331,0152	-0,30
333,0456	5,90	C13H18O6S2	[M - H]-	Yes	NO	Yes	NO	333,0461	-1,52
333,0456	5,45	C13H18O6S2	[M - H]-	Yes	NO	Yes	NO	333,0461	-1,52
336,9862	5,08	C11H14O6S3	[M - H]-	Yes	NO	NO	NO	336,9869	-2,01
339,0896	5,41	C16H20O6S	[M - H]-	Yes	NO	NO	NO	339,0897	-0,25

341,036	5,03	C11H18O8S2	[M - H]-	Yes	NO	NO	NO	341,0359	0,19
344,9757	10,30	C9H14O8S3	[M - H]-	Yes	NO	NO	Yes	344,9767	-2,92
345,0306	9,84	C13H14O9S	[M - H]-	Yes	NO	Yes	NO	345,0275	9,04
346,9371	8,62	C7H8O12S2	[M - H]-	Yes	NO	NO	Yes	346,9373	-0,70
346,9374	8,29	C7H8O12S2	[M - H]-	Yes	NO	Yes	Yes	346,9373	0,16
347,0456	10,25	C13H16O9S	[M - H]-	Yes	NO	Yes	NO	347,0431	7,12
357,0305	9,68	C11H18O9S2	[M - H]-	Yes	NO	Yes	NO	357,0309	-0,98
357,0459	5,69	C15H18O6S2	[M - H]-	Yes	NO	Yes	NO	357,0461	-0,58
359,0618	5,76	C15H20O6S2	[M - H]-	Yes	NO	Yes	NO	359,0618	0,12
366,921	6,21	C14H8O4S4	[M - H]-	Yes	NO	NO	NO	366,9222	-3,18
379,0508	5,04	C14H20O8S2	[M - H]-	Yes	Yes	NO	NO	379,0516	-2,07
382,8335	6,85	C5H4O10S5	[M - H]-	Yes	NO	NO	Yes	382,8324	2,80
391,0728	5,52	C12H24O10S2	[M - H]-	Yes	NO	NO	NO	391,0727	0,22
404,9973	12,02	C11H18O10S3	[M - H]-	Yes	NO	Yes	Yes	404,9978	-1,32

Supplementary Table 4: All detected molecular formulas showing a fragmentation pattern in accordance with a sulfonic acid functional group.

Supplementary references

1. Smith, C.A., et al., *XCMS: Processing mass spectrometry data for metabolite profiling using Nonlinear peak alignment, matching, and identification.* Analytical Chemistry, 2006. **78**(3): p. 779-787.
2. Kuhl, C., et al., *CAMERA: an integrated strategy for compound spectra extraction and annotation of liquid chromatography/mass spectrometry data sets.* Anal Chem, 2012. **84**(1): p. 283-9.

3. Franca, R.D.G., et al., *Biodegradation Products of a Sulfonated Azo Dye in Aerobic Granular Sludge Sequencing Batch Reactors Treating Simulated Textile Wastewater.* ACS Sustainable Chemistry & Engineering, 2019. **7**(17): p. 14697-14706.
4. Voogt, P. and M. Saez, *Analytical chemistry of perfluoroalkylated substances.* TrAC Trends in Analytical Chemistry, 2006. **25**(4): p. 326-342.
5. Duhrkop, K., et al., *SIRIUS 4: a rapid tool for turning tandem mass spectra into metabolite structure information.* Nat Methods, 2019. **16**(4): p. 299-302.

7.2.1 Appendix Paper 2

communications chemistry

ARTICLE

https://doi.org/10.1038/s42004-023-01021-1 OPEN

C2-addition patterns emerging from acetylene and nickel sulfide in simulated prebiotic hydrothermal conditions

Philippe Diederich[1], Alexander Ruf[2,3], Thomas Geisberger[4], Leopold Weidner[1,5], Christian Seitz[4], Wolfgang Eisenreich[4], Claudia Huber[4]✉ & Philippe Schmitt-Kopplin[1,5,6]✉

Chemical complexity is vital not only for the origin of life but also for biological evolution. The chemical evolution of a complex prebiotic mixture containing acetylene, carbon monoxide (CO), and nickel sulfide (NiS) has been analyzed with mass spectrometry as an untargeted approach to reaction monitoring. Here we show through isotopic 13C-labelling, multiple reaction products, encompassing diverse CHO and CHOS compounds within the complex reaction mixture. Molecules within the same chemical spaces displayed varying degrees of 13C-labelling, enabling more robust functional group characterization based on targeted investigations and differences in saturation levels among the described classes. A characteristic C2-addition pattern was detected in all compound classes in conjunction with a high diversity of thio acids, reminiscent of extant microbial C2-metabolism. The analysis involved a time-resolved molecular network, which unveiled the behavior of sulfur in the system. At the onset of the reaction, early formed compounds contain more sulfur atoms compared to later emerging compounds. These results give an essential insight into the still elusive role of sulfur dynamics in the origin of life. Moreover, our results provide temporally resolved evidence of the progressively increasing molecular complexity arising from a limited number of compounds.

[1] Helmholtz Munich, Research Unit Analytical BioGeoChemistry, Neuherberg, Germany. [2] Excellence Cluster ORIGINS, Boltzmannstraße 2, 85748 Garching, Germany. [3] LMU Munich, Faculty of Physics, Schellingstraße 4, 80799 Munich, Germany. [4] Technical University of Munich, TUM School of Natural Sciences, Department of Bioscience, Bavarian NMR Center (BNMRZ), Structural Membrane Biochemistry, Lichtenbergstr. 4, 85748 Garching, Germany. [5] Comprehensive Foodomics Platform, Chair of Analytical Food Chemistry, TUM School of Life Sciences, Technical University of Munich, Maximus-von-Imhof-Forum 2, 85354 Freising, Germany. [6] Center for Astrochemical Studies, Max Planck Institute for Extraterrestrial Physics, Gießebachstraße 1, 85748 Garching bei München, Germany. ✉email: claudia.huber@tum.de; schmitt-kopplin@helmholtz-muenchen.de

In 1953, Reppe pioneered the synthesis of fatty acids from acetylene and carbon monoxide[1]. In conjunction with a nickel carbonyl catalyst, both gases yielded acrylic acid and longer unsaturated fatty acids. However, nickel carbonyl, a water-labile compound, is not the only catalyst capable of lowering the required energy to accelerate this reaction. Recently, this reaction was reinterpreted in an origin-of-life context as fatty acids play structural and energetic roles in living organisms. Experimental evidence that describes the formation of a variety of fatty acids of different lengths and degrees of saturation was achieved under volcanic hydrothermal conditions, utilizing a nickel sulfide catalyst compatible with aqueous early earth conditions[2].

So far, acetylene has been underrepresented in origin-of-life research. Literature is scarce, but new evidence for its relevance emerges. Acetylene is formed from methane irradiated by UV light[3]. Multiple planetary bodies show an atmosphere partially made from acetylene gas, like the Saturn moon Titan[4,5] and the Jovian planet Jupiter[6]. The atmosphere of Enceladus, another moon of Saturn, contains acetylene in addition to phosphorous[7] and exhibits hydrothermal volcanic activity[8]. The existence of acetylene in the atmosphere of early Earth was also hypothesized[9] and can be found nowadays in fumaroles of geothermal areas[10]. Spark discharge experiments of gaseous nitrogen and methane mixtures also lead to the formation of acetylene[11]. Extant microorganisms in anaerobic aqueous environments can use acetylene as an energy and carbon source, increasing the likelihood of its presence at early evolutionary stages. Specifically, *Pelobacter acetylenicus* can grow from acetylene[12] alone and therefore demonstrates that acetylene has the potential to fuel a complete metabolism on its own. Acetylene is transformed into acetyl-coenzyme (Co)A, a thio ester, via the hydration of acetylene into acetaldehyde. Acetyl-CoA is then used to build metabolites with C2-units.

The role of sulfur in the origin of life is still an elusive and extensively researched topic. Undoubtedly sulfur is essential for extant life, as it is part of methionine and cysteine, acetyl-CoA, and multiple hydrogenases[13]. Popular hypotheses for the origin of life also include sulfur as a critical element in a more indirect way. Inspired by the "iron-sulfur world" theory of Wächtershäuser[14], transition-metal sulfides were used as catalysts in origin-of-life experiments. This theory proposed a mineral surface metabolism, starting from simple inorganic precursors and evolving into complex bioorganic molecules. This hypothetical chemoautotrophic evolution proceeds *via* thio acids or thioesters in reductive autocatalytic cycles[15]. Incubation of carbon monoxide with methyl mercaptan over transition-metal sulfides leads to the well-coveted activated thioester[16], a molecular part of acetyl-CoA. These seminal results sparked the discovery of other reactions, possible in a hydrothermal environment and yielding prebiotically-relevant compounds, including acetaldehyde[17], Krebs cycle intermediates[18], and the porphyrin building block pyrrole[19]. De Duve proposed a second hypothesis, heavily depending on sulfur compounds where thioesters contribute the energy for essential reactions[20]. Moreover, thiols were described as a possible prebiotic intermediate for peptide-bond formation[21], whereas sulfur-containing heterocycles could act as catalysts for biologically-relevant reactions[22].

A deeper comprehension of chemical complexity is vital not only for the origin of life but also for biological evolution. We combined ^{13}C-labelling with untargeted ultrahigh-resolution mass spectrometry to tackle the challenging analysis of highly complex evolving abiotic systems. We describe an analytical approach based on known chemical reactions that allows us to categorize detected elemental compositions into individual compound classes via the degree of ^{13}C-labelling. In this study, we expanded our knowledge of the diversity of compound classes formed from prebiotically relevant gases. We recognized C2-addition as a driving factor for compound diversity in a given compound class. In addition, we identified new functional classes, such as thio ethers and thio acids. Through labeling, we discovered that there are two pathways leading to thio acids, which are crucial molecular components of acetyl-CoA. Thioacids formed solely from acetylene also enabled comparison with Pelobacter acetyleneicus. Lastly, this approach succeeded in detecting a sulfur-specific trend that led to the reduction of sulfur atoms per molecule after the initial introduction of sulfur to the gases. This trend led to compounds with low numbers of sulfur, more aligned with biomolecules in extant organisms, shedding light on sulfur dynamics in abiotic systems.

Results

Compositional complexity increases over time. We incubated acetylene with carbon monoxide over water containing nickel sulfide for varying time periods at 105 °C and measured the evolving mixture at different time points. After 2 h, the first signals belonging to reaction products were analyzed by direct infusion Fourier transform ion cyclotron resonance mass spectrometry (FT-ICR-MS). Longer incubation times increased the chemical diversity and complexity of organic compounds, meaning a functional and compositional variety of molecules. Visualization of the increasing diversity of elemental CHO and CHOS compositions found in the one-pot reaction can be seen in Fig. 1. The mass-to-charge ratio was plotted against the hydrogen-to-carbon ratio. This separation allowed an overview of the chemical composition of the system resolved by the mass and the degree of saturation of the individual compounds. We separately focused on the chemical space of CHO and CHOS compounds. We observed an increase in detected signals over time for both chemical spaces, strongly suggesting a diversification of reaction products by a factor of ~9. The main group of the detected compounds is highly unsaturated, as the average H/C ratio is 1.4 for both chemical spaces after 7 days. This strong bias toward unsaturated compounds is in line with the utilized reactants (acetylene possessing a triple bond) and targeted GC-MS measurements of formed highly unsaturated carboxylic acids in the mixture[2]. Further, the mass of the compounds increased over time. The overall diversity increases as well, as the number of

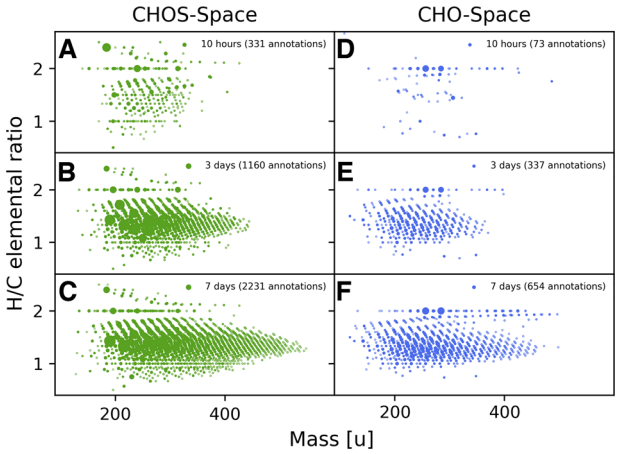

Fig. 1 Overview of the CHO and CHOS space over time. Overview of two different chemical spaces within the reaction mixture (acetylene/CO/H_2O/NiS). The annotated elemental compositions are plotted with the ratio of hydrogen atoms to carbon atoms (H/C) against the mass of the elemental composition. Different panels represent different time points for CHO (**D**–**F**, blue) and CHOS (**A**–**C**, green). Marker sizes represent relative detected intensity.

detected CHO and CHOS compounds increases from 328 annotated signals after 2 h to 2885 annotated signals present after 7 days.

The compositional space visualization of the ongoing reactions gives an overview of the system, but elemental compositions alone do not provide information about isomers and, more importantly, functional groups. The determination of such functional groups remains a determining factor if specific reactions need to be characterized.

Resolving functional diversity by ^{13}C-labelling. Comparing unlabeled setups to setups with ^{13}C-labelled carbon monoxide allowed us to characterize functional groups and compound class diversity better. Categorizing the elemental annotations by ^{13}C-labelling improved the amount of information, where ^{13}C-carbons convey specific functional insights into the onset of an early evolving system. This additional dimension allowed us to resolve different compound classes with the same number of heteroatoms. The origin of the label (carbon monoxide in our experimental setup) provided insight into the functional groups present in elemental subspaces after chemical reactions. Targeted GC-MS analysis of this mixture revealed that carbon monoxide is mainly reacted into a carboxylic acid group[2], in agreement with Reppe´s chemistry[1].

In line with published data[2,18], we were able to differentiate distinct populations of CHO and CHOS compounds in our model, as some compounds are labeled once, twice, or higher. $C_xH_yO_3$-compounds form the first elemental composition with more heteroatoms than pure fatty acids (Fig. 2). The elemental compositions with a single ^{13}C-label show a saturation level on average higher (1.38) than the saturation of the double-labeled compositions (1.20). This result strengthens the hypothesis that carbon monoxide is introduced as a carbonyl group. The carbonyl group reduces the H/C ratio compared to a hydroxy group or ether. Mono-labeled compounds, therefore, belong to carboxylic acids carrying an additional hydroxy or ether group. The addition of water to a double bond is likely responsible for the increase in oxygen in molecules without the need for carbon monoxide. We further observed that the number of oxygens in compounds with one ^{13}C label positively correlates with the H/C ratio of the detected compounds, further strengthening the claim that the

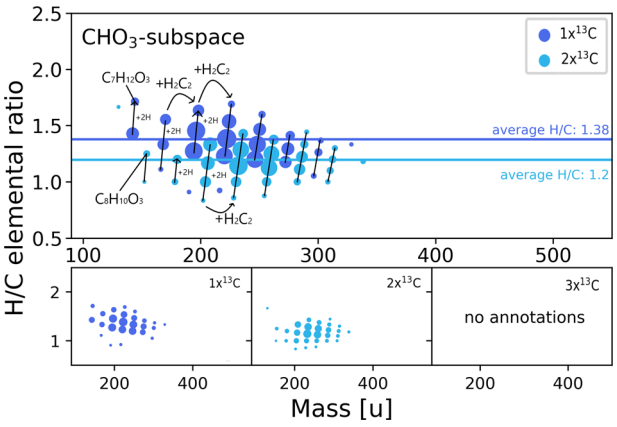

Fig. 2 CHO_3-subspace Elemental compositions in the $C_xH_yO_3$-subspace colored by the degree of ^{13}C-labelling. Differences in acetylene and hydrogen building blocks are highlighted by black arrows. Exemplary structures belonging to the identified compound class are shown for both degrees of ^{13}C-labelling. Horizontal colored lines show the average H/C ratio for the different degrees of labeling. Marker sizes represent relative detected intensity.

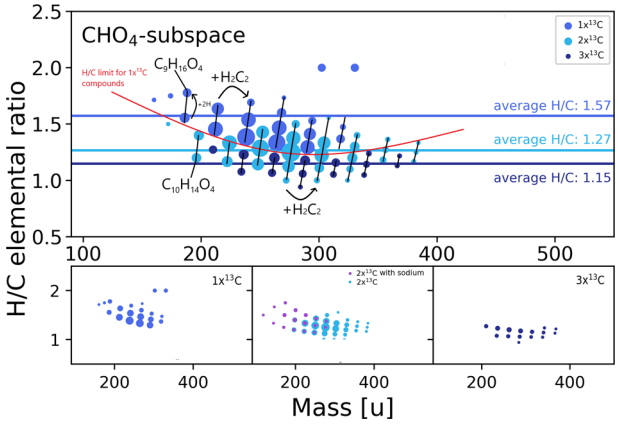

Fig. 3 CHO_4-subspace. Elemental compositions in the $C_xH_yO_4$-subspace colored by the degree of ^{13}C-labelling. Violet color shows sodium adducts. Red line marks the clear border in saturation between mono-and triple-labeled compounds. Differences in acetylene and hydrogen building blocks are highlighted by black arrows. Exemplary structures belonging to the identified compound class are shown for all degrees of ^{13}C-labelling and adducts. Horizontal colored lines show the average H/C ratio for the different degrees of labeling. Marker sizes represent relative detected intensity.

introduction of oxygen via water consumes a double bond (supplementary fig. 1). These results suggest a separation of the CHO_3 space into keto acids and either hydroxy acids or carboxylic acids with an ether (cyclic unsaturated ethers like furans, for example). Similar carboxylated heterocycles with sulfur, namely thiophenes, were already described in the system[23].

The recurring pattern of molecules reflecting C2-addition originating from acetylene is important to mention. Compounds of a specific subspace with the same amount of ^{13}C label increase in mass only via the addition of acetylene or reduction of double bonds. This addition of C2-units is reminiscent of the C2-metabolism carried out by acetyl-CoA. This behavior of mass increase via acetylene can be seen for all identified compound classes.

Additional heteroatoms increase the number of potential isomers and functional groups. This labeling approach further allows distinguishing at least three different compound classes in the CHO_4-subspace (Fig. 3). Mono-labeled compounds show the expected behavior of an increase in H/C-ratio compared to the CHO_3-subspace (from 1.38 to 1.57). This is the result of the consumption of a double bond during the introduction of water into the molecule. The mono-labeled compounds belong to the group of dihydroxy-acids and were not yet described in the system. Double-labeled compounds present a challenge, as the labeling still allows the formation of dicarboxylic acids or hydroxy-keto acids. The information that carbon monoxide is converted into a carbonyl group is insufficient for categorization. Further categorization requires the inclusion of an additional element, namely sodium. Our data suggested that dicarboxylic acids are prone to form sodium adducts after negative electrospray ionization. A double-deprotonated species can carry a positively charged sodium ion while still being negatively charged. This observation allows for the separation of double-labeled compounds into two potential subgroups.

Compositions labeled twice and showing sodium adducts can be categorized as dicarboxylic acids. The presence of succinic acid in the system was already shown in a previous publication[18]. Notably, no annotations with a single label (tentatively one carboxylic group) and a sodium adduct are detected. The same applies to the triple-labeled compounds that will be discussed

later. This fact strengthens the hypothesis that this behavior is specific to dicarboxylic acids in the CHO_4 subspace. A further sign of the occurrence of dicarboxylic acids is the strongly increased average H/C ratio (1.39) of compounds falling into this category compared to the average of this class (1.27). The introduction of a further carboxylic group consumes a double bond if the underlying mechanism complies with the reaction hypothesis of Reppe. This consumption of a double bond would raise the saturation level of the compounds and explain the strong deviation from the remaining double-labeled annotations. The categorization is still ambiguous, as compounds with higher mass may lead to reduced formation of sodium adducts. Notably, all sodium adducts are detected in a lower mass range than non-sodium-adduct-forming compounds. Strong evidence, however, for the presence of a mix of dicarboxylic acids and hydroxy-keto acids in the double-labeled CHO_4-subspace is the fact that a triple-labeled group is present. No sodium adducts are observed in this group, and the H/C ratio is, on average, lower (1.15). These results strengthen the annotation as diketo acids and make the presence of hydroxy-keto acids for double-labeled compounds more likely. CHO_5 and CHO_6 subspaces follow the same trends described for the previous subspaces.

Compounds containing sulfur show similar patterns. The CHO_1S_1 is the first elemental subspace in the category of CHOS compounds. Our results distinguished two groups (Fig. 4). Unlabeled compounds originate from acetylene alone, whereas mono-labeled compounds are derived from acetylene and a single carbon monoxide molecule. No double- or triple-labeled CHO_1S_1 compounds were detected. CHO_1S_1 compounds match the elemental composition of thio acids. The possibility of a modified Reppe chemistry with hydrogen sulfide instead of water leading to thio acids was already shown in earlier works of Reppe[1]. Having both labeled and unlabeled species of this compound class is surprising, as the pathway described by Reppe requires carbon monoxide. However, the probability that the unlabeled compounds belong to a different class of compounds is low, as hydroxy and thiol groups alone do not efficiently ionize in negative ionization mode. Those unlabeled species are also mostly fully labeled if acetylene is used with two labeled carbons instead of carbon monoxide (Fig. 4, black circled dots), excluding contamination. The formation of thio acetic acid could be detected in high amounts at early time points in the system with NMR (see Supplementary Fig. 2), further strengthening the presence of thio acids formed without carbon monoxide. If no more than two oxygen atoms are present in the molecule, the amount of labeled carbon does not exceed one ^{13}C. This result suggests that sulfur cannot completely exchange oxygen in this system. Oxygen originating from carbon monoxide stays attached to its labeled carbon.

The increased number of hetero atoms in the CHOS subspaces progressively leads to ambiguity. Relevant information can still be gained from ^{13}C labeling. The CHO_3S subspace behaves similarly to the CHO_3 rather than the CHO_4 subspace. Only mono- and double-labeled compounds can be detected. In addition, no sodium adducts are detected. This result suggests that compounds carrying a carboxylic and a thiocarboxylic acid group simultaneously are absent from the system. CHO_4S is similar in this regard. The diversity in sodium adducts for this subspace exceeds the diversity of the non-sodium-adduct-forming fraction of double-labeled compounds. However, the complete absence of triple-labeled compounds is very surprising in this subspace, likely because double-labeled CHO_4S belong to thioethers. Two carboxylic acids are linked to each other via a sulfur ether. To further strengthen this claim, the detected elemental composition of $C_6H_{10}O_4S$ was identified and validated as thiobispropanoic acid via targeted GC-MS analysis by comparing retention time and the fragmentation pattern to a commercially available standard (Supplementary Fig. 3). Adding one sulfur to reach the CHO_4S_2 subspace shows only double-labeled sodium adducts as a coherent homologous series. The result suggests the presence of two carboxylic acids linked by a sulfur bridge, reminiscent of protein sulfur bridges allowing their tertiary structure (Supplementary Fig. 4).

Further interpretations of higher heteroatom combinations were deemed too ambiguous, but a table showing all annotations with the corresponding labels can be found as a supplementary Excel sheet (Supplementary Data 1). One source of ambiguity is the presence of "mixed" ^{13}C annotations where the same elemental composition is present in different degrees of ^{13}C labeling. Due to this, it is almost impossible to reliably assign functional groups to a detected signal. However, it is still interesting to investigate how the percentage of "mixed" annotations changes for different subspaces in such a complex mixture. A reaction scheme summarizing all proposed mechanisms and 13C-patterns can be found in S.I. (supplementary fig. 5).

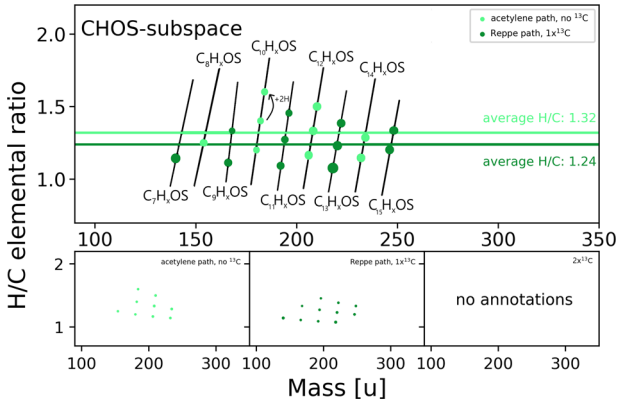

Fig. 4 $C_xH_yO_1S_1$-subspace. Elemental compositions in the CxHyO1S1-subspace representing thio acids, colored by the degree of 13C-labelling. Black encircled dots could also be confirmed to consist solely of acetylene building blocks. Differences in hydrogen building blocks are highlighted by black arrows. Horizontal colored lines show the average H/C ratio for the different degrees of labeling. Marker sizes represent relative detected intensity.

Isomer frequency has an unpredictable variance in analyzed subspaces. ^{13}C labeling of the sample allowed additional dimension for untargeted analysis, which is otherwise inaccessible in direct-infusion mass spectrometry. The labeling revealed that some of the identical elemental compositions existed as a mixture of ^{13}C labeled species, as labeled experiments yielded signals compatible with multiple degrees of labeling. A representative comparison between labeled and unlabeled spectra can be found in S.I. (supplementary fig. 6). We investigated the percentage of mixed and pure annotations for different chemical subspaces and observed unexpected behaviors. With an increasing number of hetero atoms, we expected a steady increase in the fraction of mixed annotations compared to pure annotations. This, however, was not always the case. The CHO space showed an increase of mixed annotations from two (7.7%) to three (17.4%) oxygens per molecule. The CHO_4-subspace, however, only shows 12.9%, and the CHO_5 subspace 4.9% of mixed annotations. The CHOS space showed increased mixed annotations compared to the CHO space. However, no clear trend could be elucidated. CHO_1S_1 and CHO_2S_3 showed 0% mixed annotations, in contrast to CHO_3S_2, with 39% mixed annotations. These results highlight the unpredictability of isomer populations in untargeted FT-ICR-MS.

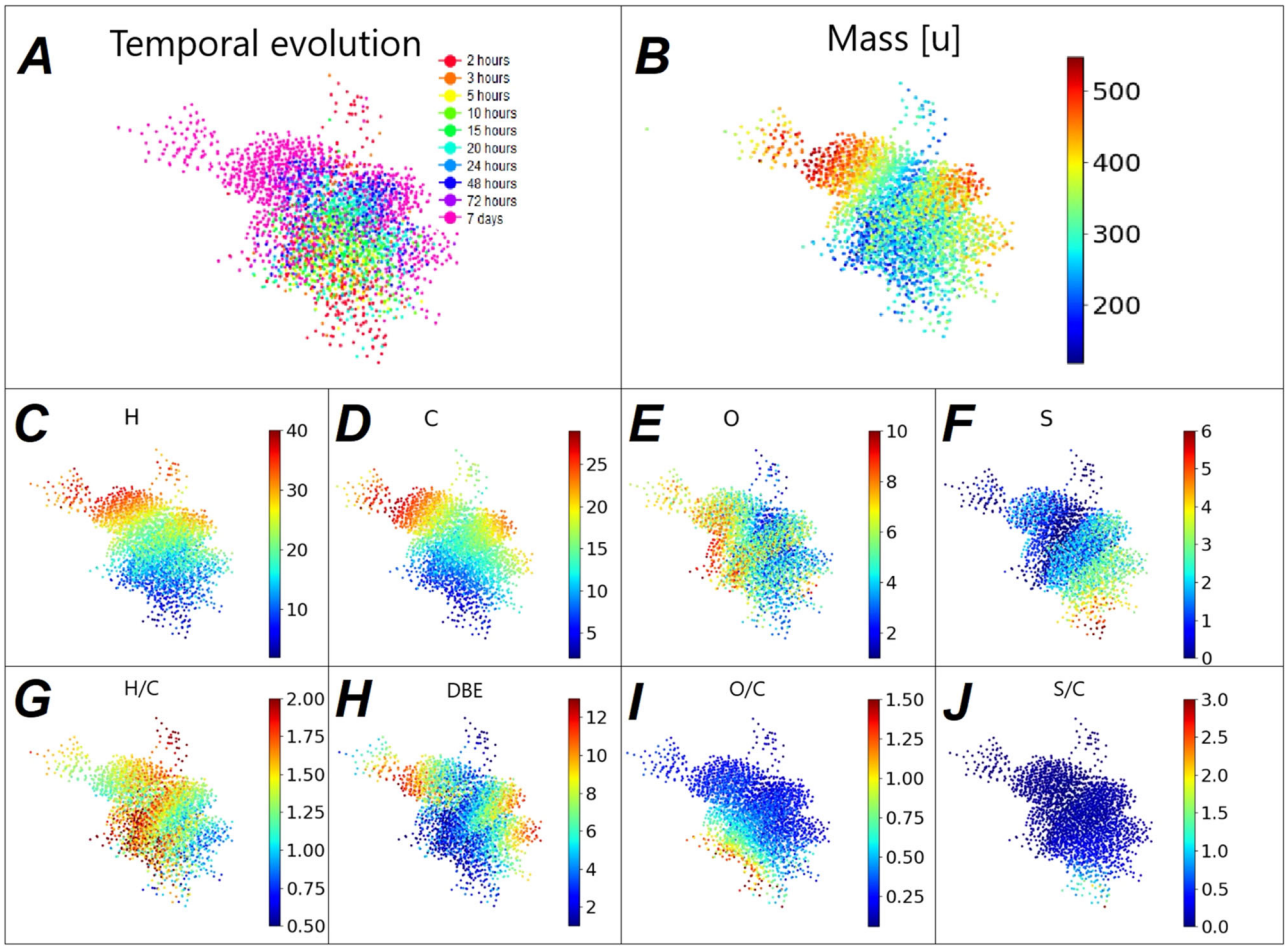

Fig. 5 Molecular network of all annotated signal. A Time-resolved molecular network evolving from red (2 h) at the bottom to pink at the top (7 days). **B** Mass-resolved molecular network showing an increase in mass correlated with the increase in time. Molecular network colored by the number of assigned elements (**C**–**F**) or elemental ratios (**G**–**J**).

Table 1 Mass differences used as edges in the molecular network to connect all annotated formulas.

Possible reaction	Elemental difference	Exact mass difference (u)
Water addition	+ H_2O	18.01057
Hydrogen sulfide addition	+ H_2S	33.98772
Dimerization/ Oligomerization	+ C_2H_2	26.01565
Carbonylation (with H_2O)	+ CH_2O_2	46.00548
Carbonylation (with H_2S)	+ CH_2OS	61.98264
Reduction	+ H_2	2.01565

Using ^{13}C labeling allows a definite distinction between impurities and experimental sample components[24]. This result is difficult to achieve with FT-ICR-MS, as removing blank signals potentially removes specific results corresponding to compound isomers in solvents or other sources of contamination. In some instances, compounds like fatty acids can be in the solvent and the investigated system.

Temporal evolution of the system. The system was visualized over time via a temporal molecular network (Fig. 5). In this network, individual nodes represent detected annotated signals. Overall, 6 elemental compositions were chosen as possible edges, all representing differences in molecular weight after specific reactions. Based on previous publications or available reactants, the 6 chosen mass differences (Table 1) represent possible reactions likely to happen in the system. Edges can represent the addition of acetylene[25], the simultaneous addition of carbon monoxide and water to a double or triple bond to form a carboxylic acid group. The same reaction can be slightly altered with hydrogen sulfide instead of water resulting in a thio acid[1]. The addition of water[26], hydrogen sulfide[27], or hydrogen represents the loss of a double or triple bond, potentially through reduction. This limited number of possible edges allowed to interconnect 97.5% of all annotated signals.

The overall temporal path taken by the system is visualized by a molecular network (Fig. 5A). Molecular networks and mass-difference analysis were developed for biological samples[28] and used in recent untargeted investigations of astrochemical reactions[29] allowing a comprehensive overview of the chemical system. The masses increase over time, and later detected molecules show the highest masses (>500 u) (Fig. 5B). The amount of hydrogen and carbon follow a nearly identical trend compared to the mass (Fig. 5C and D). The percentage of compounds containing high numbers of sulfur atoms per molecule (>2) sulfur) is highest at early time points (Fig. 5F). The percentage of CHO_xS_3 annotations starts at 29% of overall sulfur annotations after 2 h and is lowered to 17% after 7 days, even though the absolute amount of CHO_xS_3 annotations is

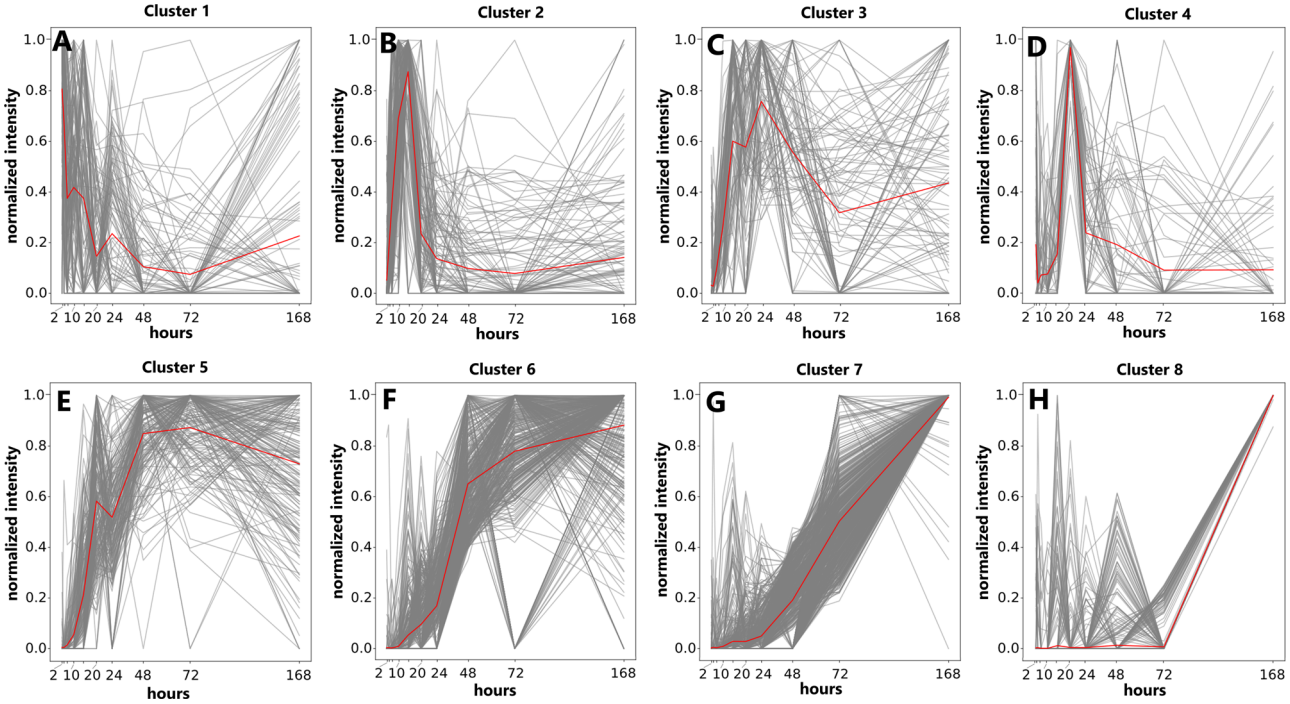

Fig. 6 SOM analysis. SOM clusters showing intensity traces for all annotated masses (gray) and an average path taken (red), with different intensity maxima for different clusters. **A**–**G** are ordered by peak time. **A** Cluster 1 peaks after 2 h and decreases over time. **B** Cluster 2 peaks after 15 h. **C** Cluster 3 peaks between 15 and 24 h. **D** Cluster 4 peaks after 20 h. **E** Cluster 5 peaks after 72 h. **F**–**H** Cluster 6–8 shows maximum intensity after 168 h with different slopes.

increasing (from 60 annotations after 2 h to 388 after 7 days). CHO_XS_4 compounds start at 39 annotations after 2 h and go down to 22 after 7 days (from 17 to 1% of total CHO_xS_4 annotations). The CHO_xS_5-subspace disappears completely after 3 days. Compounds annotated with 1–2 sulfur show the opposite trend. The percentage of CHO_xS_1 increases from 27% to 44.5% over the time of the experiment. We observe an inverted picture for the relative abundance of CHO compounds. CHO compounds with 2–3 oxygen represent 27–34% of all CHO annotations after 2 h of incubation. This percentage is reduced to 13–15% after 7 days of incubation.

We have further used self-organizing maps (SOM) classification theory[30] to characterize time-dependent molecular profiles in greater detail. This technique allows the clustering of temporal mass abundance profiles that follow the same evolutional trend over time. Masses following a similar intensity change over time are clustered together. The approach was already successfully used in other untargeted FT-ICR-MS analyses to categorize the temporal evolution of detected mass signals[31] in food samples. Our results show 8 different main clusters (Fig. 6). These clusters show groups of masses reaching their maximum intensity at different time points. We can confirm two trends that were suggested in the temporal network.: Clusters with maximum intensity at earlier time points show elemental compositions with lower masses on average than elemental compositions in clusters with late maxima. Compounds with higher amounts of sulfur reach their intensity maximum earlier than compounds with less sulfur. This fact shows that the continuous addition of sulfur to the unsaturated olefinic molecules is unlikely.

The profiles of the different groups give insight into the changing reactions over time, as compounds do not all linearly accumulate in the system but have different peak times. Some compounds are mostly depleted after 7 days (Fig. 6A, B, D). The behavior of sulfur over time is particularly interesting (Fig. 7). Sulfur-containing compounds with 3 or 4 sulfur atoms appear earlier and degrade quickly (Fig. 7A, B). The peak time appears later for annotations with lower numbers of sulfur (Fig. 7C, D). This effect differs for CHO compounds, where the compounds have a peak time of 7 days (or later) and mostly show steady signal increases over time.

Based on our results, the addition of acetylene or other mass-increasing reactions compensates for the loss of mass due to lower amounts of sulfur. However, an exchange of sulfur through other mass-increasing building blocks can only be hypothesized. 84% of all annotated thio acids follow the trend of cluster 6 (Fig. 6H). The observed behavior of the higher mass thio acids is different from their low mass counterpart thio acetic acid, which is present after 2 h in high amounts and then reacts away throughout the experiment (supplementary fig. 2), partially by hydrolyzing to acetic acid.

Discussion

The described system demonstrated its potential in previous publications to produce different prebiotically-relevant substances like aldehydes, fatty acids, and thiophenes[2,17,23]. The formation of pyrrole[19] and amino acids from aldehydes[17] via the Strecker reaction was also demonstrated in previously published experiments that included nitrogen. Our study now expands these targeted observations to reveal a dynamic chemical landscape of functional groups derived from basic building blocks, emphasizing sulfur-containing molecules and the deconvolution of functional groups with the help of ^{13}C labeling. The size of the investigated molecules also continues to grow progressively over time, mainly via a C2-unit increase, reminiscent of the C2-metabolism including the formation of fatty acids, polyketides, and terpenes from acetyl-CoA units in extant organisms[32]. Some prokaryotes even use acetylene as a main carbon source for their metabolism. The Gram-negative bacterium *Pelobacter acetylenicus* lives in anoxic oceanic sediments and converts acetylene into acetyl-CoA via acetaldehyde to fuel its C2-metabolism[12]. Capitalizing on our previous findings of a primordial conversion

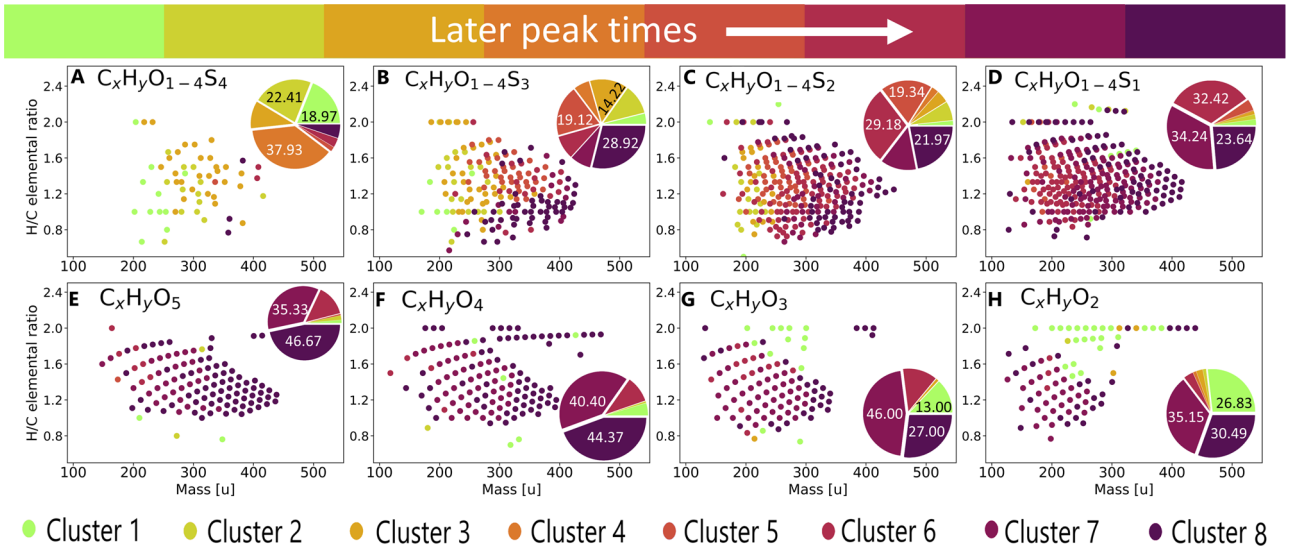

Fig. 7 SOM-clustering for different chemical spaces. $CHO_{1-4}S$ (panels **A**–**D**) and CHO (pannels **E**–**H**) subspaces colored by their maximum peak intensity through SOM-clustering, showing predominantly earlier peak times for compounds with high sulfur numbers. Green color indicates early peak times and evolves to violet for later emerging compounds. Pie charts on the right side of the plots show the percentage of annotations for the different peak times/clusters.

of acetylene into fatty acids and related organic molecules, this primitive bacterium could therefore be seen as the link between a purely abiotic acetylene-based C2-metabolism and the C2-metabolism in extant organisms. The formation of acetaldehyde and thio acetic acid S-methyl ester (a simple analog to acetyl-CoA) from acetylene was already shown in this system[16,17].

Isotope labeling uncovered the system's hidden diversity in functional groups. We could separate functional groups with the same number of hetero atoms by FT-ICR-MS. Separating functional groups with the same number of hetero atoms is difficult for FT-ICR-MS-based analysis. The problem could be solved by ^{13}C isotope labeling of the starting materials. This approach made it possible to trace the origin and chemical nature of hetero atoms based on the literature[1,18,25]. The CHO_3-subspace shows hydroxy acids and keto acids. Hydroxy acids continue to gain interest in the origin-of-life field. α-hydroxy acids can enhance peptide-bond formation in dry-down reactions[33], even though our analysis does not allow for the exact identification of the position of the functional group. The same can be said of keto acids, which play a central role in an ancestral analog of the Krebs cycle[34,35]. Dicarboxylic acids gained recent attention due to their ability to form co-polymers with glycol nucleic acids with a hypothesized potential to perform genetic or catalytic functions[36]. The diverse compound classes from multiple species have already proven to be significant in the origin of life.

After the primary introduction of varying amounts of sulfur to the initial reactants, we observed a percentual decrease of sulfur atoms per molecule over time instead of a continuous increase. This decrease in sulfur is true for all sulfur-containing groups that could be resolved and categorized in this study. The behavior of sulfur differs from that of the other elements in the system. The disappearance of sulfur from the formed compounds is an interesting observation. Sulfur represents an important element for origin-of-life reactions. In extant organisms, sulfur is less abundant than other relevant elements like carbon, nitrogen, and phosphate. Nonetheless, the remaining sulfur plays a crucial role in extant organisms. Indeed, thioesters like acetyl-CoA belong to the metabolically essential sulfur molecules. It is challenging to provide conclusive evidence for the precise process that leads to a sulfur reduction in the resulting compounds. Still, it can only be hypothesized with this untargeted approach.

We conducted and analyzed a 7-day experiment to study the evolution of a system with progressively decreasing sulfur levels. This system can be considered a fast motion of early evolution on Earth.

The analysis of the fraction of isomers revealed an unexpected distribution. Instead of a steady increase in isomer diversity, some chemical subspaces, mainly the sulfur-containing ones, showed very high variance in mixed annotations. This result shows an unknown amount of directed synthesis in the system, as some subspaces keep a certain amount of functional purity and do not uncontrollably diversify over time.

It is also relevant to mention the presence of thio acids in a large diversity. The present investigation reveals the full extent of the possible molecular diversity of pure thio acids and describes different formation pathways. One pathway requires acetylene and carbon monoxide; the other relies on acetylene alone. Independent of the pathway, the increase in mass and many saturation levels remain comparable. The temporal analysis of the mixture also revealed that larger thio acids reach their maximum intensity much later than thio acetic acid, most of them belonging to the SOM cluster reaching a maximum after 3 days. Thio acetic acid, on the other hand, decays quickly and becomes undetectable via NMR after 8 h.

Acetylene is the main driver of the increased mass of the detected molecules. Labeled atoms stemming from carbon monoxide remain in the single digits independently of the size of the molecule. Compounds detected after 7 days show between 15 and 27 carbon atoms within the mass range of 230–500 m/z but present only up to four carbon labels from ^{13}CO.

Acetylene is still a building block often overlooked. Still, our finding turns it into an important tool to increase molecular mass or as a C2-spacer to optimize the spatial arrangement of functional groups. All compound classes exhibit a noticeable increase in two-carbon mass, known as C2-chemistry. This phenomenon closely resembles the C2-metabolism of contemporary organisms, which is mediated by acetyl-CoA.

Conclusion

This work revealed a new dimension of complexity in a hydrothermal system based on the "metal-sulfur" world theory. Utilizing isotope labeling to categorize the functional groups enhanced the understanding of the reactions in the system.

Unexpected behavior was observed for sulfur, as its number was lowered in detected compounds over time, leading to sulfur numbers more akin to the biological molecules in contemporary organisms. We have discovered several ways to produce thio acids, indicating that this group of compounds is easily accessible in the environment we investigated. Furthermore, the role of acetylene as the main building block for synthesizing higher-mass compounds was shown by differentiating carbon originating from carbon monoxide and acetylene. We revealed a reoccurring pattern of C2-addition to all formed compounds through acetylene, a nutrient used by *Pelobacter acetylenicus* to fuel its fatty acid synthesis via a similar C2-metabolism. These results show new paths for further investigations that require the described functional groups or deliver a framework to tackle the analysis of even more complex systems containing nitrogen or phosphor.

Methods

Reaction bottle setup. In a typical run, a 125 ml glass serum bottle was charged with 1.0 mmol $NiSO_4 \bullet 6\ H_2O$ (99%, Aldrich) and sealed with a silicon stopper. The bottle underwent three cycles of evacuation and argon filling, ultimately reaching a deaerated state. Subsequently, the bottle was filled with argon-saturated water (calculated for the end volume of 5 ml), with 1.0 mL argon-saturated 1 M Na_2S (solid Na_2S: 99.99%, Aldrich) solution, with 1.0 mL 1 M NaOH solution and finally with 60 ml unlabeled CO and 60 ml unlabeled acetylene (acetone-free), using gastight syringes for the injections. Reactions were carried out at 105 °C. Following a reaction time of up to 7 days, the reaction mixture was cooled down. To conduct labeling experiments, ^{13}CO was utilized, while in a control run with the same composition, acetylene and CO were substituted with argon.

FT-ICR mass spectrometry. Samples were taken from the serum bottle with a syringe and centrifuged for 5 min at 15000 *rpm*. 100 µl of the supernatant were diluted in 900 µl methanol and centrifuged again to remove the precipitated salt. 70 µl of the centrifuged sample were diluted again in 930 µl methanol. For the timepoints 2 h, 1 day, 2 days, 3 days, 7 days and 7 days (13 C labeled) three different bottles were analyzed as biological replicates. Time points 3 h to 20 h were measured with two biological replicates. Every biological replicate was measured as three technical replicates. Only signals appearing in >66% of a triplicate were kept for annotation. Only annotated signals with a H/C ratio between 0.5 and 2.5 were kept. O/C ratios had to be below 1.5 for all annotations.

Analysis was performed on a high-field Fourier Transform Ion Cyclotron Resonance mass spectrometer from Bruker Daltonics —Solarix with a 12 T magnet from Magnex. The mass spectra were acquired with a 4-megaword (MW) time domain. The system was calibrated with L-Arginine clusters in negative ionization mode (5 mg L^{-1} L-arginine solved in methanol). For each sample, 200 scans were accumulated in negative ion mode in the mass range of 122–1000 amu. Ions were accumulated for 300 ms. The pressure in the hexapole was 3×10^{-6} mbar, and the pressure in the ICR vacuum chamber was 6×10^{-6} mbar. An Apollo ii (Bruker Daltonics) ESI source was used. The supernatant was injected via a microliter pump system (flow rate: 120 µl h^{-1}).

Data were recalibrated post data collection via a calibration list based on fatty acids with different chain lengths. Peaks were picked automatically in Data Analysis (Bruker) with a s/n threshold of 4. Mass lists were exported, filtered with two in-house filters removing wiggles artifacts and natural 34 S isotopes.

Formula assignment was done through a mass difference network approach[37]. The transformation list can be found in the excel sheet supplementary data.

Annotation of the labeling degree was done by comparing the 7-day setup with a CO-^{13}C- or acetylene ^{13}C labeled 7-day setup. In CO-labeled setups, compounds were categorized as labeled if the corresponding signal in the labeled sample showed a signal that surpassed the expected signal intensity of the natural ^{13}C (1% times the number of carbon atoms in an elemental composition) by 100%. ^{13}C acetylene signals were checked manually and had to fulfill the same requirements.

Molecular networks were generated and analyzed via the method mol2net (https://zenodo.org/record/7025094; Ruf & Danger 2022).

SOM-clustering. The data were preprocessed by the sklearn MinMaxScaler function. The SOM model was implemented on a 2×4 grid with a learning rate of 0.1. A Gaussian neighborhood function on top of a rectangular topology was used. Euclidean activation distances were used for model calculations. The compiled model was trained for 50,000 iterations. Aggregated clusters were extracted from the winning map and plotted with respective averaged cluster centers.

Data availability

The authors declare that [the/all other] data supporting the findings of this study are available within the paper [and in Supplementary Data 1]. Further data that support the findings of this study are available from the corresponding author upon reasonable request.

Received: 18 July 2023; Accepted: 3 October 2023;
Published online: 12 October 2023

References

1. Reppe, W. Carbonylierung I. Über die Umsetzung von Acetylen mit Kohlenoxyd und Verbindungen mit reaktionsfähigen Wasserstoffatomen Synthesen α,β-ungesättigter Carbonsäuren und ihrer Derivate. *Justus Liebigs Ann. der Chem.* **582**, 1–37 (1953).
2. Scheidler, C., Sobotta, J., Eisenreich, W., Wächtershäuser, G. & Huber, C. Unsaturated C3,5,7,9-Monocarboxylic Acids by Aqueous, One-Pot Carbon Fixation: Possible Relevance for the Origin of Life. *Sci. Rep.* **6**, 27595 (2016).
3. Ormeland, R. S. & Voytek, M. A. Acetylene as Fast Food: Implications for Development of Life on Anoxic Primordial Earth and in the Outer Solar System. *Astrobiology* **8**, 45–58 (2008).
4. Abbas O. & Schulze-Makuch D. Acetylene-based pathways for prebiotic evolution on Titan. *Exo-Astrobiology* **518**, 345–348 (2002).
5. Cable, M. L., Vu, T. H., Maynard-Casely, H. E., Choukroun, M. & Hodyss, R. The Acetylene-Ammonia Co-crystal on Titan. *ACS Earth Space Chem.* **2**, 366–375 (2018).
6. Melin, H., Fletcher, L. N., Irwin, P. G. J. & Edgington, S. G. Jupiter in the Ultraviolet: Acetylene and Ethane Abundances in the Stratosphere of Jupiter from Cassini Observations between 0.15 and 0.19 µm. *Astronom. J.* **159**, 291 (2020).
7. Postberg, F. et al. Detection of phosphates originating from Enceladus's ocean. *Nature* **618**, 489–493 (2023).
8. Waite, J. H. Jr. et al. Cassini ion and neutral mass spectrometer: Enceladus plume composition and structure. *Science* **311**, 1419–1422 (2006).
9. Rimmer, P. B. & Shorttle, O. Origin of Life's Building Blocks in Carbon- and Nitrogen-Rich Surface Hydrothermal Vents. *Life* **9**, 12 (2019).
10. Capaccioni, B. et al. Light hydrocarbons in gas-emissions from volcanic areas and geothermal fields. *Geochem. J.* **27**, 7–17 (1993).
11. Sanchez, R. A., Ferris, J. P. & Orgel, L. E. Cyanoacetylene in Prebiotic Synthesis. *Science* **154**, 784–785 (1966).
12. Schink, B. Fermentation of acetylene by an obligate anaerobe,Pelobacter acetylenicus sp. nov. *Arch. Microbiol.* **142**, 295–301 (1985).
13. Diender, M., Stams, A. J. M. & Sousa, D. Z. Pathways and Bioenergetics of Anaerobic Carbon Monoxide Fermentation. *Front. Microbiol.* **6**, 1275 (2015).
14. Wächtershäuser, G. Before enzymes and templates: theory of surface metabolism. *Microbiol. Rev.* **52**, 452–484 (1988).

15. Wächtershäuser, G. Evolution of the first metabolic cycles. *Proc. Natl Acad. Sci.* **87**, 200–204 (1990).
16. Huber, C. & Wächtershäuser, G. Activated acetic acid by carbon fixation on (Fe,Ni)S under primordial conditions. *Science* **276**, 245–247 (1997).
17. Diederich, P. et al. Formation, stabilization and fate of acetaldehyde and higher aldehydes in an autonomously changing prebiotic system emerging from acetylene. *Commun. Chem.* **6**, 38 (2023).
18. Sobotta, J. et al. A Possible Primordial Acetyleno/Carboxydotrophic Core Metabolism. *Life* **10**, 35 (2020).
19. Seitz C., Eisenreich W. & Huber C. The Abiotic Formation of Pyrrole under Volcanic, Hydrothermal Conditions—An Initial Step towards Life's First Breath? *Life* **11**, 980 (2021).
20. de Duve C. Chapter 7 Harnessing Energy. In: *Blueprint for a cell: the nature and origin of life*. (N. Patterson in 1991).
21. Frenkel-Pinter, M. et al. Thioesters provide a plausible prebiotic path to proto-peptides. *Nat. Commun.* **13**, 2569 (2022).
22. Closs, A. C., Bechtel, M. & Trapp, O. Dynamic Exchange of Substituents in a Prebiotic Organocatalyst: Initial Steps towards an Evolutionary System. *Angew. Chem. Int. Ed.* **61**, e202112563 (2022).
23. Geisberger, T., Sobotta, J., Eisenreich, W. & Huber, C. Formation of Thiophene under Simulated Volcanic Hydrothermal Conditions on Earth—Implications for Early. *Life Extraterrest. Planets? Life* **11**, 149 (2021).
24. Giavalisco, P. et al. High-Resolution Direct Infusion-Based Mass Spectrometry in Combination with Whole 13C Metabolome Isotope Labeling Allows Unambiguous Assignment of Chemical Sum Formulas. *Anal. Chem.* **80**, 9417–9425 (2008).
25. Nieuwland, J. A., Calcott, W. S., Downing, F. B. & Carter, A. S. Acetylene polymers and their derivatives. I. The controlled polymerization of acetylene. *J. Am. Chem. Soc.* **53**, 4197–4202 (1931).
26. Kutscheroff, M. Ueber eine neue Methode direkter Addition von Wasser (Hydratation) an die Kohlenwasserstoffe der Acetylenreihe. *Ber. der Dtsch. Chem. Ges.* **14**, 1540–1542 (1881).
27. Jones, S. O. & Reid, E. E. The Addition of Sulfur, Hydrogen Sulfide and Mercaptans to Unsaturated Hydrocarbons. *J. Am. Chem. Soc.* **60**, 2452–2455 (1938).
28. Moritz, F. et al. The compositional space of exhaled breath condensate and its link to the human breath volatilome. *J. Breath. Res.* **9**, 027105 (2015).
29. Ruf, A. & Danger, G. Network Analysis Reveals Spatial Clustering and Annotation of Complex Chemical Spaces: Application to Astrochemistry. *Anal. Chem.* **94**, 14135–14142 (2022).
30. Kohonen, T. Self-organized formation of topologically correct feature maps. *Biol. Cybern.* **43**, 59–69 (1982).
31. Weidner, L., Hemmler, D., Rychlik, M. & Schmitt-Kopplin, P. Real-Time Monitoring of Miniaturized Thermal Food Processing by Advanced Mass Spectrometric Techniques. *Anal. Chem.* **95**, 1694–1702 (2023).
32. Cronan J. E., Thomas J. Chapter 17 Bacterial Fatty Acid Synthesis and its Relationships with Polyketide Synthetic Pathways. In: *Methods in Enzymology*). (Academic Press, 2009).
33. Frenkel-Pinter, M., Sargon, A. B., Glass, J. B., Hud, N. V. & Williams, L. D. Transition metals enhance prebiotic depsipeptide oligomerization reactions involving histidine. *RSC Adv.* **11**, 3534–3538 (2021).
34. Stubbs, R. T., Yadav, M., Krishnamurthy, R. & Springsteen, G. A plausible metal-free ancestral analogue of the Krebs cycle composed entirely of α-ketoacids. *Nat. Chem.* **12**, 1016–1022 (2020).
35. Pulletikurti, S., Yadav, M., Springsteen, G. & Krishnamurthy, R. Prebiotic synthesis of α-amino acids and orotate from α-ketoacids potentiates transition to extant metabolic pathways. *Nat. Chem.* **14**, 1142–1150 (2022).
36. Yi, R. et al. Alternating co-synthesis of glycol nucleic acid (GNA) monomers with dicarboxylic acids via drying. *Chem. Commun.* **59**, 6865–6868 (2023).
37. Tziotis, D., Hertkorn, N. & Schmitt-Kopplin, P. Kendrick-Analogous Network Visualisation of Ion Cyclotron Resonance Fourier Transform Mass Spectra: Improved Options for the Assignment of Elemental Compositions and the Classification of Organic Molecular Complexity. *Eur. J. Mass Spectrom.* **17**, 415–421 (2011).

Acknowledgements

This research was funded by the Deutsche Forschungsgemeinschaft (DFG, German Research Foundation) – Project-ID 364653263 – TRR 235 (CRC 235). C.S. and C.H. thank the Hans-Fischer-Gesellschaft (D-Munich) for financial support. Furthermore, this project was funded by the Deutsche Forschungsgemeinschaft (DFG, German Research Foundation) under Germany´s Excellence Strategy - EXC 2094 - 390783311 (A.R.).

Author contributions

P.D. conceived and designed the analysis, collected the data, performed experiments, performed data analysis, and wrote the paper. A.R., L.W., T.G., C.S., and C.H. contributed analysis tools. T.G. and C.S. performed experiments. C.H., W.E., P.S.K., A.R., and L.W. edited the paper. P.S.K., C.H., and W.E. provided funding, supervised the project, and edited the paper.

Funding

Open Access funding enabled and organized by Projekt DEAL.

Competing interests

The authors declare no competing interests.

Additional information

Supplementary information The online version contains supplementary material available at https://doi.org/10.1038/s42004-023-01021-1.

Correspondence and requests for materials should be addressed to Claudia Huber or Philippe Schmitt-Kopplin.

Peer review information *Communications Chemistry* thanks Malak Tfaily and the other anonymous reviewers for their contribution to the peer review of this work.

Reprints and permission information is available at http://www.nature.com/reprints

Publisher's note Springer Nature remains neutral with regard to jurisdictional claims in published maps and institutional affiliations.

7.2.2 Appendix Supplementary 2

Supplementary Information

C2-addition patterns emerging from acetylene and nickel sulfide in simulated prebiotic hydrothermal conditions

Philippe Diederich [a], Alexander Ruf [b,c], Thomas Geisberger [d], Leopold Weidner [a,e] Christian Seitz [d], Wolfgang Eisenreich [d], Claudia Huber [d*], Philippe Schmitt-Kopplin [a, e, f*]

[a] Helmholtz Munich, Research Unit Analytical BioGeoChemistry, Neuherberg, Germany.

[b] Excellence Cluster ORIGINS, Boltzmannstraße 2, 85748 Garching, Germany
[c] LMU Munich, Faculty of Physics, Schellingstraße 4, 80799 Munich, Germany
[d] Technical University of Munich, TUM School of Natural Sciences, Department of Bioscience, Bavarian NMR Center (BNMRZ), Structural Membrane Biochemistry, Lichtenbergstr. 4, 85748 Garching, Germany

[e] Comprehensive Foodomics Platform, Chair of Analytical Food Chemistry, TUM School of Life Sciences, Technical University of Munich, Maximus-von-Imhof-Forum 2, 85354 Freising, Germany

[f] Max Planck Institute for Extraterrestrial Physics, Center for Astrochemical Studies, Gießebachstraße 1, 85748 Garching bei München, Germany.

[*]Corresponding authors: Research Unit Analytical BioGeoChemistry, Helmholtz Zentrum München–German Research Center for Environmental Health, Neuherberg, Germany and Technical University of Munich, TUM School of Natural Sciences, Department of Bioscience, Bavarian NMR Center (BNMRZ), Structural Membrane Biochemistry, Lichtenbergstr. 4, 85748 Garching, Germany

Emails: schmitt-kopplin@helmholtz-muenchen.de, claudia.huber@tum.de

Correlation between number of oxygen atoms per molecule and the H/C ratio for different compound classes

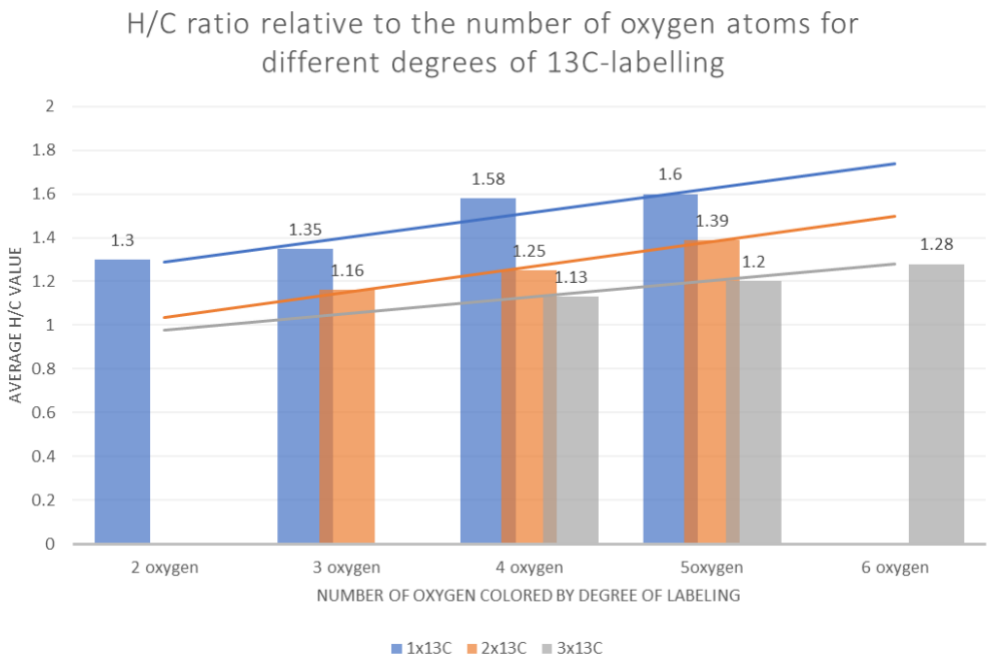

Supplementary Figure 1: Barplot showing the increasing H/C ratio with increasing amounts of oxygen atoms per molecule.

Spiking experiment with thio acetic acid standard

To prove the presence of thio acetic acid at early time points and its disappearance later, we measured the mixture after 2 hours and 7 days. To confirm the presence of thio acetic acid, a standard was spiked to the 7-day sample, and its chemical shift was compared to the signal after 2 hours (Supplementary Figure 1, gray line).

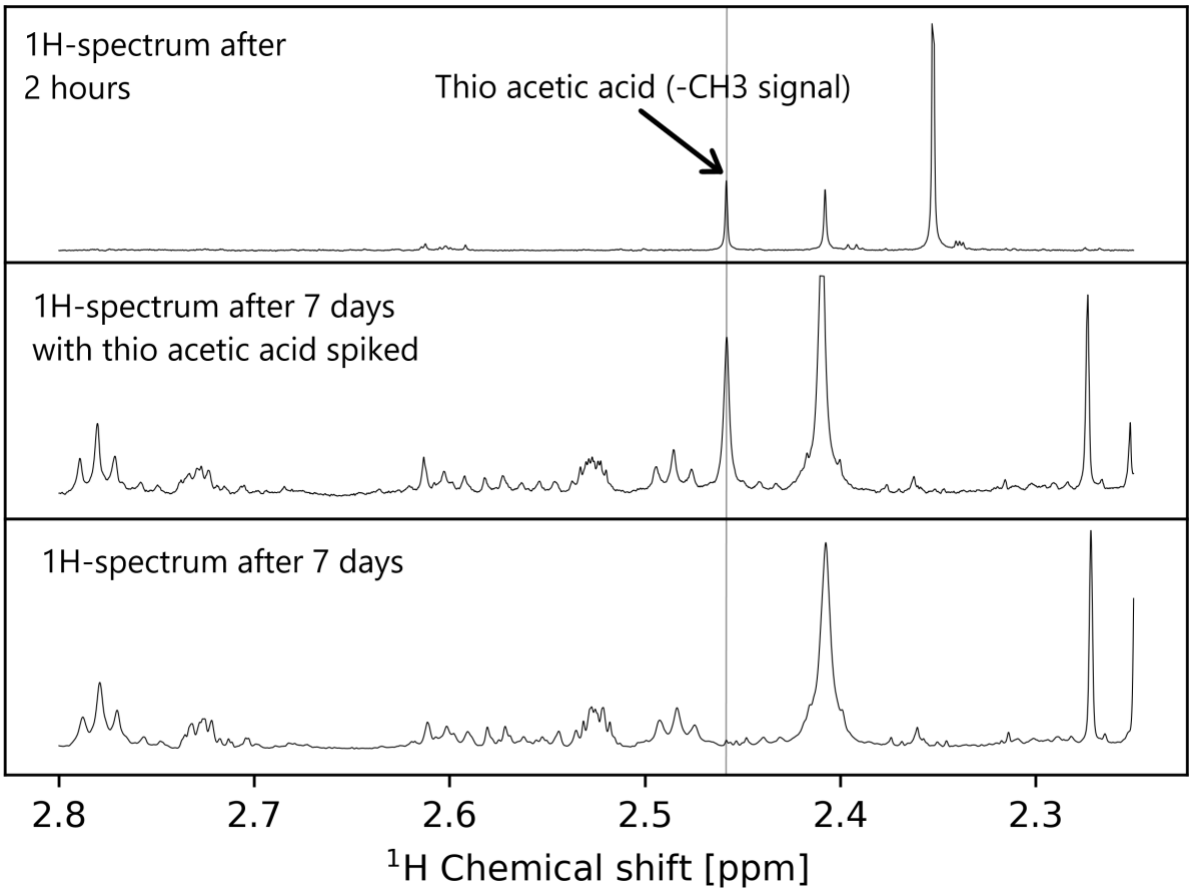

Supplementary Figure 2: ^{1}H-spectrum of the investigated setup after 2 hours and 7 days. Thio acetic acid was spiked into the 7-day experiment to confirm this compound. The gray line marks the chemical shift of thio acetic acid.

Identification of 3,3´-thiobispropanoic acid

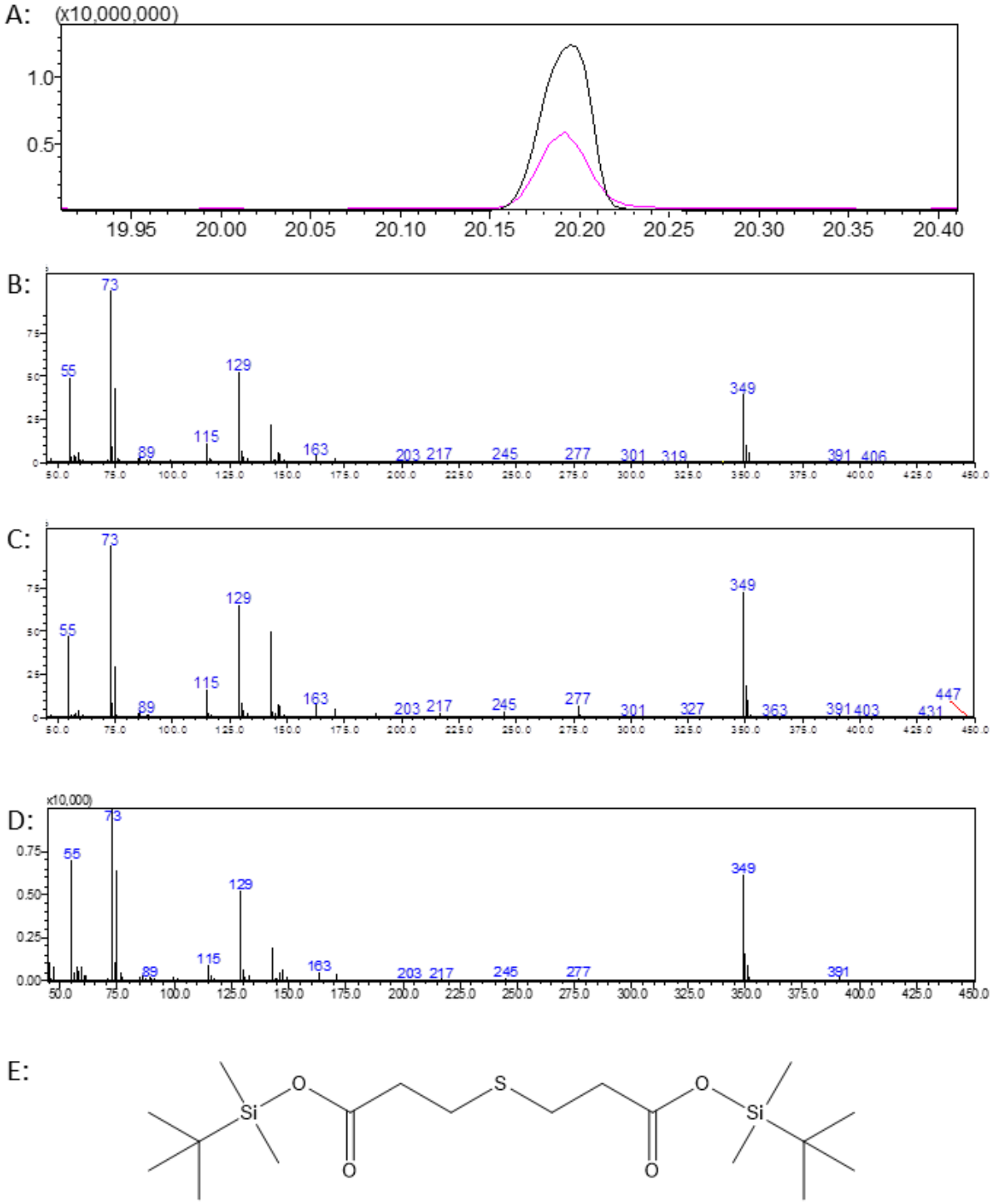

Supplementary Figure 3: GC-MS chromatogram and mass spectra from TBDMS derivatized 3,3´-thiobispropanoic acid. Sample preparation and GC-MS conditions are described in [15]

A: Chromatogram showing mass traces from a commercially available standard (black) and 3,3´-thiobispropanoic acid from the reaction supernatant (pink).

B: Mass spectrum from the commercially available 3,3´-thiobispropanoic acid

C: Mass spectrum from the reaction supernatant

D: Mass spectrum taken from library NIST14.

E: Structure of TBDMS derivatized 3,3´-thiobispropanoic acid (characteristic fragments: M-15 (methyl group): m/z 391; M-57 (tert-butyl group): m/z 349

Higher sulfur compounds showing homologous series of sodium adducts

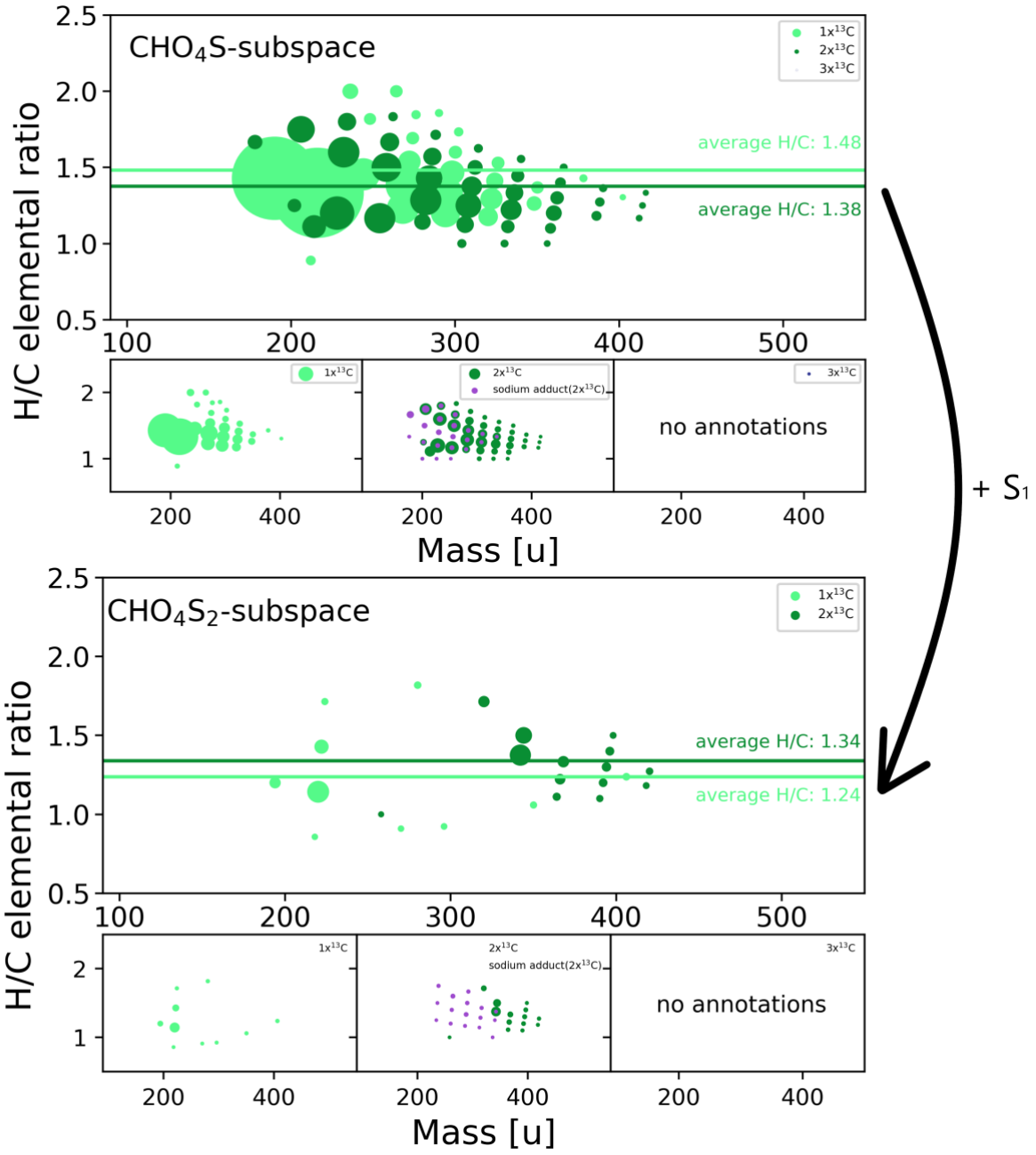

Supplementary Figure 4: Comparison of CHO_4S-subspace and CHO_4S_2-subspace. The two subspaces show interesting similarities to the CHO_4-subspace, mainly consisting of dicarboxylic acids. Comparing the two sulfur subspaces shows the nearly identical level of saturation and labeling between the fractions of sodium adducts (violet). This suggests that they are structurally very similar and are potentially only differentiated by a longer sulfur chain.

Proposed reaction schemes for the categorized compound classes

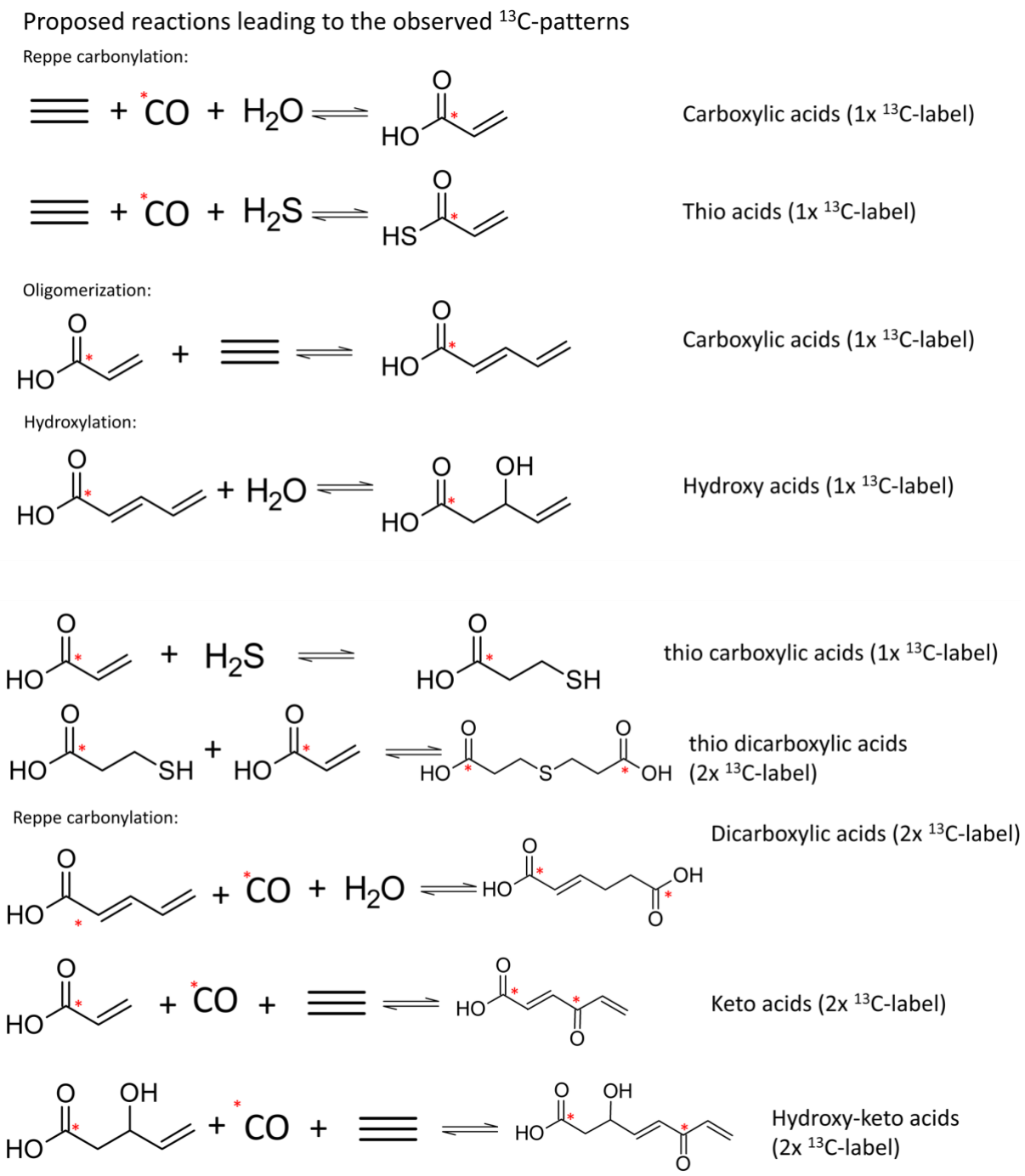

Supplementary Figure 5: Reactions with carbon monoxide leading to different degrees of 13C-labeling

Spectral manifestation of 13C-labeling. Unlabeled setup compared to labeled carbon monoxide spectrum

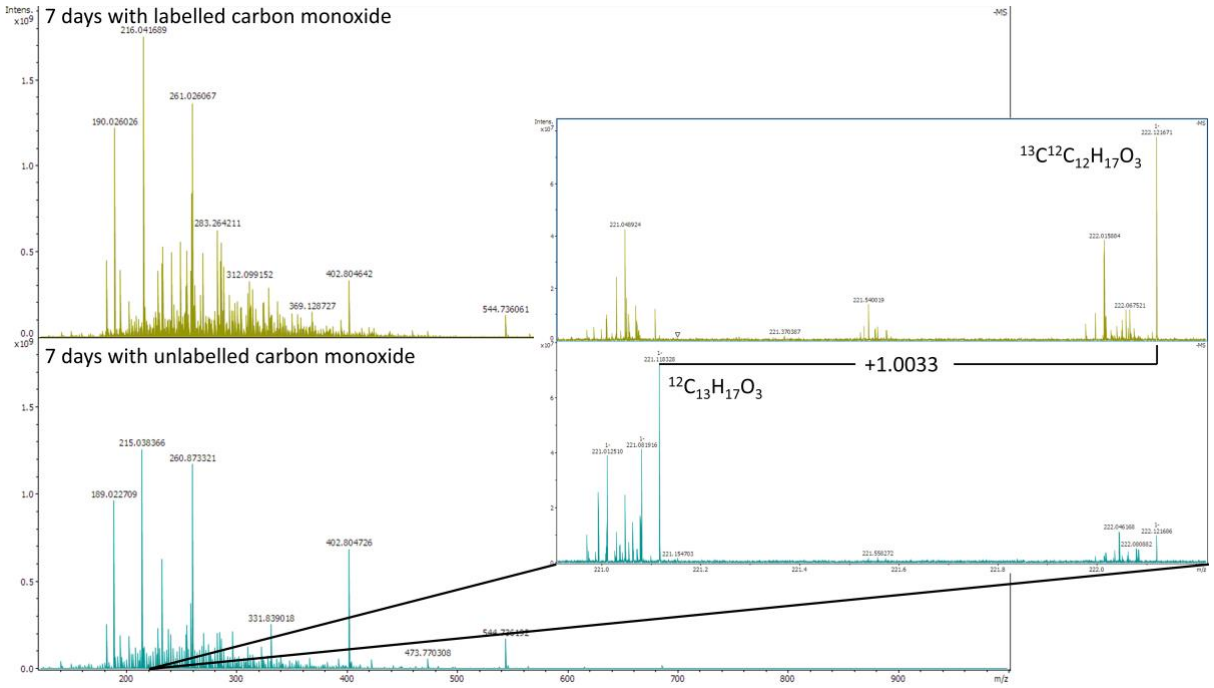

Supplementary Figure 6: Figure showing the spectral appearance of an unlabeled setup versus a lebaled setup. The magnification shows how the mass of a labeled signal shifts by exactly 1.0033 amu.

7.3.1 Appendix Paper 3

communications chemistry

Article

https://doi.org/10.1038/s42004-024-01119-0

Nickel-organo compounds as potential enzyme precursors under simulated early Earth conditions

Philippe Diederich[1], Christian Seitz[2], Lance Buckett[1], Liesa Salzer[1], Thomas Geisberger[2], Wolfgang Eisenreich[2], Claudia Huber[2] & Philippe Schmitt-Kopplin[1,3,4]

The transition from inorganic catalysis through minerals to organic catalysis by enzymes is a necessary step in the emergence of life. Our work is elucidating likely reactions at the earliest moments of Life, prior to the existence of enzymatic catalysis, by exploring essential intersections between nickel bioinorganic chemistry and pterin biochemistry. We used a prebiotically-inspired acetylene-containing volcanic hydrothermal experimental environment to shed light on the efficient formation of nickel-organo complexes. The simplest bis(dithiolene)nickel complex $(C_2H_2S_2)_2Ni$ was identified by UV/Vis spectroscopy, mass spectrometry, nuclear magnetic resonance. Its temporal progression and possible function in this simulated early Earth atmosphere were investigated by isolating the main bis(dithiolene)nickel species from the primordial experimental setup. Using this approach, we uncovered a significant diversity of nickel-organo compositions by identifying 156 elemental annotations. The formation of acetaldehyde through the subsequent degradation of these organo-metal complexes is intriguing, as it is reminiscent of the ability of *Pelobacter acetylenicus* to hydrate acetylene to acetaldehyde *via* its bis(dithiolene)-containing enzyme acetylene hydratase. As our findings mechanistically characterize the role of nickel sulfide in catalyzing the formation of acetaldehyde, this fundamental pre-metabolic reaction could play the role of a primitive enzyme precursor of the enzymatic acetylene metabolism and further strengthen the role of acetylene in the molecular origin of life.

Initially, bis(dithiolene)nickel compounds garnered attention solely for their synthetic properties. However, their resemblance to enzyme catalytic centers was later recognized, leading to renewed attention for those nickel-organo compounds. The synthesis of thiophene from acetylene and pyrite (FeS_2) by Steinkopf and Kirchhoff[1] originally inspired Schrauzer and Mayweg to investigate the reactions between diphenyl acetylene and nickel sulfides in toluene[2]. Schrauzer's discovery of bis(diphenyldithiolene)nickel, a nickel-sulfur complex with highly covalent metal-ligand bonds, led to the successful synthesis of various derivatives of this compound class, including the synthetically challenging unsubstituted complex $(C_2H_2S_2)_2Ni$, obtained from halogenated non-gaseous precursors and dissolved nickel ions[3].

Several extant enzymes possess metal-dithiolene active cores binding to transition metals like tungsten or molybdenum[4]. One example is acetylene hydratase (AH) expressed by the anaerobic bacterium *Pelobacter acetylenicus*. This organism is frequently discussed in the context of the origin of life because of its unique ability to hydrate acetylene into acetaldehyde, leading to acetyl-CoA and acetate building blocks. Hyperthermophile Archaea thriving in the vicinity of volcanic hydrothermal vents express aldehyde ferredoxin oxidoreductase (AFO) with a tungstopterin center catalyzing the oxidation of aldehydes into carboxylic acids at 100 degrees Celsius (C°)[4]. Interestingly, the catalytic ability of enzymes relying on metal-dithiolenes can be enhanced by exchanging molybdenum with

[1]Helmholtz Munich, Research Unit Analytical BioGeoChemistry, Neuherberg, Germany. [2]Technical University of Munich, TUM School of Natural Sciences, Department of Bioscience, Bavarian NMR Center (BNMRZ), Structural Membrane Biochemistry, Lichtenbergstr. 4, 85748 Garching, Germany. [3]Comprehensive Foodomics Platform, Chair of Analytical Food Chemistry, TUM School of Life Sciences, Technical University of Munich, Maximus-von-Imhof-Forum 2, 85354 Freising, Germany. [4]Max Planck Institute for Extraterrestrial Physics, Center for Astrochemical Studies, Gießebachstraße 1, 85748 Garching bei München, Germany. e-mail: schmitt-kopplin@helmholtz-muenchen.de

nickel in molybdopterin-like catalysts[5]. Regardless of the presence of an enzyme structure, the nickel bis(dithiolene) complex alone is an excellent electron transporter as it exists in three oxidation states (0, −1, −2). As a result, these complexes activate hydrogen more efficiently than most hydrogenases in Nature[6], which aligns with the abiogenesis theory of prebiotic synthesis of organic molecules.

The role of acetylene as a building block of terrestrial life remains a topic of speculation. Still, there is growing evidence for its presence in the atmosphere of interstellar bodies such as Titan[7] or Jupiter[8]. Additionally, its existence on early Earth is hypothesized[9,10], emphasizing the importance of investigating the role of acetylene in the emergence of life. Previous hypotheses regarding the role of acetylene in the origin of life have suggested that it contributes to the formation of polycyclic aromatic hydrocarbons[11] and small biomolecules[12]. Its popularity increased after it was proposed as a "fast food" for organisms in Earth's early biosphere[9]. Recent literature analyzed the potential of acetylene under the same conditions to form distinct unsaturated fatty acids in combination with carbon monoxide[13]. Moreover, a route to pyrrole was demonstrated in the presence of ammonia, leading to the elemental unit of porphyrin, another metal complexing scaffold indispensable for life as we know it today. Acetylene, combined with nickel sulfide, forms a large diversity of prebiotic organic compounds, including acetaldehyde and alanine, in a one-pot setup[14].

Nickel plays a fundamental role in enzymes found in most organisms, independent of the bis(dithiolene) framework. Nickel sites in extant enzymes show a large variety in nickel coordination and redox chemistry over a potential range of 1500 mV in proteins[15]. The metal center in superoxide dismutase (SOD) catalyzes redox processes with potentials ranging from +890–−160 mV[16]. In methyl-coenzyme M reductase (MCR) and carbon monoxide dehydrogenase (CODH), the active sites reach potentials as low as −600 mV[17].

Anaerobic nickel-containing CODH isoforms are found in organisms capable of heterotrophy, autotrophy, fermentation, or anaerobic respiration[18,19]. In hydrogenogenic CO oxidizers, CO oxidation is coupled with proton reduction to produce hydrogen (H_2)[20]. In the presence of water, required as an electron acceptor, a hydrogenase, and an ATP synthase are sufficient to ensure respiration. This straightforward mechanism highlights the significance of nickel-based catalysis in ancient energy preservation[21].

Nickel sulfide plays a crucial role in recent prebiotic chemistry, as they were shown to promote multiple relevant reactions. Thioesters were synthesized on nickel sulfide through geoelectrochemical CO2 fixation[22]. Another study reported the promotion of a protometabolism in an alkaline hydrothermal vent environment[23]."

Ni-organo catalysts are pivotal in various organic reactions, including cross-coupling reactions (e.g., Suzuki, Kumada, or Negishi couplings)[24], carbon-heteroatom bond-forming[25] reactions and the hydrogenation of organic compounds[26]. Our experimental setup finds its roots in the "Iron-sulfur world" theory of Wächtershäuser who considered nickel or iron sulfide salts as catalytically active species due to their redox potential and limited solubility in water, which allows surface catalysis.

We now further investigated the previously mentioned one-pot setup[14] with a focus on the formation mechanism of acetaldehyde and its link to the presence of nickel-organo compounds. The one-pot setup already showed a progressing system that generated acetaldehyde over time and also changed its pH in the process due to formed acids, ultimately leading to a changed reaction path for the formed acetaldehyde. Building on the knowledge about the presence of acetaldehyde, we provide the first mechanistic evidence of abiogenic acetylene processing based on nickel bis(dithiolene), a molecular structure reminiscent of active centers of contemporary enzymes. Considering the resemblance with molybdopterin coenzymes, we postulate that nickel bis(dithiolene) was a transition catalyzer, allowing early acetaldehyde formation from acetylene in a prebiotic environment.

Results

Formation and identification of nickel-organo complexes

The investigated prebiotic system consisted of an oxygen-free carbon monoxide and acetylene atmosphere in equal amounts in the headspace of water containing water-insoluble nickel sulfide salt (NiS). The setup was contained in a sealed glass bottle and was incubated at 105 °C for varying periods of time.

The presence of nickel complexes was detected using Fourier-transform ion-cyclotron-resonance mass spectrometric (FT-ICR-MS) measurements after 2 h of incubation. FT-ICR-MS analysis allowed a reliable elemental annotation of the nickel-organo complexes in the complex reaction mixture. $C_4H_4S_4Ni$ was the most abundantly detected nickel-

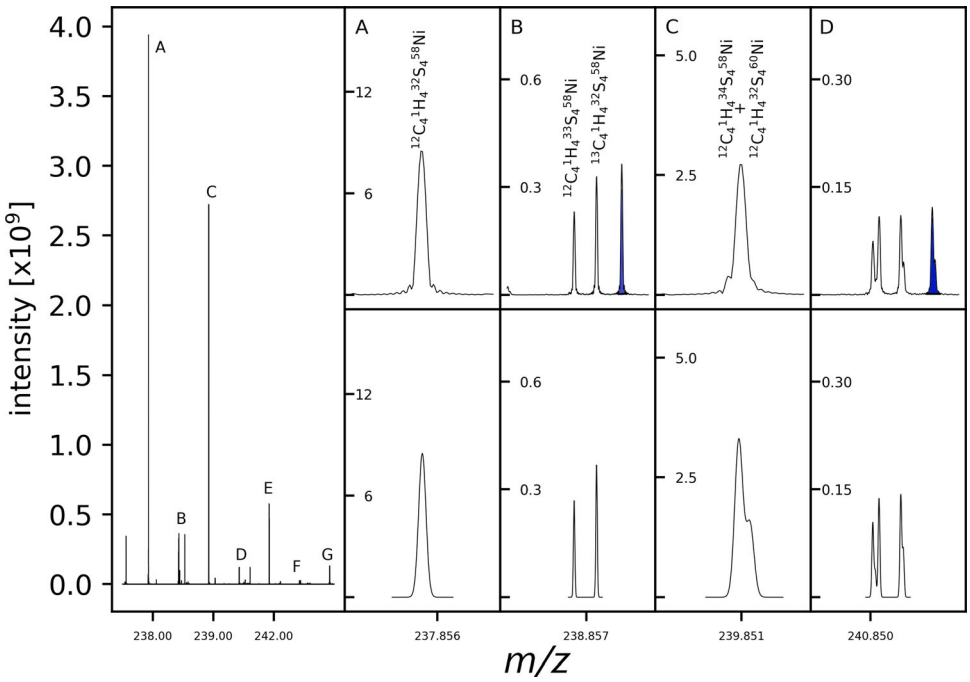

Fig. 1 | True isotopic pattern of nickel bis (dithiolene). FT-ICR-MS mass spectrum (left) with its annotated isotope pattern signals (top right) in comparison to the theoretical pattern (bottom right) enlarged in (**A**–**C**). **D** shows a further cluster of isotope signals made up of permutations of the isotopes in (**A**–**C**). Additional signals in blue highlight the -2 charge state. Signals marked **E**–**G** are further isotopic patterns belonging to the compound not shown in a zoomed in panel.

organo species by intensity. This annotation fits the simplest dithiolene-nickel species that can be obtained from two acetylene molecules, four sulfur, and one nickel atom. Due to its high abundance in the system, the composition could be further validated with its isotopic fine structure, excluding the possibility of false elemental annotation due to an isobaric compound (Fig. 1).

Samples showing the highest intensity of this compound in MS-spectra display a pink color (Suppl. Fig. 1). This color and the mass spectra signals for $C_4H_4S_4Ni$ decreased over time and were lost after 3 days of incubation.

A closer inspection of the isotope pattern revealed a further signal (Fig. 1, B+D highlighted in blue) not explained by the theoretical simulated isotope pattern. The mass difference between this additional peak and the isotope peak of the previous nominal mass amounts to the mass of one hydrogen atom. This result can be explained by the different possible oxidation states of nickel-bis(dithiolenes). The main peak belongs to the M^{-1} species. The additional peaks belong to the $[X^{-2} + H^{+1}]^{-1}$ species, with X being any isotopic species with a sufficiently high intensity to detect the second oxidation state species. The same observation was made for sodium ions but with lower signal intensity.

UV/VIS spectroscopy of the colored reaction product in water showed two absorption maxima at 500 and 855 nm. The second maximum is in the near-infrared at 855 nm. Absorption in the near-infrared is characteristic of bis(dithiolene)nickel compounds[27]. The maximum at 500 nm explained the observed pink color as absorption of green light results in red transmitted light and is also expected to be associated with the detected complex. Degradation of the complex in water happened relatively fast, and the corresponding UV/Vis signals nearly disappeared completely after 4 h at room temperature (Fig. 2, A). The degradation of the compound was accompanied by a color change of the solution from pink to yellow.

Isolation of the nickel-organo complex

We isolated the described complex from the aqueous solution *via* liquid-liquid extraction using methyl tert-butyl ether (MTBE). The MTBE phase took on a strongly violet color after the extraction of the aqueous phase. The MTBE phase was completely dried under N_2 flow, and a dark blue solid remained in the glass vial. This color is also reported by Schrauzer, who synthesized the compound through a different non-aqueous route with halogenated reactants, incompatible with currently hypothesized conditions on early Earth[3]. We weighed the remaining solid of two different experimental setups in triplicates, differing in the composition of the gaseous atmosphere (Table 1). The setup with carbon monoxide produced 5.97 mg of the complex with a theoretical yield of 1.79%. In contrast, a setup with twice the volume of acetylene in the absence of carbon monoxide generated 6.92 mg with a yield of 1.14%. Utilizing twice the volume of acetylene increased the absolute yield as expected but decreased the theoretical yield. These yields are comparable to those reported by Schrauzer, who obtained a 3% yield using a more elaborate synthetic route. One triplicate of the CO/acetylene setup only showed very faint coloration. This triplicate also showed the lowest residual mass. A reaction scheme and discussed compounds can be found in the supplementary information (Suppl. Fig. 2).

The near insolubility of the isolated compound at room temperature in purified water strengthened our hypothesis of a changed charge state. Even though the color change could result purely from the solvent change, another explanation is the change of the complexes' oxidation state from a charged water-soluble state to an uncharged lipophilic state. The solid only slowly dissolved at temperatures >50 °C, resulting in the expected pink coloration, followed by rapid degradation. Furthermore, adding the original reaction medium did not solubilize the compound at room temperature, excluding the possibility of a solubility-enhancing effect through molecules or salts formed in the experimental setup. Extraction of the residual solid phase in the reaction bottle with MTBE, expected to be mainly solid nickel sulfide salt, did not yield any amount of the target compound (no coloration of the MTBE used for extraction). We concluded that the compound remained solubilized during the experiment without precipitation and changed its oxidation state during extraction.

The isolated compound was further analyzed *via* LC-MS/MS to validate the hypothesized structure. LC-MS analysis of the dried extracted solid dissolved in methanol resulted in a violet solution with the same appearance as the MTBE solution. We detected the expected mass previously found in the initial mixture identified as $(C_2H_2S_2)_2Ni^-$. Fragmentation was performed with a UHPLC-IM-Q-ToFMS system to gather fragmentation data (Fig. 2, B) and report its collision cross section (CCS) value of 130 $Å^2$.

Fate of the formed nickel complex

The isolated water-insoluble complex became soluble at around 50 °C and above. Dissolution of the complex also resulted in a color change back to pink, comparable to the color of the unextracted aqueous mixture, reflecting the presence of the charged state in water.

Incubation of the isolated complex in water at pH 11 for 15 and 30 h resulted in the degradation of the complex. The degradation route and degradation products are temperature-dependent. The complex degraded into formic acid and acetaldehyde at temperatures reflecting the initial experimental conditions (100 °C) (Fig. 3). This result confirms the previously observed characteristics of those two compounds in the system and sheds light on the exact mechanism of their formation with nickel sulfide[11]. Incubation at 24 °C yielded no acetaldehyde. NMR measurements of the incubated sample showed increased signals in the olefinic ppm range. This observation shows the formation of new carbon-carbon bonds via this complex during its degradation. The complex degraded into unsaturated acetylene polymers. NMR spectra can be found in Supplementary data 1.

In the degradation process, nickel sulfide is consistently formed. The identification was made by observing an insoluble black solid in the reaction vessel. However, likely, the nickel and sulfur released during degradation precipitated at least partially into nickel sulfide. This particular process provides the complex with the ability to dissolve nickel sulfide, making it

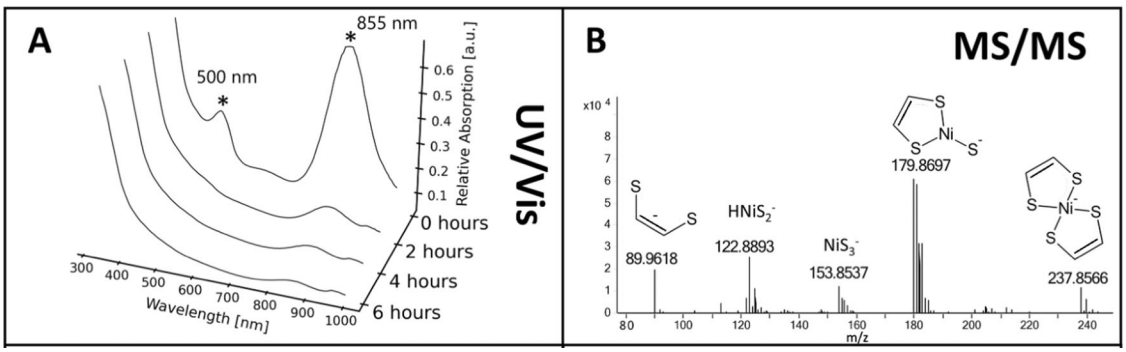

Fig. 2 | Identification of bis(dithiolene) nickel. A UV/Vis spectrum of the complete aqueous 2 h reaction product degrading over time. **B** MS/MS of the m/z 237.85 with suggested structures for the detected fragments.

Table 1 | Nickel bis(dithiolene) yield.

Gas mixture	Gas Ratio (%)	All yields (mg)	Mean Yield (mg)	Theoretical yield (%)	Relative Standard deviation (%)
CO/acetylene	50/50	5.97/5.98/(1.92)*	5.97	1.79	0.1%
Acetylene	100	6.81/7.19/6.76	6.92	1.14	3.4%

Yields from triplicate experiments with two different atmospheres determined by weighing after drying. Gas ratio describes the ratio of the two gases used in the setups. Every yield is shown for each triplicate. The *marked triplicate was excluded from the yield determination.

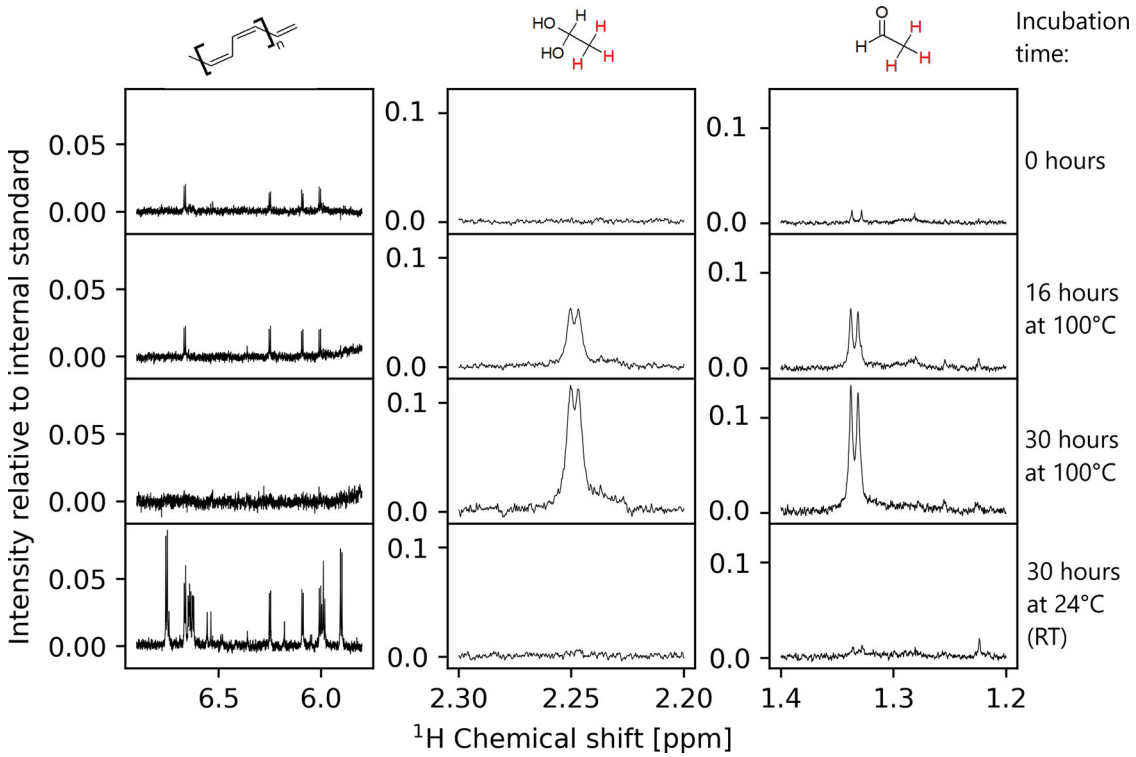

Fig. 3 | Temporal progression of the isolated nickel complex over time. The ppm range with the main changes is zoomed in. Structures on top show the observed hydrogen in red for acetaldehyde. As the structure of the olefinic species could not be determined, only the structure of an olefinic chain is shown. The incubation time indicates the time the sample was kept at 100 °C or room temperature, respectively.

soluble, transport this highly insoluble salt and relocate it via diffusion processes.

Identification and characterization of diverse nickel-organo species

The compound with the elemental composition $(C_2H_2S_2)_2Ni$ is not the only nickel-containing annotation in the mixture. 156 different elemental compositions were annotated, some containing various amounts of oxygen. The addition of oxygen to the sulfur atoms in those complexes was already described and discussed by Schrauzer[28]. The detected diversity of nickel-organo compounds is vast and sometimes challenging to interpret, as some elemental compositions contain odd amounts of carbon atoms, a fact hinting at a carbon cleavage pathway with nickel-organo compounds as intermediates. This hypothesis is also strengthened by the detection of formic acid after the degradation of the complex. Most annotations show the NiS_4-core of the bis(dithiolene)nickel complex, followed in number by NiS_3-"cores" (Fig. 4). It cannot be excluded that some or all NiS_3-annotations result from in-source fragmentation, as the fragmentation pattern of $[(C_2H_2S_2)_2Ni]^-$ also showed a fragment with the formula $[C_2H_2S_3Ni]^-$. Nickel-organo annotations become increasingly scarce with higher amounts of sulfur atoms in the molecule. The NiS_6-"core"-group is nearly devoid of signals. Only the $[C_6H_xNiS_6]^-$ compositions (highlighted in yellow in Fig. 4) show some diversity in their homologous hydrogen series and could belong to the trimer, carrying an additional dithiolene unit.

Discussion

The formation of the reported bis(dithiolene) nickel complex after 2 h of incubation of the evolving reaction mixture showed the feasibility of its existence in early earth scenarios. The similarity of the formed bis(dithiolene) nickel complex with the active center of AH found in *Pelobacter acetylenicus* living in anaerobic aqueous systems is very intriguing, as the setting of the experiment is situated in a prebiotic oxygen-free atmosphere. Acetaldehyde is obtained from acetylene in the presence of NiS via the formed nickel bis(dithiolene) and then oxidized to acetic acid[14](Fig. 5). This oxidation corresponds to a reaction performed by the hyperthermophilic archaeon *Pyroccocus furiosus via* AFO, another molybdopterin-containing enzyme. The likeness of the habitat of this microorganism is even more striking, as it lives near hydrothermal vents at 100 °C.

The described transportation role of the complex is also worth mentioning. The ability to extract nickel sulfide from minerals, to be later redeposited after degradation, leads to new scenarios, where nickel-catalyzed reactions like the reduction of double bonds[29] can occur on primitive Earth. The change in polarity, from an ionic form into a highly lipophilic organic form, could also lead to enhanced complex uptake into vesicles with less permeable and hydrophobic properties. This aspect makes the reported complex not only relevant for early prebiotic stages but also for later stages during a transition from reactions in an aqueous bulk to an evolving metabolism in protocells. Its chemical nature facilitates its introduction into vesicular protocells. This hypothesis is strengthened by a

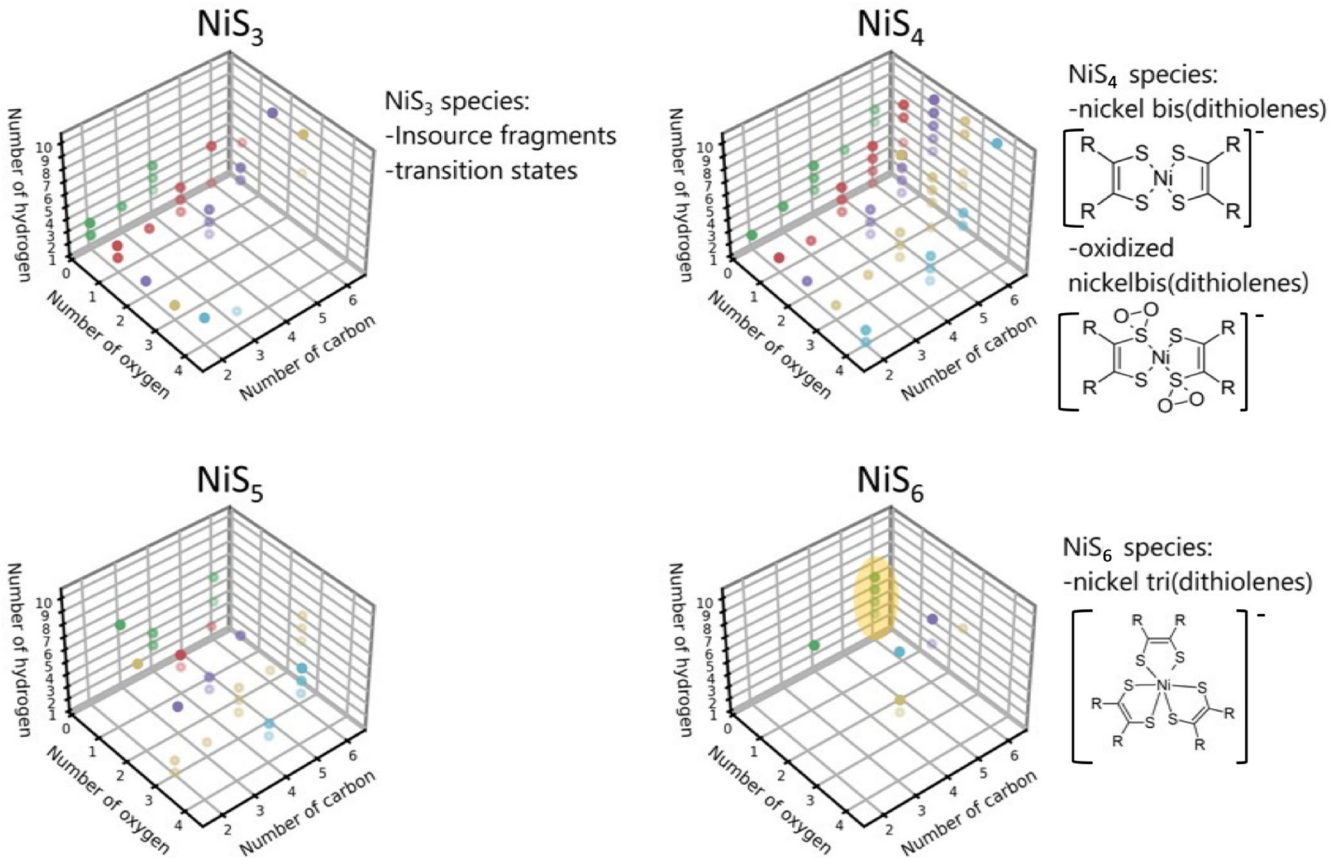

Fig. 4 | Nickel-organo complexity. 3 dimensional plots show the diversity in elemental composition for detected signals containing nickel and 3,4,5 or 6 sulfur atoms. Potential explanations for the NiS_x motives are given next to the plots. NiS_5 annotations most likely belong to insource fragmentation, but their exact identity is not known. The color of the dot represents the number of oxygen (0 for green, 1 for red, 2 for violet, 3 for yellow and 5 for blue). A yellow ellipse highlights the only homologous hydrogen series for compounds with one nickel and six sulfur. Residuals marked as R consist of carbon, hydrogen, and/or oxygen but cannot be further characterized.

recently published report of vesicle formation in the described set-up, where the formed long-chain fatty acids showed the potential to form vesicles[30].

The described complexity of the nickel-organo complexes has the potential for the derivatization of this core motif for co-enzymes. Derivatization of the elemental nickel bis(dithiolene) alters its reactivity and potential to catalyze different reactions. The literature on nickel bis(-dithiolene) complexes provides a large list of catalyzed reactions involved in the energy management of microorganisms. The reduction of hydrogen atoms to form hydrogen gas is among the most interesting. Bis(dithiolene) nickel complexes lower the reduction potential required for proton reduction resulting from formed acids[6]. Ameerunisha et al. reported the reduction of protons from p-toluene sulfonic acid through a nickel bis(dithiolene) complex[6]. The fact that this environment produced a large diversity of unsaturated carboxylic acids from carbon monoxide and acetylene[13] increases the relevance of this mechanism, as those acids dissociate readily under aqueous conditions. The second origin of hydrogen cations in the system is acetic acid. Another reduction performed by those complexes is the reduction of CO_2 into formic acid[31]. The ability of nickel bis(dithiolene) to act as an electron transporter and to exist in several oxidation states lets it perform energy transfer roles.

The formation of carboxylic acids synergizes well with the redox reactions catalyzed by this compound class. Metal-bis(dithiolene) compounds are potent hydrogenases. Nickel bis(dithiolene) complexes can reduce protons from organic acids to hydrogen gas[6]. One characteristic of the investigated system is the production of many highly unsaturated acids *via* Reppe chemistry[13] and other acids. A compound reinforcing the suspected hydrogen activation is propanoic acid. Acrylic acid is the primary product of acetylene and carbon monoxide via the chemistry described by Reppe in 1953[32]. Detection of its reduced form of propanoic acid[33] in the mixture indirectly indicates a possible reduction with hydrogen gas.

In addition to its redox capabilities, bis(dithiolene) nickel compounds act as intermediates for many organo-sulfur compounds[34]. One main follow-up product of bis(dithiolene) nickel is thiophene, proven to exist in large amounts in the investigated mixture[35].

Electron transfer is a vital mechanism of all living systems and is performed by NAD(H)/NADP(H) to allow ATP synthesis in extant organisms. The fact that acetylene is transformed to a large degree into aldehydes and additionally leads to a complex very similar to several active centers in enzymes connected to the metabolism of those compounds is a meaningful coincidence. A recent paper even showed its potential to oxidize glucose into gluconolactone[36]. Extant enzymes with pterin co-factors contain mostly molybdenum or tungsten. Yet nickel is a much more frequent element on Earth[37] with an elemental abondance of 1.86% compared to Mo with 2.35 ppm and W with 180 ppb; therefore, the early existence of precursors of active centers with nickel is a plausible hypothesis. Additionally, nickel is found in the active centers of 9 contemporary enzymes (known so far)[38]. Further studies have to be performed to investigate what prebiotic conditions allow for an exchange of nickel through molybdenum or tungsten."

Our findings revealed a pathway from acetylene to acetaldehyde via a nickel-organo complex. This discovery strengthens the relevance of nickel-organo compounds for the origin of life, as they now present an intermediate product for a prebiotic synthesis pathway of higher aldehydes, the amino acid alanine and potentially higher amino acids. Furthermore, this finding now paves the way for investigations about the exact catalytical nature and other roles in prebiotic chemistry of this nickel-organo compound.

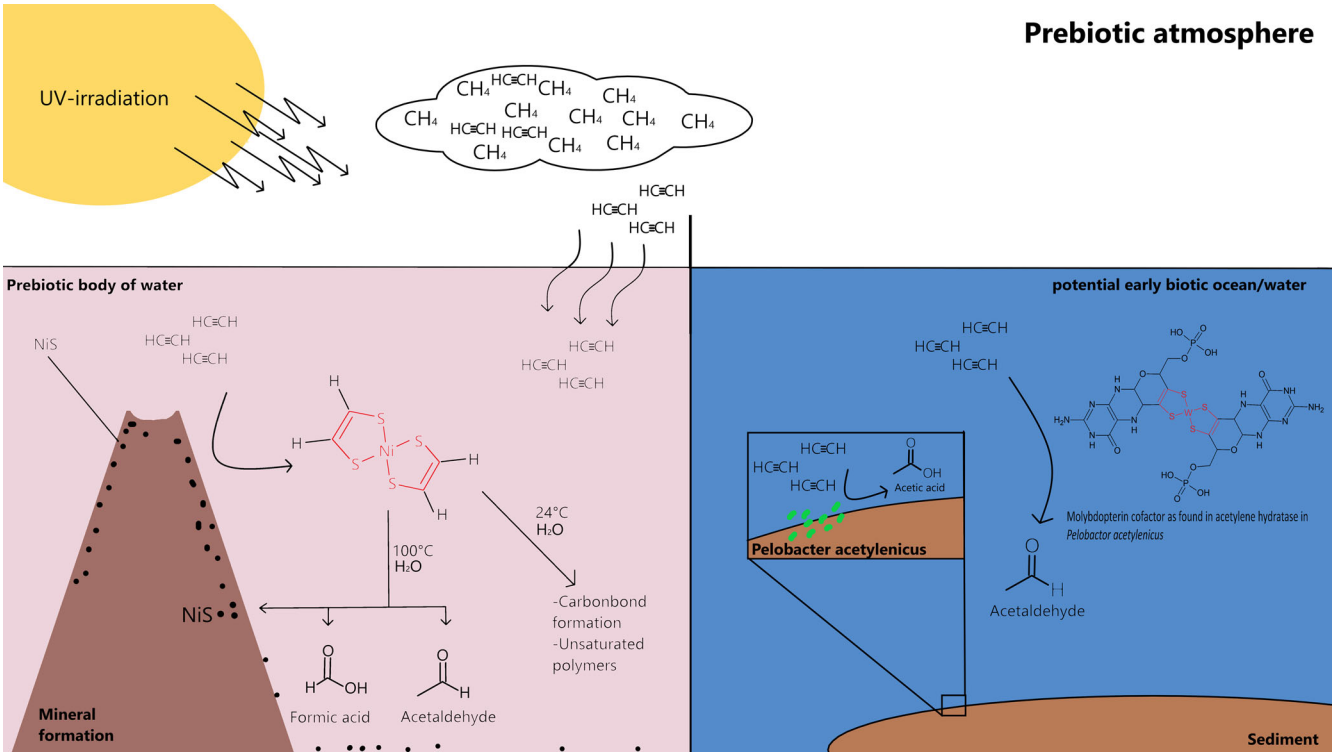

Fig. 5 | Overview of a potential scenario forming acetaldehyde from acetylene via nickel bis(dithiolene). A Reaction scheme showing a plausible pathway under early earth conditions leading to bis(dithiolene) nickel and its follow-up products. **B** Structure of the molybdopterin cofactor in Pelobacter acetylenicus and the enzymatic transformation of acetylene into acetaldehyde in a potentially more modern body of water that, however, still contains acetylene.

Conclusion

This work showed the feasibility of forming bis(dithiolene) nickel under simulated early Earth atmosphere imitating hydrothermal volcanic conditions in the presence of acetylene. Even though the main nickel-organo compound $(C_2H_2S_2)_2Ni$ is nearly water-insoluble, its spontaneous self-assembly from acetylene allows its charged existence in water. We characterized the structure of the detected nickel bis(dithiolene). We showed an intriguing similarity between the transformation of acetylene to acetaldehyde by the tungstopterin co-enzymes and the formation of acetaldehyde *via* the degradation of the self-assembled nickel bis(dithiolene). The structural resemblance between bis(dithiolene) and extant co-enzymes supports the hypothesis that metal bis(dithiolenes) may have been among the first protoenzymes. Altogether, our work explores an essential intersection between nickel bioinorganic chemistry and pterin biochemistry, elucidating likely reactions at the earliest moments prior to the existence of enzymatic catalysis.

Methods

Bottle setup

A 125 ml glass serum bottle was charged with 1.0 mmol $NiSO_4 \cdot 6\ H_2O$ (99%, Aldrich) and sealed with a silicon stopper. The bottle underwent three cycles of evacuation and argon filling, ultimately reaching a deaerated state. Subsequently, the bottle was filled with argon-saturated water (calculated for the end volume of 5 ml), with 1.0 mL argon-saturated 1 M Na_2S (solid Na_2S: 99.99%, Aldrich) solution, with 1.0 mL 1 M NaOH solution and finally with 60 ml CO and 60 ml acetylene (acetone-free), using gastight syringes for the injections. Reactions were carried out at 105 °C. Following a reaction time of up to 3 days, the reaction mixture was cooled down.

FT-ICR-MS analysis

Samples were taken from the serum bottle with a syringe and centrifuged for 5 min at 15000 rpm. 100 µl of supernatant were diluted in 900 µl methanol and centrifuged to remove the precipitated salt. 70 µl of the centrifuged sample were diluted in 930 µl methanol to obtain the final sample dilution. Samples were measured in triplicates. All measurements were done in negative ionization mode.

Analysis was performed on a high-field Fourier Transform Ion Cyclotron Resonance mass spectrometer from Bruker Daltonics—Solarix. The magnet is a 12 T magnet from Magnex. The mass spectra were acquired with a 4 mega word (MW) time domain. The system was calibrated with L-arginine clusters in negative mode (5 mg L^{-1} L-arginine solved in methanol). For each sample, scans were accumulated in the mass range of 122–1000 amu. Ions were accumulated for 300 ms. The pressure in the hexapole was 3×10^{-6} mbar, and the pressure in the ICR vacuum chamber was 6×10^{-6} mbar. An Apollo ii (Bruker Daltonics) ESI source was used. The supernatant was injected via a microliter pump system (flow rate: 120 µl h^{-1}).

Formula assignment was achieved through a network approach[39].

LC-IM-Q-ToFMS analysis

LC-IM-MS/MS was carried out using a 6560 Ion Mobility LC/Q-TOF system (Agilent Technologies, Santa Clara, CA) coupled with a 1290 infinity II UHPLC (Agilent Technologies, Santa Clara, CA). Before the analysis, the MS was tuned within the parameters recommended by Agilent. The sample was injected onto a Waters ACQUITY UPLC BEH C8 (150 mm × 11 mm, 1.7 µm) column, with a starting gradient of 99% ACN (LC-MS/MS grade, Supelco LiChroSolv hypergrade for LC-MS) lowered linearly to 50% over 1 min with Milli-Q grade water and a total run time of 9 min at a flow rate of 0.2 mL/min. During the entire analysis, a reference mass mixture containing purine and hexakis(1H,1H,3H-tetrafluoropentoxy)phosphazene (Agilent Technologies, Santa Clara, CA) was introduced at a flow rate of 0.5 µL/min. The MS method used negative polarity with all ion fixed 2 ramped mode selected following drift time 0–59 with 10–40 CE in the second phase and a mass range from 50–1700. The gas temp was set at 250 °C with a flow of 12 L/min. The nebulizer was set at 40 psi, the sheath gas at 320 °C with a flow of 11 L/min, and vcap set at 5500 V. The IM measurements were conducted

in N_2 gas at ~4 Torr and 25 °C with a trap fill time of 2000 µs and release of 300 µs.

The raw file was calibrated to the reference mixture using an IM-MS reprocessor (Agilent Technologies, Santa Clara, CA), and the CCS was calibrated using a calibration mixture (Agilent Technologies, Santa Clara, CA) introduced to the IM-MS prior with a single field setting in Masshunter IM-MS browser (Agilent Technologies, Santa Clara, CA) result was applied to the sample measurement. Feature finding was carried out using an automatic and unbiased option in the mass profiler, and the CCS value resulted accordingly.

NMR analysis

D_2O (for analysis, Merck KGaA) was prepared with added sodium trimethylsilylpropanoate (2 mM) (98 atom %D, Aldrich) as the internal standard. This solution was used to reference and quantify signals in 1D-1H experiments. The pH of the sodium phosphate buffer was adjusted to 11 with sodium hydroxide. This solution was used to keep the dissolved complex at pH 11. The buffer was deoxygenated by nitrogen purging.

Detection of degradation products

1D ^{1}H spectra were acquired in triplicates for the dissolved complex in deoxygenated buffered water (100 mM sodium phosphate at pH11) after 0, 15, and 30 h of incubation at 100 °C. The sample at room temperature was prepared identically and measured after 30 h. 150 µl dissolved complex were spiked with 40 µl phosphate buffer and 10 µl D2O containing 2 mM TSP. The pulse program consisted of a simple 90° pulse followed by acquisition. 8 scans were acquired for each sample with a relaxation delay of 26 s and an acquisition time of 4 s. On-resonance pre-saturation was used during the relaxation delay to suppress the water signal. The optimized 90° pulse had a duration of 10.35 µs. Relative quantification was done by comparing the sum of the integrals after baseline correction of the hydrate single hydrogen signal and the methyl hydrogens signal to the TSP internal reference integral. The average for every time point was calculated. The acquired FID was apodized with an exponential function (LB = 0.3), and Fourier transformed.

Isolation of nickel bis(dithiolene)

We isolated the described complex from the aqueous solution *via* liquid-liquid extraction with methyl tert-butyl ether (MTBE). 9 mL of the reaction mixture was extracted with 3 × 9 mL of MTBE in a 50 ml falcon tube. The MTBE phase became strongly violet after the vortexing of the two-phase system. The MTBE phase was separated from the aqueous phase by carefully pipetting the MTBE off. The 3 × 9 ml of MTBE were combined and dried with an N_2 flow. After reducing the volume to about 1 ml, the residual sample was transferred to a 1.5 ml glass vial that was weighed beforehand. The residual sample was then dried to completeness and weighed to determine the amount of solid in the glass vial. A dark blue solid remained in the glass vial. This procedure was repeated three times for the two examined gas ratios.

Data availability

The authors declare that [the/all other] data supporting the findings of this study are available within the paper [and its supplementary information files]. Further data that support the findings of this study are available from the corresponding author upon reasonable request. All NMR spectra can be found in Supplementary Data 1. Data for Fig. 4 can be found in Supplementary Data 2.

Received: 21 October 2023; Accepted: 1 February 2024;
Published online: 15 February 2024

References

1. Steinkopf, W. & Kirchhoff, G. Studien in der thiophenreihe. I. die darstellung von thiophen aus acetylen. *Justus Liebigs Ann. der Chem.* **403**, 1–11 (2006).
2. Schrauzer, G. N. & Mayweg, V. Reaction of diphenylacetylene with nickel sulfides. *J. Am. Chem. Soc.* **84**, 3221–3221 (2002).
3. Schrauzer, G. N. & Mayweg, V. P. Coordination compounds with delocalized ground states, bisdithioglyoxalnickel and related complexes1a,b. *J. Am. Chem. Soc.* **87**, 3585–3592 (2002).
4. Chan, M. K., Mukund, S., Kletzin, A., Adams, M. W. & Rees, D. C. Structure of a hyperthermophilic tungstopterin enzyme, aldehyde ferredoxin oxidoreductase. *Science* **267**, 1463–1469 (1995).
5. Fogeron, T. et al. A bioinspired nickel(bis-dithiolene) complex as a homogeneous catalyst for carbon dioxide electroreduction. *ACS Catal.* **8**, 2030–2038 (2018).
6. Begum, A., Moula, G. & Sarkar, S. A nickel(II)-sulfur-based radical-ligand complex as a functional model of hydrogenase. *Chemistry* **16**, 12324–12327 (2010).
7. Cable, M. L., Vu, T. H., Maynard-Casely, H. E., Choukroun, M. & Hodyss, R. The acetylene-ammonia co-crystal on titan. *ACS Earth Space Chem.* **2**, 366–375 (2018).
8. Melin, H., Fletcher, L. N., Irwin, P. G. J. & Edgington, S. G. Jupiter in the ultraviolet: acetylene and ethane abundances in the stratosphere of Jupiter from Cassini observations between 0.15 and 0.19 µm. *Astron. J.* **159**, 291 (2020).
9. Oremland, R. S. & Voytek, M. A. Acetylene as fast food: implications for development of life on anoxic primordial Earth and in the outer solar system. *Astrobiology* **8**, 45–58 (2008).
10. Rimmer, P. B. & Shorttle, O. Origin of life's building blocks in carbon and nitrogen-rich surface hydrothermal vents. *Life (Basel)* **9**, 12 (2019).
11. Menor-Salvan, C., Ruiz-Bermejo, M., Osuna-Esteban, S., Munoz-Caro, G. & Veintemillas-Verdaguer, S. Synthesis of polycyclic aromatic hydrocarbons and acetylene polymers in ice: a prebiotic scenario. *Chem. Biodivers.* **5**, 2729–2739 (2008).
12. Abbas O. & Schulze-Makuch D. Acetylene-based pathways for prebiotic evolution on titan. *Exo-Astrobiology* **518**, 345–348 (2002).
13. Scheidler, C., Sobotta, J., Eisenreich, W., Wachtershauser, G. & Huber, C. Unsaturated C3,5,7,9-Monocarboxylic acids by aqueous, one-pot carbon fixation: possible relevance for the origin of life. *Sci. Rep.* **6**, 27595 (2016).
14. Diederich, P. et al. Formation, stabilization and fate of acetaldehyde and higher aldehydes in an autonomously changing prebiotic system emerging from acetylene. *Commun. Chem.* **6**, 38 (2023).
15. Ragsdale, S. W. Nickel-based enzyme systems. *J. Biol. Chem.* **284**, 18571–18575 (2009).
16. Miller, A. F. Redox tuning over almost 1 V in a structurally conserved active site: lessons from Fe-containing superoxide dismutase. *Acc. Chem. Res* **41**, 501–510 (2008).
17. Holliger, C., Pierik, A. J., Reijerse, E. J. & Hagen, W. R. A spectroelectrochemical study of factor F430 nickel(II/I) from methanogenic bacteria in aqueous solution. *J. Am. Chem. Soc.* **115**, 5651–5656 (2002).
18. Inoue, M. et al. Structural and phylogenetic diversity of anaerobic carbon-monoxide dehydrogenases. *Front Microbiol.* **9**, 3353 (2018).
19. Aragao, D., Mitchell, E. P., Frazao, C. F., Carrondo, M. A. & Lindley, P. F. Structural and functional relationships in the hybrid cluster protein family: structure of the anaerobically purified hybrid cluster protein from Desulfovibrio vulgaris at 1.35 A resolution. *Acta Crystallogr D. Biol. Crystallogr* **64**, 665–674 (2008).
20. Fox, J. D., Kerby, R. L., Roberts, G. P. & Ludden, P. W. Characterization of the CO-induced, CO-tolerant hydrogenase from Rhodospirillum rubrum and the gene encoding the large subunit of the enzyme. *J. Bacteriol.* **178**, 1515–1524 (1996).
21. Schoelmerich, M. C. & Muller, V. Energy conservation by a hydrogenase-dependent chemiosmotic mechanism in an ancient metabolic pathway. *Proc. Natl Acad. Sci. USA* **116**, 6329–6334 (2019).
22. Kitadai, N. et al. Thioester synthesis through geoelectrochemical CO(2) fixation on Ni sulfides. *Commun. Chem.* **4**, 37 (2021).

23. Kitadai, N. et al. Metals likely promoted protometabolism in early ocean alkaline hydrothermal systems. *Sci. Adv.* **5**, eaav7848 (2019).
24. Muto, K., Yamaguchi, J., Musaev, D. G. & Itami, K. Decarbonylative organoboron cross-coupling of esters by nickel catalysis. *Nat. Commun.* **6**, 7508 (2015).
25. Hartwig, J. F. Carbon-heteroatom bond formation catalysed by organometallic complexes. *Nature* **455**, 314–322 (2008).
26. Kamble, P. A., Vinod, C. P., Rathod, V. K. & Kantam, M. L. Hydrogenation of levulinic acid to gamma-valerolactone over nickel supported organoclay catalyst. *Catal. Today* **408**, 36–49 (2023).
27. Miao, Q. et al. Syntheses and characterization of several nickel bis(dithiolene) complexes with strong and broad Near-IR absorption. *Inorg. Chim. Acta.* **376**, 619–627 (2011).
28. Schrauzer, G. N., Zhang, C. & Chadha, R. The cis-bis(cis-2-mercaptostilbene-1-sulfinato)nickel(II) dianion: a product of the irreversible oxidation of the bis(cis-stilbene-1,2-dithiolato)nickel(II) dianion. *Inorg. Chem.* **29**, 4104–4107 (2002).
29. Rauscher, S. A. & Moran, J. Hydrogen drives part of the reverse krebs cycle under metal or meteorite catalysis. *Angew. Chem. Int Ed. Engl.* **61**, e202212932 (2022).
30. Geisberger, T. et al. Formation of vesicular structures from fatty acids formed under simulated volcanic hydrothermal conditions. *Sci. Rep.* **13**, 15227 (2023).
31. Zhou, Y. et al. In(III) metal-organic framework incorporated with enzyme-mimicking Nickel Bis(dithiolene) ligand for highly selective CO(2) electroreduction. *J. Am. Chem. Soc.* **143**, 14071–14076 (2021).
32. Reppe, W. Carbonylierung I. Über die umsetzung von acetylen mit kohlenoxyd und verbindungen mit reaktionsfähigen wasserstoffatomen synthesen α,β-ungesättigter carbonsäuren und ihrer derivate. *Justus Liebigs Ann. der Chem.* **582**, 1–37 (2006).
33. Sobotta, J. et al. A possible primordial acetyleno/carboxydotrophic core metabolism. *Life (Basel)* **10**, 35 (2020).
34. Schrauzer, G. N. Coordination compounds with delocalized ground states, transition metal derivatives of dithiodiketones and ethylene-1,2-dithiolates (metal dithienes). *Acc. Chem. Res.* **2**, 72–80 (2002).
35. Geisberger, T., Sobotta, J., Eisenreich, W. & Huber, C. Formation of thiophene under simulated volcanic hydrothermal conditions on earth-implications for early life on extraterrestrial planets. *Life (Basel)* **11**, 149 (2021).
36. Zhou, Y. et al. A metal-organic framework based on a Nickel Bis(dithiolene) connector: synthesis, crystal structure and application as an electrochemical glucose sensor. *J. Am. Chem. Soc.* **142**, 20313–20317 (2020).
37. Morgan, J. W. & Anders, E. Chemical composition of Earth, Venus, and Mercury. *Proc. Natl Acad. Sci. USA* **77**, 6973–6977 (1980).
38. Alfano, M. & Cavazza, C. Structure, function, and biosynthesis of nickel-dependent enzymes. *Protein Sci.* **29**, 1071–1089 (2020).
39. Tziotis, D., Hertkorn, N. & Schmitt-Kopplin, P. Kendrick-analogous network visualisation of ion cyclotron resonance fourier transform mass spectra: improved options for the assignment of elemental compositions and the classification of organic molecular complexity. *Eur. J. Mass Spectrom. (Chichester)* **17**, 415–421 (2011).

Acknowledgements

This research was funded by the Deutsche Forschungsgemeinschaft (DFG, German Research Foundation) – Project-ID 364653263 – TRR 235 (CRC 235). CS and CH thank the Hans-Fischer-Gesellschaft (D-Munich) for financial support.

Author contributions

PD conceived and designed the analysis, collected the data, performed experiments, performed data analysis, and wrote the manuscript. CS, LB, LS, TG, and CH contributed analysis tools. TG and CS performed experiments. LB, LS, WE, CH, and PSK edited the manuscript. PSK, CH, and WE provided funding and supervised the project.

Funding

Open Access funding enabled and organized by Projekt DEAL.

Competing interests

The authors declare no competing interests.

Additional information

Supplementary information The online version contains supplementary material available at https://doi.org/10.1038/s42004-024-01119-0.

Correspondence and requests for materials should be addressed to Philippe Schmitt-Kopplin.

Peer review information *Communications Chemistry* thanks all the anonymous reviewer for their contribution to the peer review of this work. A peer review file is available.

7.3.2 Appendix Supplementary 3

Supplement

Nickel-organo compounds as potential enzyme precursors under simulated Early Earth conditions

Philippe Diederich [a], Christian Seitz [b], Lance Buckett [a], Liesa Salzer [a], Thomas Geisberger [b], Wolfgang Eisenreich [b], Claudia Huber [b], Philippe Schmitt-Kopplin [a, c, d*]

[a] Helmholtz Munich, Research Unit Analytical BioGeoChemistry, Neuherberg, Germany.

[b] Technical University of Munich, TUM School of Natural Sciences, Department of Bioscience, Bavarian NMR Center (BNMRZ), Structural Membrane Biochemistry, Lichtenbergstr. 4, 85748 Garching, Germany

[c] Comprehensive Foodomics Platform, Chair of Analytical Food Chemistry, TUM School of Life Sciences, Technical University of Munich, Maximus-von-Imhof-Forum 2, 85354 Freising, Germany

[d] Max Planck Institute for Extraterrestrial Physics, Center for Astrochemical Studies, Gießebachstraße 1, 85748 Garching bei München, Germany.

[*]Corresponding author: Research Unit Analytical BioGeoChemistry, Helmholtz Zentrum München–German Research Center for Environmental Health, Neuherberg, Germany.

Email: schmitt-kopplin@helmholtz-muenchen.de

Color correlates with the bis(dithiolene)nickel signal

The color of the analyzed samples correlates with the intensity of the mass of nickel bis(dithiolene). The bar plot presents the signal intensity at different time points. The corresponding sample is located directly beneath the respective bar and displays the reported color.

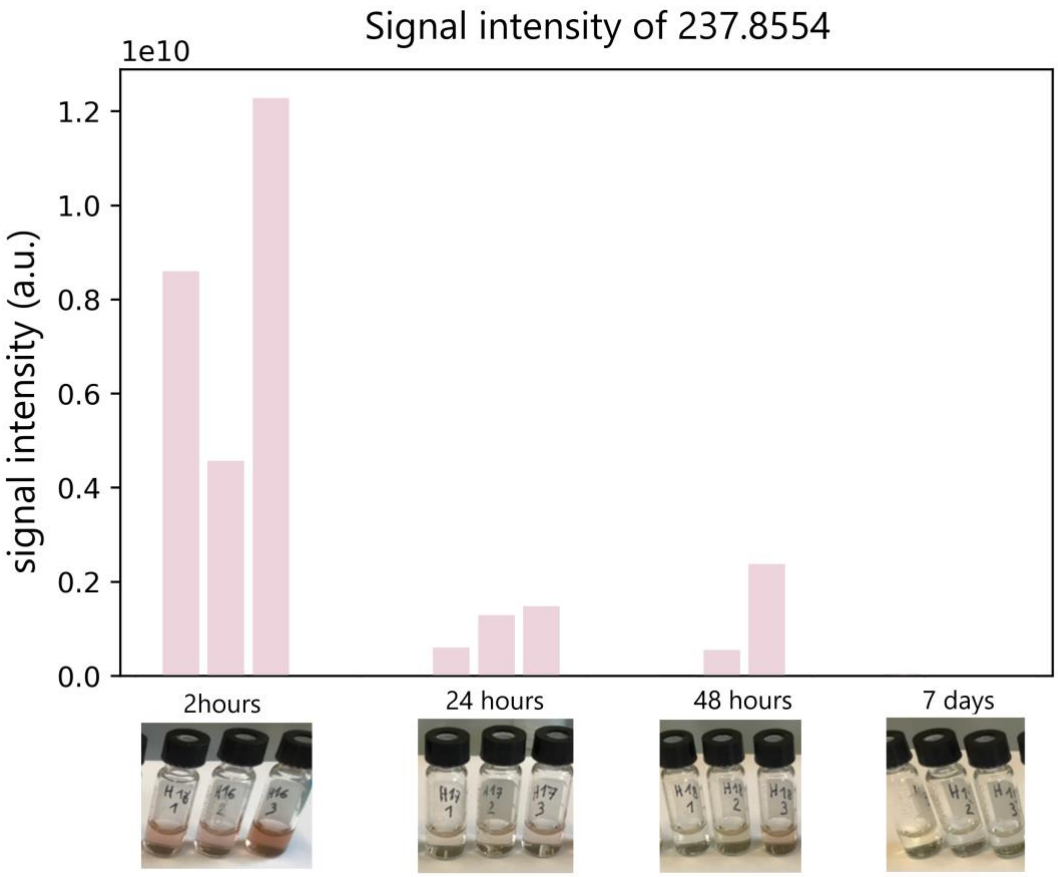

Supplementary figure 1: Bar plot showing the correlation between the detected intensity for the mass 237.8554 and the pinkish color of the prepared samples at different timepoints.

Reaction scheme and discussed compounds

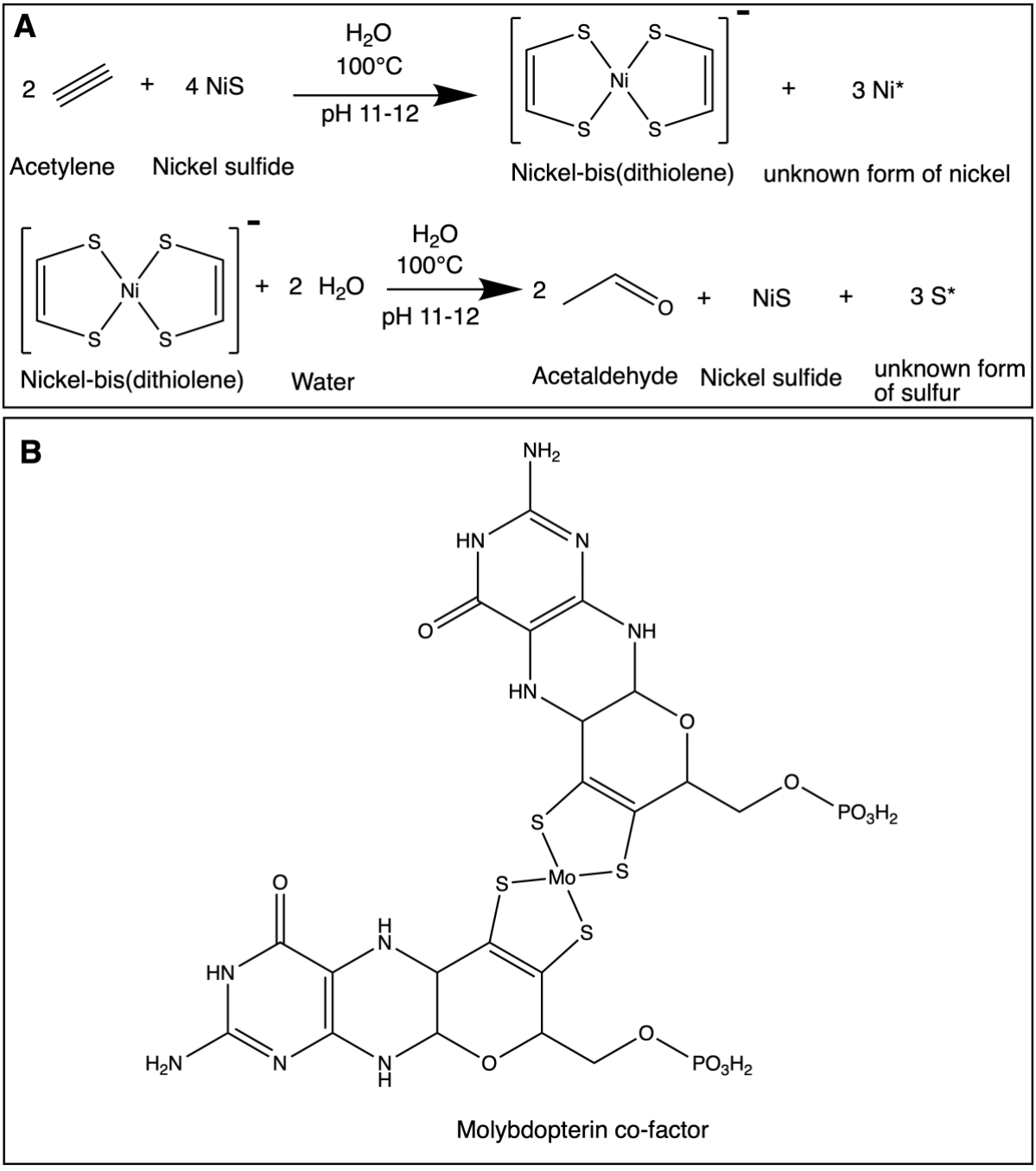

*Supplementary figure 2: Reaction scheme overview. Panel A shows the hypothesized formation pathway of nickel bis(dithiolene) and acetaldehyde. Panel B shows the structure of a molybdopterin co-factor found in extant enzymes. *Unknown form.*

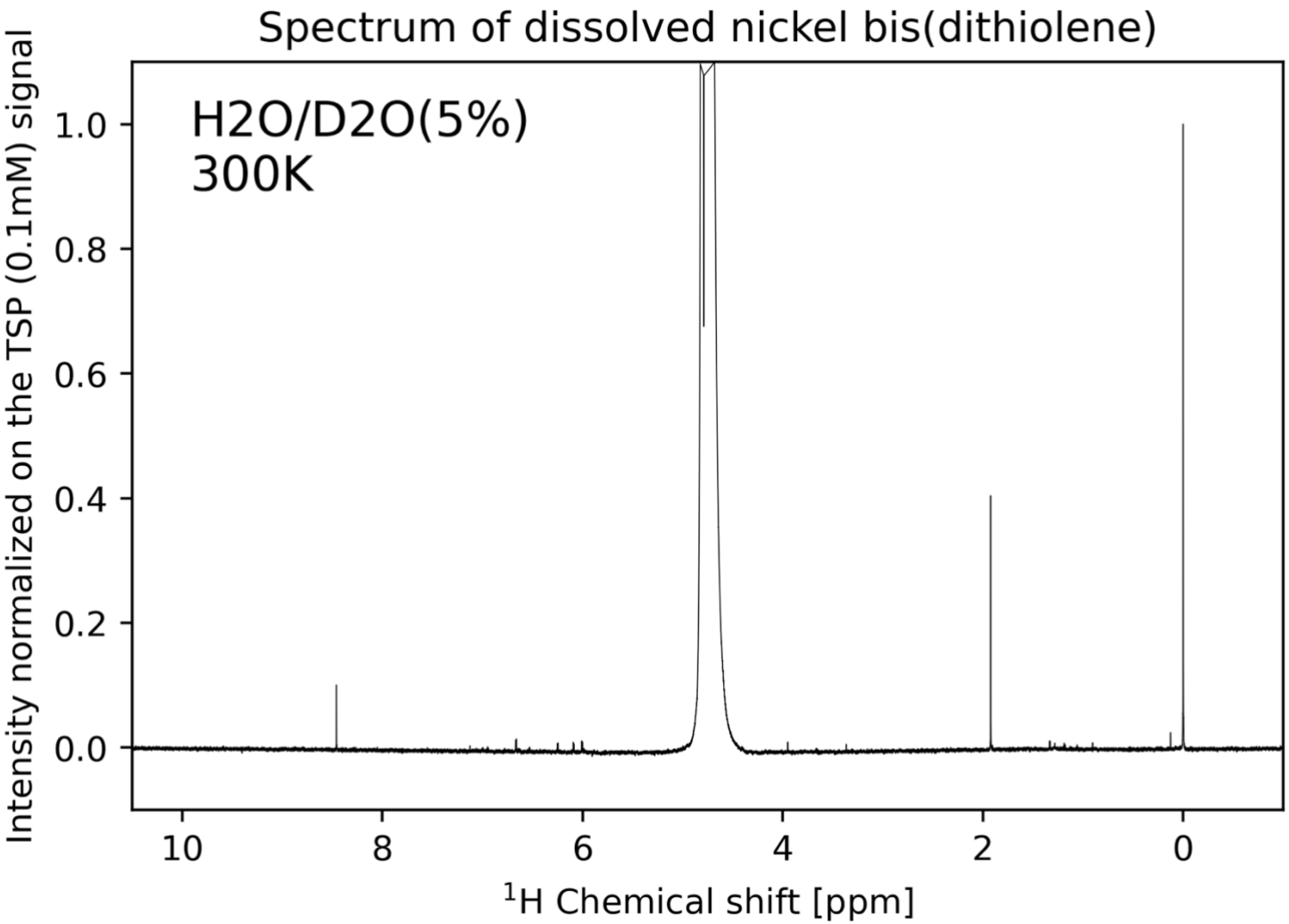
Spectrum of dissolved nickel bis(dithiolene)
H2O/D2O(5%)
300K
Intensity normalized on the TSP (0.1mM) signal
1.0
0.8
0.6
0.4
0.2
0.0
10
8
6
4
2
0
^{1}H Chemical shift [ppm]

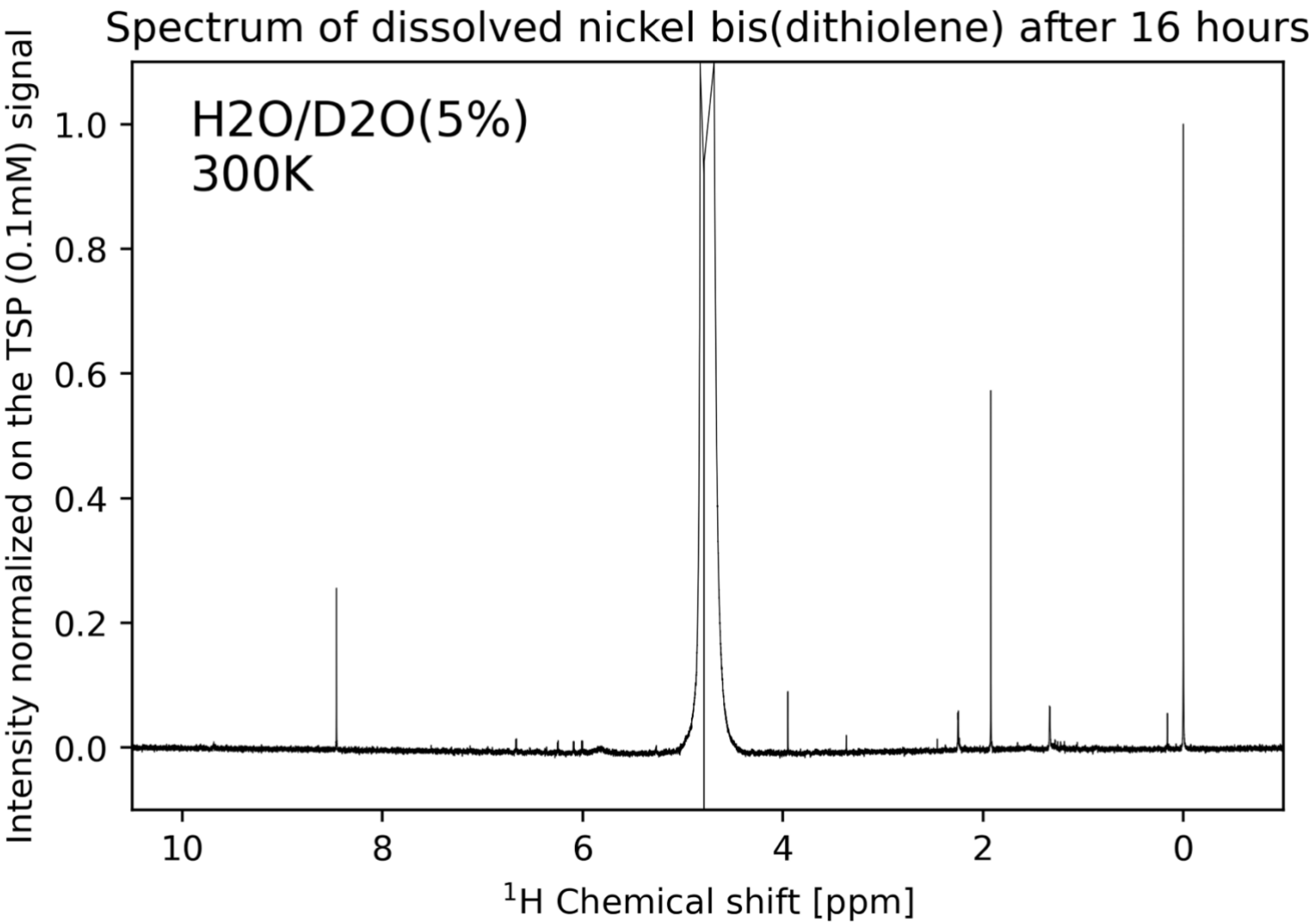
Spectrum of dissolved nickel bis(dithiolene) after 16 hours
H2O/D2O(5%)
300K
Intensity normalized on the TSP (0.1mM) signal
1.0
0.8
0.6
0.4
0.2
0.0
10
8
6
4
2
0
^{1}H Chemical shift [ppm]

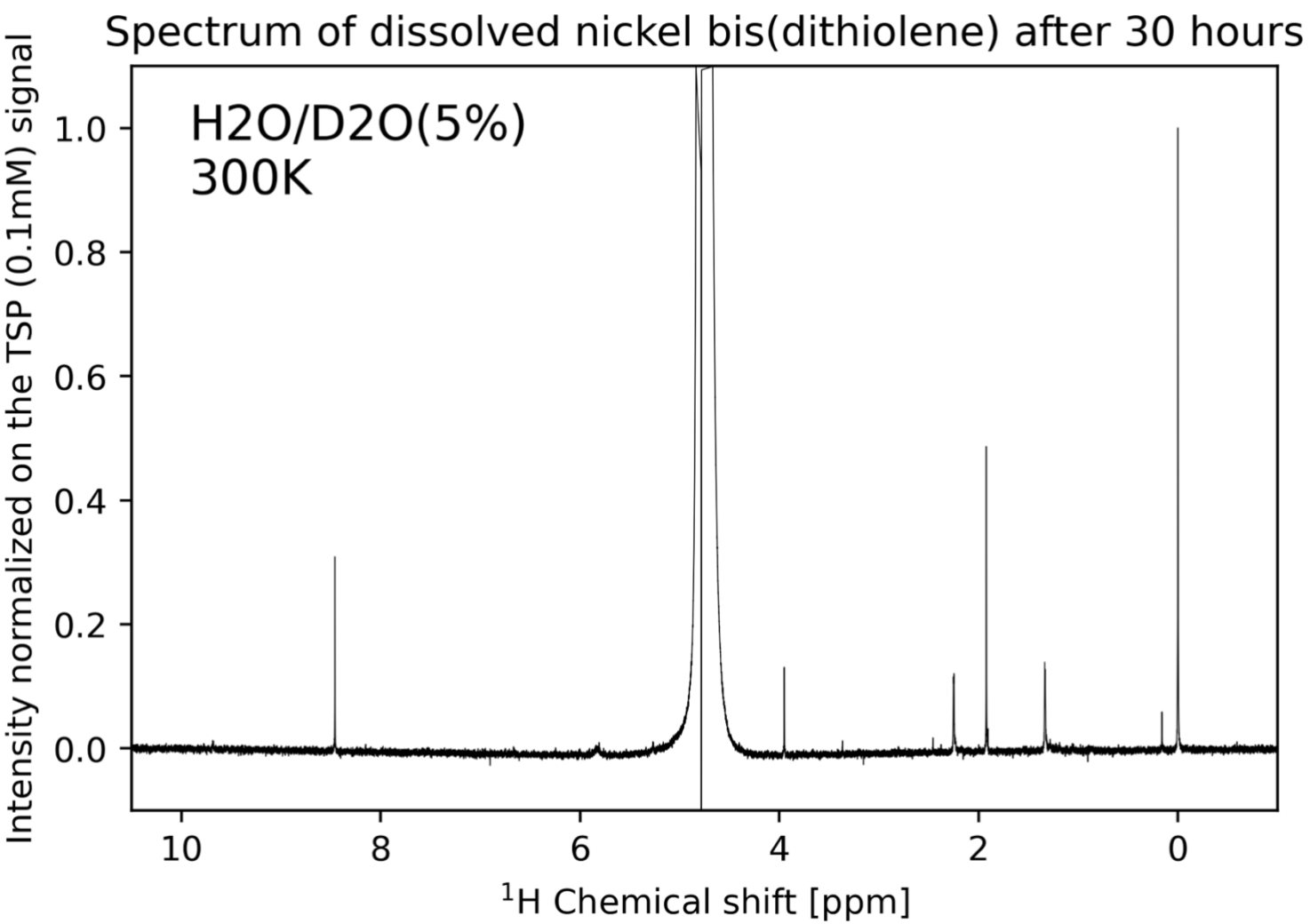
Spectrum of dissolved nickel bis(dithiolene) after 30 hours
H2O/D2O(5%)
300K
Intensity normalized on the TSP (0.1mM) signal
1.0
0.8
0.6
0.4
0.2
0.0
10
8
6
4
2
0
^{1}H Chemical shift [ppm]

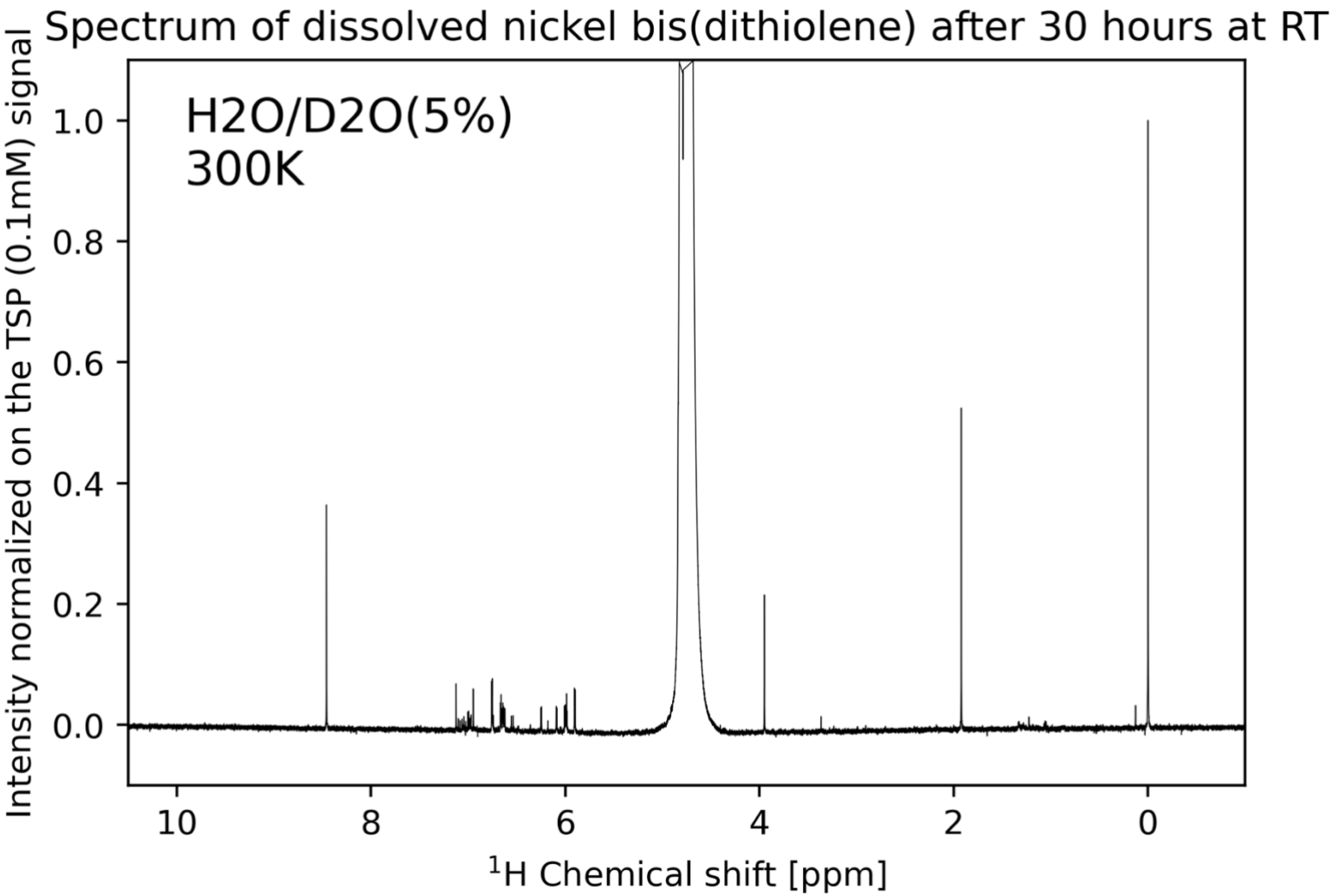
Spectrum of dissolved nickel bis(dithiolene) after 30 hours at RT
H2O/D2O(5%)
300K
Intensity normalized on the TSP (0.1mM) signal
1.0
0.8
0.6
0.4
0.2
0.0
10
8
6
4
2
0
^{1}H Chemical shift [ppm]

8. Bibliography

1. Orgel LE. The origin of life--a review of facts and speculations. Trends Biochem Sci. 1998;23(12):491-5.
2. Fry I. The origins of research into the origins of life. Endeavour. 2006;30(1):24-8.
3. Sutherland JD. Opinion: Studies on the origin of life — the end of the beginning. Nature Reviews Chemistry. 2017;1(2):0012.
4. Malaterre C, Jeancolas C, Nghe P. The Origin of Life: What Is the Question? Astrobiology. 2022;22(7):851-62.
5. Hanczyc MM. Engineering Life: A Review of Synthetic Biology. Artif Life. 2020;26(2):260-73.
6. Endy D. Foundations for engineering biology. Nature. 2005;438(7067):449-53.
7. Pereto J, Bada JL, Lazcano A. Charles Darwin and the origin of life. Orig Life Evol Biosph. 2009;39(5):395-406.
8. Oldroyd DR. Charles Darwin's theory of evolution: A review of our present understanding. Biology & Philosophy. 1986;1(2):133-68.
9. Ruiz-Mirazo K, Briones C, de la Escosura A. Prebiotic systems chemistry: new perspectives for the origins of life. Chem Rev. 2014;114(1):285-366.
10. Kitadai N, Maruyama S. Origins of building blocks of life: A review. Geoscience Frontiers. 2018;9(4):1117-53.
11. Rimmer PB, Shorttle O. Origin of Life's Building Blocks in Carbon- and Nitrogen-Rich Surface Hydrothermal Vents. Life (Basel). 2019;9(1):12.
12. Lunine JI. Physical conditions on the early Earth. Philos Trans R Soc Lond B Biol Sci. 2006;361(1474):1721-31.
13. Muller UF, Elsila J, Trail D, DasGupta S, Giese CC, Walton CR, et al. Frontiers in Prebiotic Chemistry and Early Earth Environments. Orig Life Evol Biosph. 2022;52(1-3):165-81.
14. Mutschler H, Wochner A, Holliger P. Freeze-thaw cycles as drivers of complex ribozyme assembly. Nat Chem. 2015;7(6):502-8.
15. Bada JL. Volcanic Island lightning prebiotic chemistry and the origin of life in the early Hadean eon. Nat Commun. 2023;14(1):2011.
16. Damer B, Deamer D. The Hot Spring Hypothesis for an Origin of Life. Astrobiology. 2020;20(4):429-52.
17. Peters JW, Williams LD. The origin of life: look up and look down. Astrobiology. 2012;12(11):1087-92.
18. Lahav N, Nir S, Elitzur AC. The emergence of life on Earth. Prog Biophys Mol Biol. 2001;75(1-2):75-120.
19. de Duve C. Blueprint for a cell: the nature and origin of life. Burlington, N.C: N. Patterson; 1991.
20. Eschenmoser A. The search for the chemistry of life's origin. Tetrahedron. 2007;63(52):12821-44.
21. Jungclaus GA, Yuen GU, Moore CB, Lawless JG. Evidence for the Presence of Low Molecular Weight Alcohols and Carbonyl Compounds in the Murchison Meteorite†. Meteoritics. 2012;11(3):231-7.
22. Butlerow A. Bildung einer zuckerartigen Substanz durch Synthese. Justus Liebigs Annalen der Chemie. 2006;120(3):295-8.

23. Breslow R. On the mechanism of the formose reaction. Tetrahedron Letters. 1959;1(21):22-6.
24. Larralde R, Robertson MP, Miller SL. Rates of decomposition of ribose and other sugars: implications for chemical evolution. Proc Natl Acad Sci U S A. 1995;92(18):8158-60.
25. Benner SA, Kim HJ, Carrigan MA. Asphalt, water, and the prebiotic synthesis of ribose, ribonucleosides, and RNA. Acc Chem Res. 2012;45(12):2025-34.
26. Sharma C, Awasthi SK. Versatility of peptide nucleic acids (PNA s): Role in chemical biology, drug discovery, and origins of life. Chemical biology & drug design. 2017;89(1):16-37.
27. Kruse FM, Teichert JS, Trapp O. Prebiotic Nucleoside Synthesis: The Selectivity of Simplicity. Chemistry. 2020;26(65):14776-90.
28. Teichert JS, Kruse FM, Trapp O. Direct Prebiotic Pathway to DNA Nucleosides. Angew Chem Int Ed Engl. 2019;58(29):9944-7.
29. Oró J. Synthesis of adenine from ammonium cyanide. Biochemical and Biophysical Research Communications. 1960;2(6):407-12.
30. Oro J, editor Non-enzymatic formation of purines and pyrimidines. Federation Proceedings; 1963: FEDERATION AMER SOC EXP BIOL 9650 ROCKVILLE PIKE, BETHESDA, MD 20814-3998.
31. Oro J, Kimball AP. Synthesis of purines under possible primitive earth conditions. I. Adenine from hydrogen cyanide. Arch Biochem Biophys. 1961;94(2):217-27.
32. Orgel LE. Prebiotic chemistry and the origin of the RNA world. Crit Rev Biochem Mol Biol. 2004;39(2):99-123.
33. Shapiro R. Prebiotic cytosine synthesis: a critical analysis and implications for the origin of life. Proc Natl Acad Sci U S A. 1999;96(8):4396-401.
34. Ferris JP, Sanchez RA, Orgel LE. Studies in prebiotic synthesis. 3. Synthesis of pyrimidines from cyanoacetylene and cyanate. J Mol Biol. 1968;33(3):693-704.
35. Ferris JP, Zamek OS, Altbuch AM, Freiman H. Chemical evolution. 18. Synthesis of pyrimidines from guanidine and cyanoacetaldehyde. J Mol Evol. 1974;3(4):301-9.
36. Robertson MP, Miller SL. An efficient prebiotic synthesis of cytosine and uracil. Nature. 1995;375(6534):772-4.
37. Saladino R, Botta G, Pino S, Costanzo G, Di Mauro E. Genetics first or metabolism first? The formamide clue. Chem Soc Rev. 2012;41(16):5526-65.
38. Saladino R, Crestini C, Pino S, Costanzo G, Di Mauro E. Formamide and the origin of life. Phys Life Rev. 2012;9(1):84-104.
39. Sanchez R, Ferris J, Orgel LE. Conditions for purine synthesis: did prebiotic synthesis occur at low temperatures? Science. 1966;153(3731):72-3.
40. Levy M, Miller SL. The stability of the RNA bases: implications for the origin of life. Proc Natl Acad Sci U S A. 1998;95(14):7933-8.
41. Shapiro R. The prebiotic role of adenine: a critical analysis. Orig Life Evol Biosph. 1995;25(1-3):83-98.
42. Burton AS, Stern JC, Elsila JE, Glavin DP, Dworkin JP. Understanding prebiotic chemistry through the analysis of extraterrestrial amino acids and nucleobases in meteorites. Chem Soc Rev. 2012;41(16):5459-72.
43. Callahan MP, Smith KE, Cleaves HJ, 2nd, Ruzicka J, Stern JC, Glavin DP, et al. Carbonaceous meteorites contain a wide range of extraterrestrial nucleobases. Proc Natl Acad Sci U S A. 2011;108(34):13995-8.

44. Miller SL. A production of amino acids under possible primitive earth conditions. Science. 1953;117(3046):528-9.
45. Schulte M, Shock E. Thermodynamics of Strecker synthesis in hydrothermal systems. Orig Life Evol Biosph. 1995;25(1-3):161-73.
46. Masamba W. Petasis vs. Strecker Amino Acid Synthesis: Convergence, Divergence and Opportunities in Organic Synthesis. Molecules. 2021;26(6).
47. Van Trump JE, Miller SL. Prebiotic synthesis of methionine. Science. 1972;178(4063):859-60.
48. Shen C, Yang L, Miller SL, Oro J. Prebiotic synthesis of histidine. J Mol Evol. 1990;31(3):167-74.
49. Sanchez RA, Ferris JP, Orgel LE. Cyanoacetylene in prebiotic synthesis. Science. 1966;154(3750):784-5.
50. Friedmann N, Miller SL. Phenylalanine and tyrosine synthesis under primitive earth conditions. Science. 1969;166(3906):766-7.
51. Friedmann N, Miller SL. Synthesis of valine and isoleucine in primitive earth conditions. Nature. 1969;221(5186):1152-3.
52. Strecker A. Ueber die künstliche Bildung der Milchsäure und einen neuen, dem Glycocoll homologen Körper. Justus Liebigs Annalen der Chemie. 2006;75(1):27-45.
53. Frenkel-Pinter M, Sargon AB, Glass JB, Hud NV, Williams LD. Transition metals enhance prebiotic depsipeptide oligomerization reactions involving histidine. RSC Adv. 2021;11(6):3534-8.
54. Joyce G. Hydrothermal vents too hot? Nature. 1988;334(6183):564-.
55. Saladino R, Sponer JE, Sponer J, Di Mauro E. Rewarming the Primordial Soup: Revisitations and Rediscoveries in Prebiotic Chemistry. Chembiochem. 2018;19(1):22-5.
56. Ingolfsson HI, Melo MN, van Eerden FJ, Arnarez C, Lopez CA, Wassenaar TA, et al. Lipid organization of the plasma membrane. J Am Chem Soc. 2014;136(41):14554-9.
57. Paula S, Volkov AG, Van Hoek AN, Haines TH, Deamer DW. Permeation of protons, potassium ions, and small polar molecules through phospholipid bilayers as a function of membrane thickness. Biophys J. 1996;70(1):339-48.
58. Apel CL, Deamer DW, Mautner MN. Self-assembled vesicles of monocarboxylic acids and alcohols: conditions for stability and for the encapsulation of biopolymers. Biochim Biophys Acta. 2002;1559(1):1-9.
59. Deamer DW. Boundary structures are formed by organic components of the Murchison carbonaceous chondrite. Nature. 1985;317(6040):792-4.
60. Fischer F, Tropsch H. Über die direkte Synthese von Erdöl-Kohlenwasserstoffen bei gewöhnlichem Druck. (Erste Mitteilung). Berichte der deutschen chemischen Gesellschaft (A and B Series). 2006;59(4):830-1.
61. McCollom TM. Miller-Urey and Beyond: What Have We Learned About Prebiotic Organic Synthesis Reactions in the Past 60 Years? Annual Review of Earth and Planetary Sciences. 2013;41(1):207-29.
62. Horita J, Berndt ME. Abiogenic methane formation and isotopic fractionation under hydrothermal conditions. Science. 1999;285(5430):1055-7.
63. Dworkin J, Deamer D, Sandford S, Allamandola L. Self-assembling amphiphilic molecules: Synthesis in simulated interstellar/precometary ices. Proc Natl Acad Sci U S A. 2001;98(3):815-9.

64. Nooner DW, Gibert JM, Gelpi E, Oró J. Closed system Fischer-Tropsch synthesis over meteoritic iron, iron ore and nickel-iron alloy. Geochimica et Cosmochimica Acta. 1976;40(8):915-24.
65. Allen WV, Ponnamperuma C. A possible prebiotic synthesis of monocarboxylic acids. Curr Mod Biol. 1967;1(1):24-8.
66. Scheidler C, Sobotta J, Eisenreich W, Wachtershauser G, Huber C. Unsaturated C3,5,7,9-Monocarboxylic Acids by Aqueous, One-Pot Carbon Fixation: Possible Relevance for the Origin of Life. Sci Rep. 2016;6(1):27595.
67. Reppe W. Carbonylierung I. Über die Umsetzung von Acetylen mit Kohlenoxyd und Verbindungen mit reaktionsfähigen Wasserstoffatomen Synthesen α,β-ungesättigter Carbonsäuren und ihrer Derivate. Justus Liebigs Annalen der Chemie. 2006;582(1):1-37.
68. Abbas O, Schulze-Makuch D. Acetylene-based pathways for prebiotic evolution on Titan. Exo-Astrobiology. 2002;518.
69. Oremland RS, Voytek MA. Acetylene as fast food: implications for development of life on anoxic primordial Earth and in the outer solar system. Astrobiology. 2008;8(1):45-58.
70. Cable ML, Vu TH, Maynard-Casely HE, Choukroun M, Hodyss R. The Acetylene-Ammonia Co-crystal on Titan. ACS Earth and Space Chemistry. 2018;2(4):366-75.
71. Pässler P, Hefner W, Buckl K, Meinass H, Meiswinkel A, Wernicke H-J, et al. Acetylene. Ullmann's Encyclopedia of Industrial Chemistry2008.
72. Kutscheroff Acetylene Hydration. Comprehensive Organic Name Reactions and Reagents2010. p. 1710-2.
73. Kutscheroff M. Ueber eine neue Methode direkter Addition von Wasser (Hydratation) an die Kohlenwasserstoffe der Acetylenreihe. Berichte der deutschen chemischen Gesellschaft. 2006;14(1):1540-2.
74. Trotus IT, Zimmermann T, Schuth F. Catalytic reactions of acetylene: a feedstock for the chemical industry revisited. Chem Rev. 2014;114(3):1761-82.
75. Zhang S, Li J, Li G, Nie Y, Qiang L, Bai B, et al. Life cycle assessment of acetylene production from calcium carbide and methane in China. Journal of Cleaner Production. 2021;322:129055.
76. Voronin VV, Ledovskaya MS, Bogachenkov AS, Rodygin KS, Ananikov VP. Acetylene in Organic Synthesis: Recent Progress and New Uses. Molecules. 2018;23(10):2442.
77. Bertleff W, Roeper M, Sava X. In Ullmann’s Encyclopedia of Industrial Chemistry. Weinheim, Germany: Wiley-VCH; 2000.
78. Bach FH. Carbon monoxide: from the origin of life to molecular medicine. Trends Mol Med. 2006;12(8):348-50.
79. Holmen A, Olsvik O, Rokstad OA. Pyrolysis of natural gas: chemistry and process concepts. Fuel Processing Technology. 1995;42(2-3):249-67.
80. Arpe H-J. Industrial Organic Chemistry. ed t, editor. Weinheim, Germany: Wiley-VCH; 2010.
81. Dändliker G. Katalytische Cyclisierung von Acetylen und substituiertem Acetylen zu aromatischen Kohlenwasserstoffen. Helvetica Chimica Acta. 2004;52(6):1482-7.
82. Busch M, Ahlberg E, Ahlberg E, Laasonen K. How to Predict the pK (a) of Any Compound in Any Solvent. ACS Omega. 2022;7(20):17369-83.

83. Nieuwland JA, Calcott WS, Downing FB, Carter AS. Acetylene Polymers and Their Derivatives. I. The Controlled Polymerization of Acetylene. Journal of the American Chemical Society. 2002;53(11):4197-202.
84. Konn C, Charlou JL, Donval JP, Holm NG, Dehairs F, Bouillon S. Hydrocarbons and oxidized organic compounds in hydrothermal fluids from Rainbow and Lost City ultramafic-hosted vents. Chemical Geology. 2009;258(3-4):299-314.
85. Proskurowski G, Lilley MD, Seewald JS, Fruh-Green GL, Olson EJ, Lupton JE, et al. Abiogenic hydrocarbon production at lost city hydrothermal field. Science. 2008;319(5863):604-7.
86. Kaiser SK, Surin I, Amoros-Perez A, Buchele S, Krumeich F, Clark AH, et al. Design of carbon supports for metal-catalyzed acetylene hydrochlorination. Nat Commun. 2021;12(1):4016.
87. Zhang L, Lin J, Liu Z, Zhang J. Non-noble metal-based catalysts for acetylene semihydrogenation: from thermocatalysis to sustainable catalysis. Science China Chemistry. 2023;66(7):1963-74.
88. Nishiwaki K-i, Kobayashi M, Takeuchi T, Matuoto K, Osakada K. Nieuwland catalysts: investigation of structure in the solid state and in solution and performance in the dimerization of acetylene. Journal of Molecular Catalysis A: Chemical. 2001;175(1-2):73-81.
89. Carothers WH, Williams I, Collins AM, Kirby JE. Acetylene polymers and their derivatives. II. A new synthetic rubber: chloroprene and its polymers. Journal of the American Chemical Society. 1931;53(11):4203-25.
90. Kaur A, Gautrot JE, Cavalli G, Watson D, Bickley A, Akutagawa K, et al. Novel Crosslinking System for Poly-Chloroprene Rubber to Enable Recyclability and Introduce Self-Healing. Polymers (Basel). 2021;13(19):3347.
91. Oestreich M, Klare HF, Brösamlen D. The Bönnemann–Wakatsuki Pyridine Synthesis. Synfacts. 2021;18(01):0062.
92. Das T, Ghule S, Vanka K. Insights Into the Origin of Life: Did It Begin from HCN and H(2)O? ACS Cent Sci. 2019;5(9):1532-40.
93. Matthews CN, Minard RD. Hydrogen cyanide polymers, comets and the origin of life. Faraday Discuss. 2006;133(0):393-401; discussion 27-52.
94. Portella G, Terrazas M, Villegas N, Gonzalez C, Orozco M. Can A Denaturant Stabilize DNA? Pyridine Reverses DNA Denaturation in Acidic pH. Angew Chem Int Ed Engl. 2015;54(36):10488-91.
95. Whitby RA, Altwicker ER. Acetylene in the atmosphere: Sources, representative ambient concentrations and ratios to other hydrocarbons. Atmospheric Environment (1967). 1978;12(6-7):1289-96.
96. Wang C, Hazen RM, Cheng Q, Stephenson MH, Zhou C, Fox P, et al. The Deep-Time Digital Earth program: data-driven discovery in geosciences. Natl Sci Rev. 2021;8(9):nwab027.
97. Zahnle KJ. Photochemistry of methane and the formation of hydrocyanic acid (HCN) in the Earth's early atmosphere. Journal of Geophysical Research: Atmospheres. 2012;91(D2):2819-34.
98. Trainer MG, Pavlov AA, Curtis DB, McKay CP, Worsnop DR, Delia AE, et al. Haze aerosols in the atmosphere of early Earth: manna from heaven. Astrobiology. 2004;4(4):409-19.
99. Orton GS, Aumann HH. The abundance of acetylene in the atmosphere of Jupiter. Icarus. 1977;32(4):431-6.
100. Melin H, Fletcher LN, Irwin PGJ, Edgington SG. Jupiter in the Ultraviolet: Acetylene and Ethane Abundances in the Stratosphere of Jupiter from Cassini

Observations between 0.15 and 0.19 μm. The Astronomical Journal. 2020;159(6):291.
101. Buriez JCdB, C. A study of the atmosphere of Saturn based on methane line profiles near 1.1 microns. Astronomy and Astrophysics. 1980;94(2):382-90.
102. Macy W. Mixing ratios of methane, ethane, and acetylene in Neptune's stratosphere. Icarus. 1980;41(1):153-8.
103. Atreya SK, Ponthieu JJ. Photolysis of methane and the ionosphere of Uranus. Planetary and Space Science. 1983;31(8):939-44.
104. Waite JH, Jr., Young DT, Cravens TE, Coates AJ, Crary FJ, Magee B, et al. The process of tholin formation in Titan's upper atmosphere. Science. 2007;316(5826):870-5.
105. Stoker CR, Boston PJ, Mancinelli RL, Segal W, Khare BN, Sagan C. Microbial metabolism of tholin. Icarus. 1990;85(1):241-56.
106. Owen T. The atmosphere of Titan. J Mol Evol. 1982;18(3):150-6.
107. Waite JH, Jr., Combi MR, Ip WH, Cravens TE, McNutt RL, Jr., Kasprzak W, et al. Cassini ion and neutral mass spectrometer: Enceladus plume composition and structure. Science. 2006;311(5766):1419-22.
108. van ’t Hoff MLR, Harsono D, Tobin JJ, Bosman AD, van Dishoeck EF, Jørgensen JK, et al. Temperature Structures of Embedded Disks: Young Disks in Taurus Are Warm. The Astrophysical Journal. 2020;901(2):166.
109. van Dishoeck EF, Grant S, Tabone B, van Gelder M, Francis L, Tychoniec L, et al. The diverse chemistry of protoplanetary disks as revealed by JWST. Faraday Discuss. 2023;245(0):52-79.
110. Robinson PK. Enzymes: principles and biotechnological applications. Essays Biochem. 2015;59:1-41.
111. Selles Vidal L, Kelly CL, Mordaka PM, Heap JT. Review of NAD(P)H-dependent oxidoreductases: Properties, engineering and application. Biochim Biophys Acta Proteins Proteom. 2018;1866(2):327-47.
112. Gibson MI, Brignole EJ, Pierce E, Can M, Ragsdale SW, Drennan CL. The Structure of an Oxalate Oxidoreductase Provides Insight into Microbial 2-Oxoacid Metabolism. Biochemistry. 2015;54(26):4112-20.
113. Trumpower BL. The protonmotive Q cycle. Energy transduction by coupling of proton translocation to electron transfer by the cytochrome bc1 complex. J Biol Chem. 1990;265(20):11409-12.
114. Ljungdahl LG. The autotrophic pathway of acetate synthesis in acetogenic bacteria. Annu Rev Microbiol. 1986;40:415-50.
115. Fuchs G. Alternative pathways of carbon dioxide fixation: insights into the early evolution of life? Annu Rev Microbiol. 2011;65:631-58.
116. Huber C, Wachtershauser G. Activated acetic acid by carbon fixation on (Fe,Ni)S under primordial conditions. Science. 1997;276(5310):245-7.
117. Shepard EM, Broderick JB. 8.17 - S-Adenosylmethionine and Iron–Sulfur Clusters in Biological Radical Reactions: The Radical SAM Superfamily. In: Liu H-W, Mander L, editors. Comprehensive Natural Products II. Oxford: Elsevier; 2010. p. 625-61.
118. Schink B. Fermentation of acetylene by an obligate anaerobe,Pelobacter acetylenicus sp. nov. Archives of Microbiology. 1985;142(3):295-301.
119. Roy R, Menon AL, Adams MWW. [11] Aldehyde Oxidoreductases from Pyrococcus furiosus. Methods in Enzymology. 331: Academic Press; 2001. p. 132-44.

120. Schmitt-Kopplin P, Gabelica Z, Gougeon RD, Fekete A, Kanawati B, Harir M, et al. High molecular diversity of extraterrestrial organic matter in Murchison meteorite revealed 40 years after its fall. Proc Natl Acad Sci U S A. 2010;107(7):2763-8.
121. Schmitt-Kopplin P, Hertkorn N, Schulten H-R, Kettrup A. Structural Changes in a Dissolved Soil Humic Acid during Photochemical Degradation Processes under O2and N2Atmosphere. Environmental Science & Technology. 1998;32(17):2531-41.
122. Jameson CJ. Understanding Nmr Chemical Shifts. Annual Review of Physical Chemistry. 1996;47(1):135-69.
123. Beckonert O, Keun HC, Ebbels TM, Bundy J, Holmes E, Lindon JC, et al. Metabolic profiling, metabolomic and metabonomic procedures for NMR spectroscopy of urine, plasma, serum and tissue extracts. Nat Protoc. 2007;2(11):2692-703.
124. Pieczonka SA, Zarnkow M, Diederich P, Hutzler M, Weber N, Jacob F, et al. Archeochemistry reveals the first steps into modern industrial brewing. Sci Rep. 2022;12(1):9251.
125. Li S, Harir M, Schmitt-Kopplin P, Gonsior M, Enrich-Prast A, Bastviken D, et al. Comprehensive assessment of dissolved organic matter processing in the Amazon River and its major tributaries revealed by positive and negative electrospray mass spectrometry and NMR spectroscopy. Sci Total Environ. 2023;857(Pt 3):159620.
126. Li S, Harir M, Schmitt-Kopplin P, Machado-Silva F, Gonsior M, Bastviken D, et al. Distinct Non-conservative Behavior of Dissolved Organic Matter after Mixing Solimoes/Negro and Amazon/Tapajos River Waters. ACS ES T Water. 2023;3(8):2083-95.
127. Wong KC. Review of NMR Spectroscopy: Basic Principles, Concepts and Applications in Chemistry. Journal of Chemical Education. 2014;91(8):1103-4.
128. Pasek MA. Rethinking early Earth phosphorus geochemistry. Proc Natl Acad Sci U S A. 2008;105(3):853-8.
129. Çalışkanoğlu AZ, Dingwell DB, Cimarelli C, Camara ASB, Breitzke H, Buntkowsky G, et al. Reactive phosphorus via simulated lightning discharge: A role for fulgurites in pre-biotic chemistry. Chemical Geology. 2023;620:121343.
130. Hertkorn N, Benner R, Frommberger M, Schmitt-Kopplin P, Witt M, Kaiser K, et al. Characterization of a major refractory component of marine dissolved organic matter. Geochimica et Cosmochimica Acta. 2006;70(12):2990-3010.
131. Keller MA, Driscoll PC, Messner CB, Ralser M. 1H-NMR as implemented in several origin of life studies artificially implies the absence of metabolism-like non-enzymatic reactions by being signal-suppressed. Wellcome Open Research. 2018;2(52).
132. Clore GM, Iwahara J. Theory, practice, and applications of paramagnetic relaxation enhancement for the characterization of transient low-population states of biological macromolecules and their complexes. Chem Rev. 2009;109(9):4108-39.
133. Weljie AM, Newton J, Mercier P, Carlson E, Slupsky CM. Targeted profiling: quantitative analysis of 1H NMR metabolomics data. Anal Chem. 2006;78(13):4430-42.
134. Waikar SS, Srivastava A, Palsson R, Shafi T, Hsu CY, Sharma K, et al. Association of Urinary Oxalate Excretion With the Risk of Chronic Kidney Disease Progression. JAMA Intern Med. 2019;179(4):542-51.

135. Menor Salván C, Bouza M, Fialho DM, Burcar BT, Fernández FM, Hud NV. Prebiotic Origin of Pre-RNA Building Blocks in a Urea “Warm Little Pond” Scenario. ChemBioChem. 2020;21(24):3504-10.
136. Ter-Ovanessian LMP, Lambert J-F, Maurel M-C. Building the uracil skeleton in primitive ponds at the origins of life: carbamoylation of aspartic acid. Scientific Reports. 2022;12(1):19178.
137. Das T, Ghule S, Vanka K. Insights Into the Origin of Life: Did It Begin from HCN and H2O? ACS Central Science. 2019;5(9):1532-40.
138. Caillet-Saguy C, Delepierre M, Lecroisey A, Bertini I, Piccioli M, Turano P. Direct-detected 13C NMR to investigate the iron(III) hemophore HasA. J Am Chem Soc. 2006;128(1):150-8.
139. Kiontke A, Oliveira-Birkmeier A, Opitz A, Birkemeyer C. Electrospray Ionization Efficiency Is Dependent on Different Molecular Descriptors with Respect to Solvent pH and Instrumental Configuration. PLOS ONE. 2016;11(12):e0167502.
140. Pieczonka SA, Zarnkow M, Ampenberger F, Gastl M, Rychlik M, Schmitt-Kopplin P. FT-ICR-MS reveals the molecular imprints of the brewing process. Frontiers in Nutrition. 2023;10.
141. Awad H, Khamis MM, El-Aneed A. Mass Spectrometry, Review of the Basics: Ionization. Applied Spectroscopy Reviews. 2015;50(2):158-75.
142. Annesley TM. Ion Suppression in Mass Spectrometry. Clinical Chemistry. 2003;49(7):1041-4.
143. El-Aneed A, Cohen A, Banoub J. Mass Spectrometry, Review of the Basics: Electrospray, MALDI, and Commonly Used Mass Analyzers. Applied Spectroscopy Reviews. 2009;44(3):210-30.
144. Kim CH, Kim MY, Lee S-W, Jang K-S. UPLC/FT-ICR MS-based high-resolution platform for determining the geographical origins of raw propolis samples. Journal of Analytical Science and Technology. 2019;10(1):8.
145. Nikolaev EN, Kostyukevich YI, Vladimirov GN. Fourier transform ion cyclotron resonance (FT ICR) mass spectrometry: Theory and simulations. Mass Spectrometry Reviews. 2016;35(2):219-58.
146. Marshall AG, Hendrickson CL, Jackson GS. Fourier transform ion cyclotron resonance mass spectrometry: A primer. Mass Spectrometry Reviews. 1998;17(1):1-35.
147. Scigelova M, Hornshaw M, Giannakopulos A, Makarov A. Fourier transform mass spectrometry. Molecular & Cellular Proteomics. 2011;10(7).
148. Plumb RS, Gethings LA, Rainville PD, Isaac G, Trengove R, King AM, et al. Advances in high throughput LC/MS based metabolomics: A review. TrAC Trends in Analytical Chemistry. 2023;160:116954.
149. Rodgers RP, Mapolelo Mmilili M, Robbins WK, Chacón-Patiño ML, Putman JC, Niles SF, et al. Combating selective ionization in the high resolution mass spectral characterization of complex mixtures. Faraday Discussions. 2019;218(0):29-51.
150. Krutchinsky AN, Chait BT. On the mature of the chemical noise in MALDI mass spectra. Journal of the American Society for Mass Spectrometry. 2002;13(2):129-34.
151. Hordijk W, Steel M. Autocatalytic Networks at the Basis of Life’s Origin and Organization. Life [Internet]. 2018; 8(4).
152. Rajaei V, Frenkel-Pinter M, Matange K, Petrov AS, Bowman J, Williams LD, editors. Combinatorial Explosion vs. Compression: What Can We Learn From Multicomponent Systems? 2022 Astrobiology Science Conference; 2022: AGU.

153. Closs AC, Bechtel M, Trapp O. Dynamic Exchange of Substituents in a Prebiotic Organocatalyst: Initial Steps towards an Evolutionary System. Angew Chem Int Ed Engl. 2022;61(3):e202112563.
154. Socha R. Homogeneously catalyzed condensation of formaldehyde to carbohydrates VII. An overall formose reaction model. Journal of Catalysis. 1981;67(1):207-17.
155. Beyazay T, Belthle KS, Fares C, Preiner M, Moran J, Martin WF, et al. Ambient temperature CO(2) fixation to pyruvate and subsequently to citramalate over iron and nickel nanoparticles. Nat Commun. 2023;14(1):570.
156. Preiner M, Igarashi K, Muchowska KB, Yu M, Varma SJ, Kleinermanns K, et al. A hydrogen-dependent geochemical analogue of primordial carbon and energy metabolism. Nat Ecol Evol. 2020;4(4):534-42.
157. Becker HGO. Organikum: Organisch-chemisches Grundpraktikum: Deutscher Verlag der Wissenschaften; 1967.
158. Kisker C, Schindelin H, Baas D, Retey J, Meckenstock RU, Kroneck PM. A structural comparison of molybdenum cofactor-containing enzymes. FEMS Microbiol Rev. 1998;22(5):503-21.
159. Geisberger T, Diederich P, Kaiser CJO, Vogele K, Ruf A, Seitz C, et al. Formation of vesicular structures from fatty acids formed under simulated volcanic hydrothermal conditions. Sci Rep. 2023;13(1):15227.
160. Muchowska KB, Varma SJ, Chevallot-Beroux E, Lethuillier-Karl L, Li G, Moran J. Metals promote sequences of the reverse Krebs cycle. Nat Ecol Evol. 2017;1(11):1716-21.